5

ORNL-2983
UC-4 – Chemistry-General

CHEMISTRY DIVISION ANNUAL PROGRESS REPORT

FOR PERIOD ENDING JUNE 20, 1960

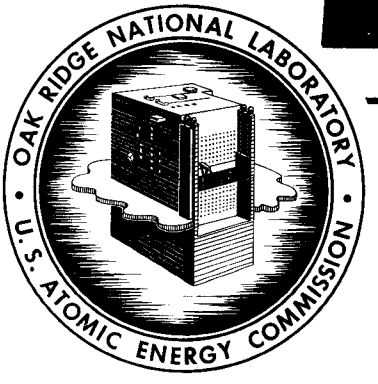

OAK RIDGE NATIONAL LABORATORY
operated by
UNION CARBIDE CORPORATION
for the
U.S. ATOMIC ENERGY COMMISSION

Printed in USA. Price $2.25. Available from the
Office of Technical Services
Department of Commerce
Washington 25, D.C.

ORNL-2983
Errata
Internal Dist.

CHEMISTRY DIVISION ANNUAL PROGRESS REPORT FOR PERIOD ENDING JUNE 20, 1960

Page	Column	Line	Errata
13	1	2	*for* methy *read* methyl
15	Table 8		(revised below)
44	2	18	*for* $10^{-4}t$ – *read* $10^{-4}t$
47	2	15	*for* has been *read* we have
48	2		brackets shown in the equation should have been parentheses
48	2	41	*for* Dowex 1-X10 *read* Dowex-1 X 10
49	1	6	*for* Dowex 50-X10 *read* Dowex-50 X 10

Table 8. Single-Stage Separation Factors and Thermodynamic Functions at 30°C for the Isotopic Exchange for Various BF_3-Organic Systems

$BF_3(g) \rightleftharpoons BF_3$-Organic Complex$(l)$

$\log \alpha = b/T - a$

Complex	a	b	$-\Delta H$ (cal/mole)	$-\Delta F$ (cal/mole)	$-\Delta S$ (cal • mole^{-1} • deg^{-1})	α at 30°C
$(CH_3)_2S \cdot BF_3$	16.9	0.0440	77.3	17.1	0.199	1.029
$(C_4H_9)_2S \cdot BF_3$	15.870	0.04007	72.7	17.2	0.183	1.029
$C_6H_5OCH_3 \cdot BF_3$	12.156	0.02814	55.7	16.4	0.130	1.028
$C_6H_5OH \cdot BF_3$	10.315	0.02433	47.2	13.7	0.111	1.023
$(C_2H_5)_3N \cdot BF_3$	11.105	0.02694	50.8	13.5	0.123	1.023

ORNL-2983
UC-4 – Chemistry-General

Contract No. W-7405-eng-26

CHEMISTRY DIVISION ANNUAL PROGRESS REPORT

for Period Ending June 20, 1960

E. H. Taylor, Director
M. A. Bredig, Associate Director

DATE ISSUED

AUG 26 1960

OAK RIDGE NATIONAL LABORATORY
Oak Ridge, Tennessee
operated by
UNION CARBIDE CORPORATION
for the
U. S. ATOMIC ENERGY COMMISSION

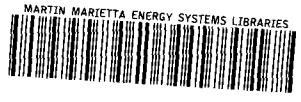

CHEMISTRY DIVISION ANNUAL PROGRESS REPORT

SUMMARY

NUCLEAR CHEMISTRY

The beta and gamma radiations of 21-hr I^{133} were investigated by single- and multicrystal scintillation spectrometers, and a scheme is proposed for the energy levels of Xe^{133}.

The level scheme of Ge^{74} was obtained by means of single- and multiple-crystal beta- and gamma-ray spectrometry using sources of Ga^{74} and As^{74}. The angular correlation for the 0.60-0.60-Mev cascade was measured.

Both beta- and gamma-ray single-crystal measurements and gamma-beta and gamma-gamma coincidence experiments were performed on the decay of I^{132}. Also, gamma-gamma angular correlations were measured for all the prominent gamma rays. This information has led to a level scheme in Xe^{132} involving excited states at 0.673, 1.448, 1.97, 2.10, 2.40, 2.59, and 2.84 Mev with spin assignments of 2, 4, 3, and 4 for the first four of these.

A study of 2.7-hr Pm^{150} established that the most energetic beta ray, at 3.16 ± 0.11 Mev, decays to the first excited state of Sm^{150} at 0.333 Mev. A partial decay scheme based on beta-gamma coincidence spectrometry was formulated with excited states in Sm^{150} at 0.333, 1.18, 1.66, and 2.08 Mev.

The measurement of the neutron absorption cross sections of Ce^{141} and Ce^{144} by the activation method is in progress. Separation of the 5.9-hr Pr^{145} daughter of the 3-min Ce^{145} produced by the (n, γ) reaction on Ce^{144} from the associated cerium isotopes was accomplished by the extraction of tetravalent cerium with di(2-ethylhexyl)phosphoric acid in *n*-heptane. Preliminary results of several irradiations of Ce^{144} in the LITR indicate an effective neutron cross section of $(6 \pm 2) \times 10^{-24}$ cm^2/atom.

Flux depressions in the vicinity of and within infinite cadmium slabs were calculated using the SNG reactor code on the IBM-704 computer at K-25. These results are pertinent to burnout calculations concerning cadmium filters during long irradiations.

An upper limit of 0.1 barn was set for the formation cross section of the 25-sec isomer of Po^{211} from Po^{210} for thermal reactor neutrons.

An upper limit of about 7×10^5 years was obtained for the half life of Bi^{208} by measuring the disintegration rate and measuring qualitatively the Bi^{208}/Bi^{209} ratio; this value is consistent with an approximate estimate of 7.5×10^5 years by C. H. Miller and co-workers at Chalk River.

A value of 870 barns was determined for the fission resonance integral of U^{233} from analyses of three fission products: Sr^{89}, Mo^{99}, and Ba^{140}. This value may be compared with two values, 900 and 820 barns, calculated from available resonance data.

Work on electron depolarization by scattering and the effect of multiple scattering on scattering asymmetry, along with changes in experimental equipment, will allow the use of weaker sources in beta-ray polarization measurements.

ISOLATION AND CHEMICAL PROPERTIES OF SYNTHETIC ELEMENTS

The solubilities at 25°C of $KTcO_4$ in water and of K_2ReCl_6 in 0.0100 *M* HCl were determined to be 0.1057 *m* and 0.1664 *m*. The standard heats of solution were measured calorimetrically as 12,765 and 10,397 cal/mole. The entropies of the ions were computed to be

$$S^0[TcO_4^-\ (aq)] = 47.9\ \text{cal}\cdot\text{deg}^{-1}\cdot\text{mole}^{-1}$$

and

$$S^0[ReCl_6^{--}\ (aq)] = 59.5\ \text{cal}\cdot\text{deg}^{-1}\cdot\text{mole}^{-1}\ .$$

The visible and near-infrared spectrum of K_2ReCl_6 in 1 *M* HCl is presented and the vibrational fine structure exhibited is discussed in relation to the excess entropy of K_2ReCl_6 over that of K_2PtCl_6.

Reduction of TcO_4^- in HCl solutions with zinc metal produces two species of technetium(III), one in high acidities and one in low acidities. Evidence is given to suggest the species are $TcCl_4^-$ and $Tc(OH)Cl_3^-$ respectively.

CHEMICAL SEPARATION OF ISOTOPES

The influence of various parameters on the separation of lithium isotopes by ion exchange was determined.

Studies of vapor pressures, heats of formation, and various other physical properties of the BF_3-organic complexes were made in an effort

to correlate these phenomena with isotopic fractionation factors.

The rate of exchange of CO gas with $Fe(CO)_5$ was found to be immeasurably slow at 25°C in the dark. Carbon-13 was depleted in CO evolved from $Fe(CO)_5$ by iodine, and by photodecomposition of the carbonyl. There was no exchange between C*O and $Mo(CO)_6$.

Pyridine and *sec*-butylamine show promise as substituents for ammonia in the cuprous ammonium lactate–CO system; other acids may be substituted for the lactic acid.

A 10-mm-ID × 40-cm-long column for distillation of NO was built and operated. Maximum isotopic fractionation was obtained with low boilup rates and low system pressures. Nitrogen 14/15 separation of 1.28 and oxygen 16/18 separation of 1.41, corresponding to 8.2 and 8.5 stages, were the largest obtained.

The addition of LiCl to an aqueous ammonia solution did not affect the nitrogen isotopic separation factor between ammonia gas and aqueous ammonia.

Operation of the Nitrox facility resulted in the separation of 203 g of N^{15} having a purity of 94 to 98% and 11.5 g of N^{15} having a purity greater than 87%.

A half time of 420 days at 35°C was observed for the NH_3 exchange between $Co(NH_3)_6Cl_3$ and NH_4OH in aqueous solution.

The atoms in N_2 molecules produced by the alkaline hypobromite oxidation of urea were found to be derived from the same urea molecule.

Oxygen isotope fractionation between $O_2(g)$ and cobalt-di(salicylal)ethylenediimine·$O_2(s)$ was redetermined. The new value of 1.012 confirms the one previously obtained.

The temperature dependence of isotope fractionation in the gas-liquid system $CO_2(g)$ vs dipropylamine carbamate(l) was measured. The C^{12}/C^{13} fractionation varies from 1.0059 at 25°C to 1.0028 at 60°C, with C^{13} enriching in the liquid. The O^{16}/O^{18} fractionation varies from 1.0081 at 25°C to 1.0096 at 60°C, with O^{18} enriching in the gas.

Revised and additional values for the single-stage fractionation factors of O^{18} for several aliphatic amine carbamates are presented.

A cascade to produce 50% O^{17} and 98% O^{18} was designed and fabricated. Installation of the equipment is in progress. Operation is expected to begin during October.

Special nonclogging constant-flow leaks were developed to remove liquid and gaseous products from the O^{17} enrichment cascade.

Exchange of calcium between calcium amalgam and aqueous calcium formate was found to be rapid. A tentative separation factor is 1.001 per stage per unit mass difference.

Infrared and Raman spectral observations and a complete vibrational frequency assignment were made on $N_2^{15}O_4$ and $N_2^{14}O_4$. Accurate isotopic partition function ratio calculations from spectral data were performed on a number of nitrogen-containing molecules. Raman spectra are reported for $B^{10}F_3\cdot(CH_3)_2O$ and $B^{11}F_3\cdot(CH_3)_2O$.

The Raman spectra of

$$Zn(N^{15}H_3)_4Br_2,\ Zn(ND_3)_4Br_2,\ \text{and}\ Zn(NH_3)_4Br_2$$

were observed, and the symmetric Zn-N stretching frequencies were compared and were found to be very close to the ratios of

$$\frac{1}{\sqrt{18}} : \frac{1}{\sqrt{20}} : \frac{1}{\sqrt{17}},$$

as predicted by theory.

Mass spectral studies of the cracking pattern of nitrous oxide are reported for all four nitrogen isotopic species. Metastable transitions were observed in the mass spectrum of nitrous oxide, and their existence was demonstrated with the various isotopic species. Pressure dependence studies showed these transitions to be spontaneous as well as collision-induced.

Routine isotopic mass analyses were performed on samples of BF_3 by peak-height measurements to give separation factors reproducible to about ±0.002. Analyses by the dual-collection, ratio technique were performed on samples of NO, $N^{15}O$, N_2, O_2, CO, and CO_2 to give separation factors generally reproducible to better than ±0.001.

RADIATION CHEMISTRY

The effect of displacement of atoms (by fast-neutron bombardment of copper) on reactions catalyzed at the surface and the relationship between catalysis and semiconductivity (using intrinsic and doped germanium) are being investigated by determining the kinetics of the H_2-D_2

exchange and the catalytic decomposition of formic acid vapor.

Tracer and adsorption studies connected the radiation-produced color centers and paramagnetic resonance in silica gel with positive holes and trapped electrons respectively. Their influence on the radiation enhancement of the catalytic activity of the gel is discussed.

The pressed alkali halide disk method for the identification and quantitative determination of organic and inorganic solids was used as a tool for study of the effect of variation of structure of the receiver on the transfer of radiation energy primarily absorbed by the alkali halide and the effect of various alkali halides on energy transfer to a given receiver.

Studies of sulfuric acid solutions containing Ce(IV) and Fe(II) showed that chemical intermediates arise on irradiation from the sulfuric acid as well as the water. The important intermediates are H, OH, HSO_4, H_2O_2, $H_2S_2O_8$, H_2SO_5, and H_2; $H_2S_2O_8$ and H_2SO_5, produced linearly with dose, may build up to appreciable concentrations in solutions containing Ce(IV).

Radiolysis of aqueous methane solutions, and also methane solutions with added ceric sulfate or ferric sulfate, indicated that methane reacts readily with OH but not with H.

The OH radical yield in Co^{60}-irradiated aqueous $NaNO_3$ solutions, 5.0 *M* and less, was observed to be constant, indicating that energy is transferred from the solute to the solvent and that the OH radical does not react with nitrate ion.

The Co^{60} irradiation of concentrated aqueous $NaNO_3$ solutions indicated that molecular hydrogen is formed by two mechanisms. These are the decomposition of excited water molecules (Samuel-Magee model) and the reaction of diffusing electrons with water molecules (Lea-Gray-Platzman model). Elimination of H_2 resulting from the Samuel-Magee mechanism may be accomplished by a high concentration of a solute that scavenges H atoms or by carrying out the irradiation at −196°C.

Experimental evidence was obtained to support the view that the alpha radiolysis of CO proceeds through ionic and excited species and that the active ionic species, CO^+, is deactivated by charge transfer to the product CO_2. There is no evident depletion of the excited species.

ORGANIC CHEMISTRY

The deamination of several diarylaminopropanols and diarylpropylamines was studied with stereochemical and radiochemical techniques. The results are best interpreted in terms of classical carbonium-ion intermediates which undergo rearrangement or nucleophilic attack more rapidly than rotation about the carbon-carbon bond takes place.

A secondary isotope effect of $k^*/k = 1.008 \pm 0.001$ was observed in the formation of the 2,4-dinitrophenylhydrazone of (aceto-2-C^{14})-phenone.

The mode of formation of substituted tetrahydropyrans among the products of the Grignard reactions of certain allylic systems was studied.

The ratio of the ionization constant of formic acid to that of formic-*d* acid (DCOOH) in aqueous solution was measured at 24 ± 0.5°C. The result fails to support a suggestion that the effect of alpha deuterium substitution on the ionization constant of phenylacetic acid is exerted mostly through an inductive mechanism.

Carbon-14 was employed in the evaluation of the deuterium kinetic isotope effects in the photochemical reactions of chlorine and bromine with formic-*d* acid.

Through the use of the mass spectrometer a search was made for an intermediate during the photochemical reaction of formic acid with chlorine. Chloroformic acid, which was reported by other workers to be an intermediate, could not be detected.

Cationic complexes with dibutylphosphoric acid were prepared in analytical purity. Metathesis of the complexes has been demonstrated with aqueous alkali.

The mutual solubility of tributylphosphine oxide and water as a function of temperature and the distribution of tributylphosphine oxide between carbon tetrachloride and water were determined refractometrically. The method that was developed for the use of the refractometer proved more useful than the synthetic method using the cloud point.

The initial reaction of tributyl phosphate upon heating is the formation of large yields of butene-1 and dibutylphosphoric acid, with lesser yields of butanol, butyl ether, and tetrabutyl pyrophosphate. The rate of decomposition increases as the amount of acid produced increases.

Differential thermal analysis has been used to define the conditions where one obtains endothermic and exothermic reactions between tributyl phosphate and nitric acid or nitrate salts. The results have been used to develop a safe and satisfactory synthesis of butyl nitrate by the dealkylation of tributyl phosphate.

Sulfuric acid (95%) and Amsco 125-82 react at 25°C to produce low-boiling hydrocarbons. This reaction removes compounds that would otherwise react in the solvent extraction process to reduce the separation factors.

CHEMISTRY OF AQUEOUS SYSTEMS

Solutions of UO_2SO_4 and $CuSO_4$ in D_2O were investigated spectrophotometrically from 4 to 280°C. The 0.42-μ band of U(VI) and the 0.82-μ band of Cu(II) showed monotonic increases in absorptivity by factors of 2.3 and 2.0, respectively, over this temperature range. A solution containing both U(VI) and Cu(II) showed a small amount of U(IV) to be present below 50°C after a thermal cycle and to disappear reproducibly on raising the temperature above 50°C.

The standard potential of the Ag, AgBr electrode was measured up to 200°C, and the activity coefficient of HBr was determined up to 200°C over the concentration range 0.005 to 0.5 m and to 150° over the range 0.5 to 1.0 m.

The standard electrode potentials of the quinhydrone electrode were measured from 25 to 55°C at 5° intervals using an Ag, AgCl reference electrode; the quinhydrone electrode is sufficiently reproducible in this temperature range to be used for activity coefficient measurements.

The Beckman amber glass electrode in conjunction with either an Ag, AgBr or an Hg, Hg_2Br_2 reference electrode was used to measure the activity coefficients of HBr solutions to 100°C. The acid error becomes higher with increasing temperature and acidity, limiting the useful range at 60°C to the millimolal region and below.

The solubility of Ag_2SO_4 was measured in UO_2SO_4 solutions to 200°C. The agreement between observed and calculated solubilities was good under all conditions when hydrolysis and complexing of the uranyl ion were taken into account. Single-parameter Debye-Hückel expressions were found to be satisfactory for representing the variation of all the equilibrium quotients with ionic strength throughout the temperature range 25 to 200°C.

Activity coefficients of silicotungstic acid (0.0004 to 0.04 M), measured by equilibrium ultracentrifugation, are in satisfactory agreement with the Debye-Hückel theory for a 1-4 electrolyte with a distance of closest approach parameter of 7.6 A. Turbidities of this system agree with the ultracentrifugation results. Equilibrium ultracentrifugations of soap solutions confirm that, if excess salt concentration is not too high, micelles are predominantly monodisperse; the micellar weights determined by this technique agree fairly well with those given by light scattering.

In a continuation of studies of anion exchange resins and their utilization for separations, adsorbability of positively charged complexes by anion exchangers was demonstrated and a new elution method for the removal of strongly adsorbed anions through complexing with cations was developed. The apparent molar volumes of exchangers in three-component systems were found to be additive. Earlier study on the adsorption of HF by anion exchangers was extended, and the selectivity coefficient of the HF_2^- ion compared with the F^- ion was evaluated, as well as the distribution coefficient of (molecular) HF. For the latter, large differences were found between anion and cation exchangers.

Investigations of the ion exchange and stability properties of various inorganic materials continued. The effect of method of preparation on the properties of zirconium phosphate was investigated as well as the stability of various phosphates to acids and bases at high temperature (200°C). Remarkable differences in the stability of zirconium and titanium phosphates to base at high temperatures were found. A survey of the properties of tantalum phosphate was carried out. A combination of two inorganic materials, one highly selective for Cs^+ over Ba^{++} and one having the reverse selectivity in the same medium, was developed for the rapid separation of short-lived Ba^{137} from its long-lived parent, Cs^{137}. The combination should have applications as a rapidly decaying, mobile radiation source.

The results of calorimetric measurements of the heat of the zinc-sodium ion exchange reaction on 2, 4, 8, 16, and 24% DVB Dowex 50 resins are discussed in terms of entropy changes.

A rigorous thermodynamic computation of the equilibrium selectivity coefficients for the exchange of bromide with chloride, iodide, or fluoride ions present in dilute aqueous solutions was performed for a series of cross-linked strong-base anion exchangers (polystyrene quaternary ammonium type) using the Gibbs-Donnan equation. Swelling pressures and activity coefficient ratios were evaluated from weight swelling measurements conducted in isopiestic vapor pressure experiments on virtually un-cross-linked and on cross-linked exchangers. Partial molar volume differences needed for the swelling free energy estimate were derived from density measurements on a weakly cross-linked exchanger. In the absence of specific interactions in the aqueous phase, the selectivity coefficient was found to be a function solely of the weight swelling.

CHEMISTRY OF CORROSION

A combination of spectrophotometric and electrochemical measurements was made for the analysis of the effect of complexing upon the rate of cathodic reduction of copper(II) species in acidic solutions. The complexing ions were sulfate and thiocyanate, and measurements of the association quotients were made at 25, 34, 49, and 63°C.

An electrical analog of a model of the passive interface on a metal was developed with the requirement that it represent the detailed phenomenology of such systems. The theory is applicable to the study of transients observed in potentiostatic and galvanostatic measurements.

The rate of growth of the corrosion film on zirconium was studied electrochemically. A similar study on Zircaloy-2 gave quite comparable results. The rate of reduction of several oxidizing agents on oxidized zirconium electrodes was determined.

The comparative rates of reduction of oxygen and several reducible inhibitors on passive iron were determined. With TcO_4^- and CrO_4^{--}, reduction of oxygen predominates, but with OsO_4 the reverse is the case. The cathodic processes are accelerated by the reduction products $Tc(OH)_4$ and $Os(OH)_4$.

In the study of the action of iodide ions as inhibitor for the dissolution of iron in acidic sulfate media, I^{131} was used to measure the extent of adsorption as a function of ionic activity and anodic current density.

Cathodic polarization measurements on iron in solutions containing benzoate ions as inhibitor established the reduction in corrosion rate in such a medium at various concentrations and its independence of the pH value over an appreciable range.

NONAQUEOUS SYSTEMS AT HIGH TEMPERATURE

Comparative studies of the rate of reaction of highly irradiated uranium with air, CO_2, and steam were conducted in an investigation of the fission product release potential in a loss-of-coolant-type accident postulated for the plutonium-producing reactors. Highly irradiated uranium was found to be more reactive, probably because of the defects in the oxide coating formed by the inclusion of fission products. Complete oxidation or melting released rare gases, iodine, and tellurium semiquantitatively in most atmospheres. Other fission products (ruthenium, cesium, and strontium) were released to a lesser extent and apparently in proportion to the amount of self-heating induced. In order of their relative tendency to promote the release of fission products the atmospheric reactants investigated could be rated in the order: air > CO_2 > steam.

In pursuit of the study of metal solutions in molten halides, the solubilities of lithium metal in molten lithium chloride and lithium iodide were found to increase between 600 and 1000°C approximately from 0.5 to 1.0 and from 1.2 to 2.5 mole % respectively; they are the smallest yet observed among the alkali-metal systems.

An electrochemical investigation of the Ce-$CeCl_3$ system was started. The data of the recent literature obtained with the use of alumina crucibles were shown to be entirely erroneous, as the dissolved cerium was found to react readily with Al_2O_3 to form CeOCl and aluminum metal.

The conductivities of three molten salts, LiI, CsF, and $CeCl_3$, were found to be quite different from values reported by others, which are thought to be in error.

The determination of the heat of fusion of the alkali halides was completed with calorimetric measurements on NaCl and the four rubidium halides.

A neutron and x-ray diffraction study of molten cesium fluoride yielded a radial distribution function and an estimate of 3.7 ± 0.1 nearest

neighbors of opposite charge at a most frequent distance of 2.85 A, significantly smaller than the number 6, at 3.12 A, in the solid at the melting point.

On the basis of new x-ray diffraction studies on molten and solid bismuth(I) chloroaluminate, the assumption of a trimeric ion, $(Bi_3)^{+++}$, was arrived at, which is likely to replace an earlier proposal of a dimeric ion, $(Bi_2)^{++}$, thought to occur in $(BiCl)_x$.

CHEMICAL PHYSICS

The low-temperature heat capacity of K_2ReBr_6 was measured and the entropy at 298.15°K calculated to be 108.47 $cal \cdot deg^{-1} \cdot mole^{-1}$.

Enthalpy measurements using a Bunsen ice calorimeter on standard Al_2O_3 are presented for the temperature range 0 to 900°C and are compared with those obtained at the National Bureau of Standards.

Work on the characteristics of thermal emission of positive ions from heated tungsten filaments and on the vapor phase association of alkali halides was completed. The product-detection component of the apparatus used to study the kinetics of the reaction between potassium and potassium bromide was redesigned to improve angular resolution and to eliminate spurious beam effects. A new apparatus was designed and substantially completed to study the hydrogen-deuterium exchange reaction.

Anomalous coherent neutron scattering from single crystals was demonstrated for the first time. Friedel's law, which requires $I_{hkl} = I_{\bar{h}\bar{k}\bar{l}}$ for Bragg scattering from single crystals, fails in CdS, CdI_2, and BP, each of which contains strong neutron absorbers. The neutron scattering amplitude in the thermal range was shown for Cd in CdS and CdI_2 to be energy-dependent.

A single-crystal neutron diffraction study of hydrazine is in progress. Preliminary results indicate that the molecular configuration is probably a staggered one.

A single-crystal neutron diffraction study of $Sr(OH)_2 \cdot 8H_2O$ is being undertaken. The hydroxide ions are hydrogen-bonded to each other in linear chains.

A computer program to produce stereoscopic pictures of crystal structures by using the cathode-ray-tube output of the IBM-704 is described.

A structure for $Na_7Zr_6F_{31}$ is proposed.

The saturation concentration of hydrogen atoms upon prolonged gamma irradiation of 0.129 mole fraction sulfuric acid at 77°K was found to be 3.4×10^{18} atoms per gram and that for 0.125 mole fraction perchloric acid was 2.9×10^{19}. The scavenging of atomic hydrogen by nitric acid and by hydrogen peroxide was studied, and an accompanying study was made on the molecular hydrogen yields.

The unpaired electron distribution on the two hydrazyl nitrogen atoms of the stable free radical α,α-diphenyl-β-picrylhydrazyl was determined by a detailed study of the anisotropic hyperfine interactions in a single crystal containing a small amount of the radical.

A paramagnetic resonance study of the two species formed in gamma-irradiated single crystals of calcium tungstate at 77°K elucidated many details of the radiation effect. One of these species is electron-deficient and contains two tungsten atoms, while the other has a surplus electron and contains a single atom of tungsten.

A paramagnetic resonance study is in progress on irradiated single crystals of sodium nitrite containing silver nitrite. Hyperfine effects from N^{14} were measured, and the results are being interpreted on the basis that NO_2 is the most likely paramagnetic species.

Molecular association energies in alkali halide vapors were studied by measuring the temperature dependence of the molecular weights of gaseous NaCl, NaBr, NaI, KCl, KI, RbCl, and CsCl. Dissociation energies for the reaction $(MX)_2 \rightleftharpoons 2MX$ at 1300°K ranged from 48.0 kcal/mole for NaCl to 34.7 for CsCl.

Free radicals and a stable intermediate displaced from the surface of a platnium catalyst have been identified by studying heterogeneous reactions at high pressure (1 mm) in a research mass spectrometer.

Chemical species having unpaired electrons, whether charged (ion-radicals) or uncharged (free radicals), were shown to undergo similar types of reactions.

Evidence was found in a negative ion–molecule reaction that rearrangement always involves the migration, or tunneling, of the hydrogen originally attached to the negative ion.

The increased yield in the radiolytic polymerization of $(CN)_2$ upon the admixture of xenon is attributed to the observed increase in negative-ion polymers and to the observed addition complex $[Xe(CN)_2]^+$.

Charge-transfer reactions producing intrinsic chemical change (methyl, methylene, and hydrogen radicals from CH_4) in the neutral molecule were proved by mass spectrometric techniques.

Mass spectrometric studies show that numerous radiation-induced charge-transfer reactions between C_2H_2 or CO and chemically inert gases go with high probability. However, not all energetically possible charge-transfer reactions go.

Ion-molecule reactions in the alpha radiolysis of C_2H_4 were studied in the alpha-particle mass spectrometer. Both pressure studies and mixture studies were employed to elucidate reaction mechanisms. Polymeric ions as large as $C_5H_9^+$ resulting from tertiary reactions were observed.

The charge spectrum of the ions formed after the beta decay of He^6 was found to agree with theoretical expectations.

DECAY OF I^{133}[1]

E. Eichler N. R. Johnson
J. W. Chase[2] G. D. O'Kelley

The beta and gamma radiations of 21-hr I^{133} have been studied by scintillation spectrometry.

An analysis of a single-crystal gamma-ray spectrum measured with a 3 × 3 in. NaI(Tl) scintillation spectrometer is shown in Fig. 1. The gamma energies in Mev (and relative intensities) are 0.24(0.1), 0.530(100), 0.700(2), 0.779(0.6), 0.874(6), 1.05(0.9), 1.23(2.0), and 1.30(2.5). Not shown in the figure is a weak transition at 0.62 Mev, which later was shown to exhibit a strong coincidence with the 0.700-Mev gamma ray.

Determinations were made of the gamma-ray spectra in coincidence with gamma radiations of 0.53, 0.70, 0.87, 1.05, 1.23, and 1.30 Mev. In some of these experiments additional weak transitions were found at 0.43, 0.36, 0.34, and 0.26 Mev. The coincidence results also showed that there were two gamma transitions of about 0.70 Mev, and that the peak at 0.874 Mev in the single-crystal spectrum includes a contribution from a gamma ray at 0.86 Mev.

Fermi analysis of the beta-ray spectrum measured with an anthracene scintillation spectrometer revealed a weak group at 1.54 Mev and more intense groups at 1.23 and about 0.9 Mev. Beta spectra in coincidence with 0.53-, 0.87-, 0.70-, and 1.23-Mev gamma rays yielded end points at 1.23, 0.89, 0.51, and 0.50 Mev respectively.

The decay scheme shown in Fig. 2 is consistent with the results of this investigation.

The 0.62-Mev gamma ray cannot populate the 1.23-Mev level, since the energy of this cascade (1.85 Mev) would exceed the total disintegration energy (1.76 Mev). To account for the coincidences with 0.70-Mev gamma rays, the 0.62-Mev transition was assigned as shown in Fig. 2. The

[1]Presented at the meeting of the Southeastern Section of the American Physical Society, Gatlinburg, Tenn., Apr. 7–9, 1960.

[2]Summer employee from the Massachusetts Institute of Technology, 1958–1959.

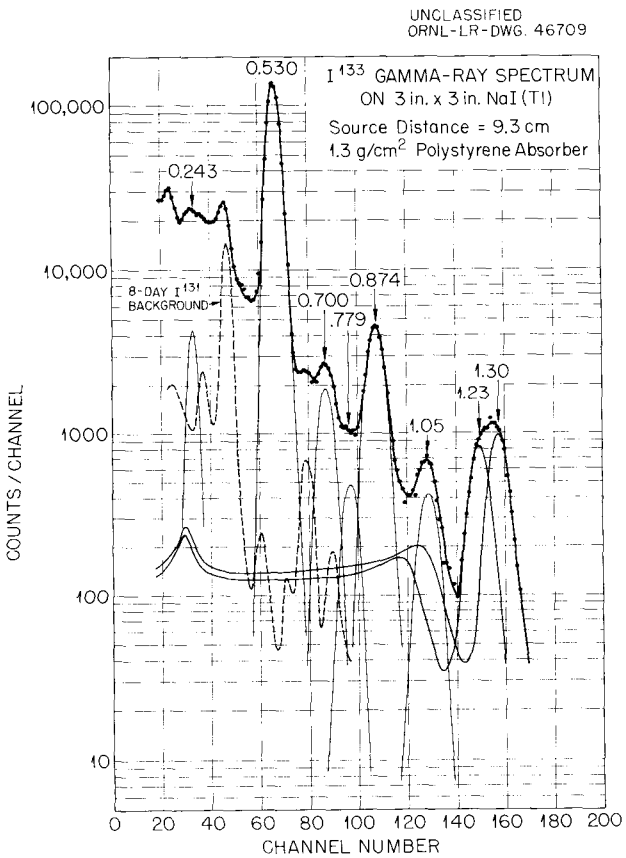

Fig. 1. Analysis of the Gamma-Ray Spectrum of 21-hr ^{133}. Energies are in Mev.

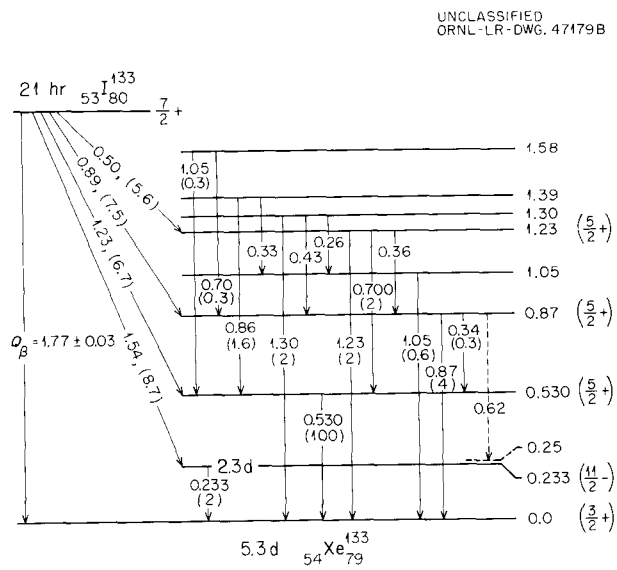

Fig. 2. Decay Scheme Proposed for I^{133}. Energies are in Mev, and the relative gamma-ray intensities are given in parentheses.

ground-state spins of I^{133} and Xe^{133} are measured values, while those shown for the 0.233-, 0.530-, 0.87-, and 1.23-Mev levels are supported by log *ft* values and single-particle transition probability calculations.

NUCLEAR LEVELS IN Ge^{74}[3]

E. Eichler G. D. O'Kelley
J. A. Marinsky[4] R. L. Robinson[5]
N. R. Johnson

The de-excitation of levels in Ge^{74} populated by the decay of Ga^{74} and As^{74} has been investigated with gamma and beta scintillation spectrometry. The single-crystal gamma-ray spectrum of Ga^{74} revealed the following gamma rays (and relative intensities): 0.38(2), 0.50(11), 0.600(100), 0.72(3), 0.87(9), 0.98(4), 1.11(5), 1.20(8), 1.33(5), 1.46(7), 1.56(2), 1.76(7), 1.93(6), 2.35(45), 2.55(3), 2.73(3), 2.97(3), 3.20(3), and 3.40(2). These data are consistent with those of Ythier *et al.*[6] Gamma-gamma coincidence experiments have been performed, gating on the 0.50-, 0.600-, 0.87-, 1.46-, and 2.35-Mev gamma rays. Figure 3 represents a typical coincidence spectrum, gating on the 0.60-Mev region. The peak at 0.60 Mev is much too large to be accounted for by random coincidences and thus indicates a 0.60-0.60-Mev gamma-ray cascade. The end point of the highest energy beta-ray group was observed at 2.7 Mev, and this same group was shown to be in coincidence with the 2.35-Mev gamma ray. These results support the level scheme given in Fig. 4.

The angular correlation between the two 0.60-Mev gamma rays was measured at ten angles using an As^{74} source. The data were compatible only with a 2, 2, 0 spin sequence and with a mixing ratio, δ, of $-3.4^{-1.1}_{+1.5}$ for the upper transition.

[3]Abstract published in *Bull. Am. Phys. Soc.* 5, 10 (1960).

[4]ORINS research participant, 1958, 1959; permanent address, University of Buffalo, Buffalo, N.Y.

[5]Physics Division.

[6]C. Ythier *et al.*, *Physica* 25, 694 (1959).

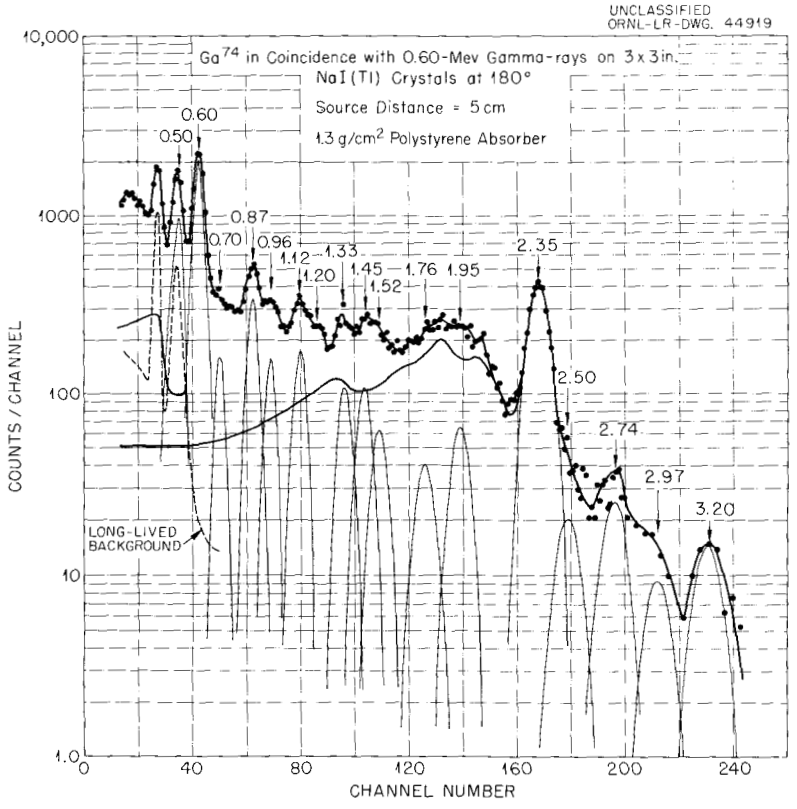

Fig. 3. Gamma-Ray Spectrum of Ga^{74} in Coincidence with 0.60-Mev Gamma Rays.

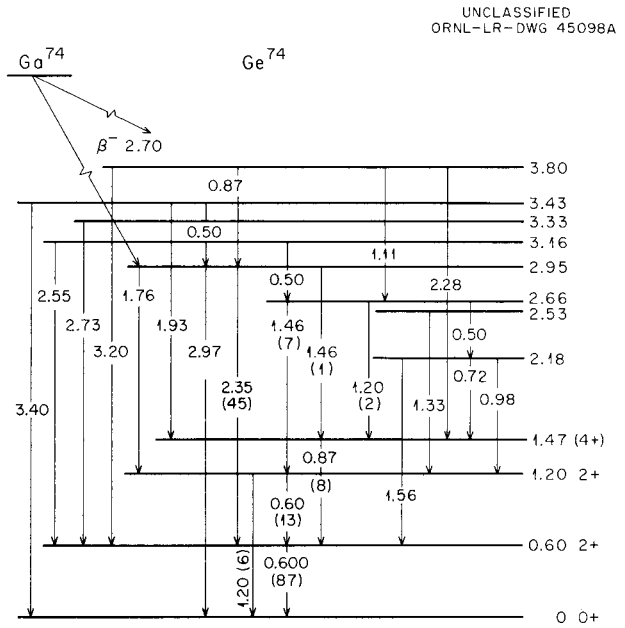

Fig. 4. Proposed Level Scheme for Ge^{74}.

This value is consistent with that of $-1^{-9}_{+0.5}$ obtained by Yamazaki *et al.*[7] and in good agreement with the value −2.8 predicted from the theory of Davydov and Filippov.[8]

DECAY OF I^{132}[1]

R. L. Robinson[5] E. Eichler N. R. Johnson

The ground-state spin of I^{132} has been measured recently as 4 by Sherwood, Ovenshine, and Parker.[9] With this information it seemed probable that the spins of some of the higher energy levels in Xe^{132} could be determined through additional studies of the decay of I^{132}. This has led us to examine both its gamma-ray and beta-ray spectra by means of scintillation spectrometers and to measure several gamma-gamma angular correlations.

The 2.3-hr I^{132} was extracted from an equilibrium mixture containing both I^{132} and its parent, 77-hr Te^{132}. The single-crystal (NaI) spectrum observed for a source-to-detector distance of 9.3 cm is shown in Fig. 5. Both the beta and gamma spectra in coincidence with the 0.515-, 0.667-, 0.775-, 0.953-, 1.142-, and 1.392-Mev gamma rays have been measured.

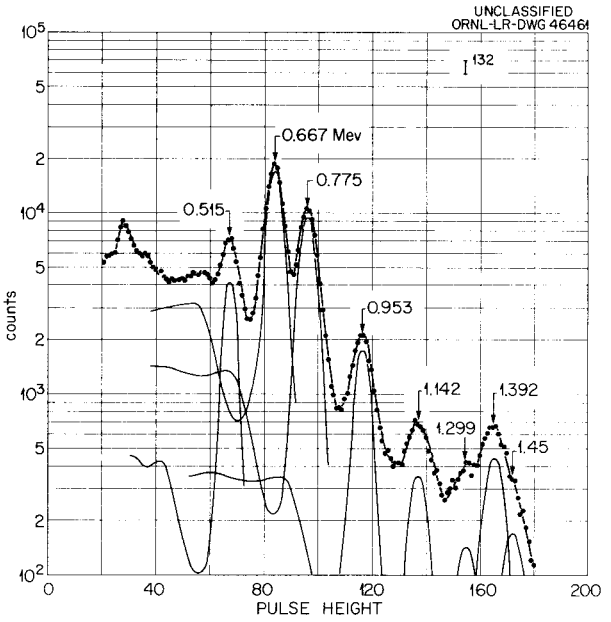

Fig. 5. Gamma-Ray Spectrum of I^{132} Taken at 9.3 cm with a 3 × 3 in. NaI(Tl) Crystal Spectrometer.

Besides elucidating the character of the I^{132} decay scheme, the coincidence studies have revealed additional low-intensity gamma rays at 0.24, 0.75, and 1.75 Mev and have shown that the 0.667-Mev peak in the singles spectrum is composed of two gamma rays with energies of 0.673 and about 0.64 Mev. A decay scheme consistent with most of our experimental results is shown in Fig. 6. It is similar to that proposed earlier by Finston and Bernstein.[10]

It can be assumed that the ground and first excited levels in Xe^{132} have respective assignments of 0^+ and 2^+. The intensities of the gamma transitions shown in Fig. 6 suggest that all levels from 1.448 Mev up are populated by beta-ray groups which have log *ft* values characteristic of once-forbidden or possibly allowed transitions, while gamma-beta coincidence measurements give

[7] T. Yamazaki, H. Ikegami, and M. Sakai, private communication.

[8] A. S. Davydov and G. F. Filippov, *Nuclear Phys.* 8, 237 (1958).

[9] J. E. Sherwood, S. J. Ovenshine, and G. W. Parker, *Bull. Am. Phys. Soc.* 4, 386 (1959). More recently this spin value was also obtained by E. Lipworth, H. L. Garvin, and W. A. Nierenberg, *Bull. Am. Phys. Soc.* 4, 353 (1959).

[10] H. L. Finston and W. Bernstein, *Phys. Rev.* 96, 71 (1954).

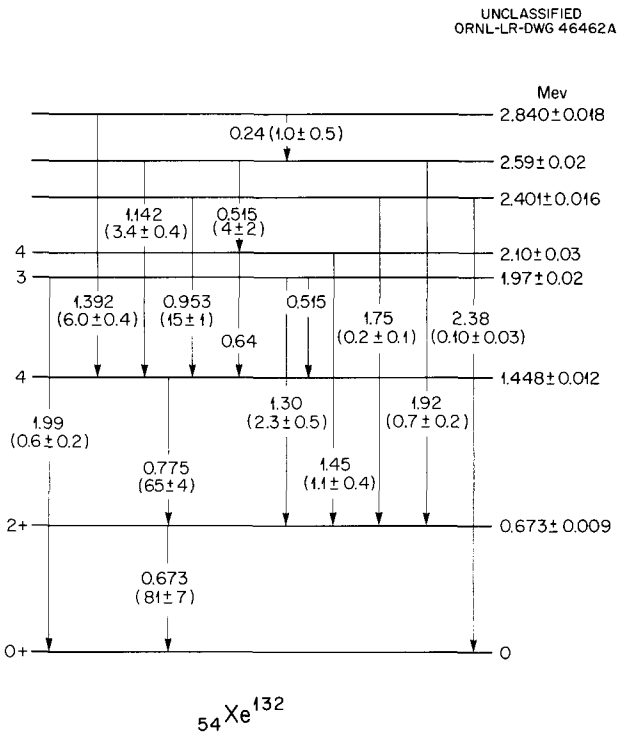

Fig. 6. Level Scheme in Xe^{132} Populated by the Decay of I^{132}. The pair of numbers associated with each transition gives its energy in Mev and relative intensity.

an upper limit of 0.3% for beta rays decaying to the 0.673-Mev level. From this information and the known systematic behavior of even-even nuclei in this region, the 1.448-Mev level is assigned spin 4^+.

To establish the spins of other levels, gamma-gamma angular correlations have been measured for all the prominent gamma rays. The data, taken every 10° between 90 and 180°, were fitted by the method of least squares to the function $W(\theta) = 1 + A_2P_2 + A_4P_4$, where P_2 and P_4 are Legendre polynomials. From these experiments the assignments for the 1.97- and 2.10-Mev levels are 3 and 4 respectively.

DECAY ENERGY OF Pm^{150} AND THE ENERGY LEVELS IN Sm^{150}

N. B. Gove[11] G. D. O'Kelley

Of all the disintegration energies determined for isotopes of the light rare earths with neutron numbers of about 83 to 94, only that of 2.7-hr Pm^{150} was found to exhibit a large deviation[12] (about 1.5 Mev) from the beta-decay systematics of Way and Wood. An examination of disintegration energies for other beta-decay pairs with 89 neutrons revealed no sharp deviations such as that reported in the literature for Pm^{150} decay, and so it was decided to re-examine its decay scheme in the hope that the beta-decay energy could be determined unambiguously.

A single-crystal gamma-ray spectrum was determined with a 3 × 3 in. NaI(Tl) scintillation spectrometer. The most intense peak of the single-crystal spectrum was at 0.333 Mev, with other prominent peaks clearly resolved at 0.41, 0.71, 0.86, 1.18, 1.33, 1.77, 1.96, 2.53, and 2.91 Mev. The analysis revealed less intense peaks at 1.0, 1.6, 2.06, 2.29, 2.41, 2.75, and 3.08 Mev.

Fermi analysis of a single-crystal beta-ray spectrum disclosed groups at 3.16 ± 0.11 Mev, 2.3 Mev, and lower energies. The gamma-ray spectrum in coincidence with beta rays of energy greater than 1.8 Mev showed a strong gamma peak at 0.33 Mev and peaks of low intensity at 0.4, 0.86, and 1.18 Mev. Beta spectra were determined in coincidence with five of the prominent gamma rays, and the results demonstrated that: the 3.16-Mev beta group is in coincidence with the 0.333-Mev gamma ray only; the 2.3-Mev beta group is coincident with gamma rays at 0.333, 0.86, and 1.18 Mev; a 1.83-Mev beta group is in coincidence with 0.86- and 1.33-Mev gamma rays; a 1.4-Mev beta group is coincident with gamma rays of 0.333, 1.33, and 1.75 Mev, and possibly others.

These results demonstrate that the most energetic beta group decays to the well-known first excited state of Sm^{150} at 0.333 Mev; hence the Pm^{150} beta disintegration energy is 3.49 ± 0.11 Mev, in good agreement with the prediction of the energy systematics.

From the above preliminary information a partial decay scheme can be formulated with excited states in Sm^{150} at 0.333, 1.18, 1.66, and 2.08 Mev. The large decay energy for Pm^{150}, the gamma-ray spectrum found here, and the Sm^{149} neutron capture gamma-ray spectrum[13] indicate

[11] Nuclear Data Project, National Academy of Sciences.

[12] V. K. Fischer and E. A. Remler, *Bull. Am. Phys. Soc.* 3, 63 (1958).

[13] L. V. Groshev *et al.*, *Atlas of Thermal Neutron Capture Gamma Rays*, Moscow, 1958.

that a number of additional energy levels are present in Sm^{150}. To this end a number of gamma-gamma spectra have been recorded, and the results are being evaluated.

EFFECTIVE NEUTRON ABSORPTION CROSS SECTION OF Ce^{144}

P. M. Lantz G. W. Parker

The need for neutron cross section values for many of the unstable fission product nuclides in reactor technology prompted us to undertake the measurement of the cross sections of 32-day Ce^{141} and 285-day Ce^{144}, which apparently have not been previously determined. Initial determinations of the cross section of Ce^{144} by the activation method have been completed, and work on determination of the Ce^{141} cross section is in progress.

Samples of purified fission product cerium containing the 140, 141, 142, and 144 isotopes were irradiated in the LITR along with cobalt and gold monitors for 3 to 4 hr. Separation of the 5.9-hr Pr^{145}, daughter of the 3-min Ce^{145} produced by an (n,γ) reaction on Ce^{144}, from the cerium isotopes was started 1 to 2 hr after the sample was removed from the reactor in order to prevent contamination from the longer lived praseodymium isotopes. Two milligrams of praseodymium carrier was added to the irradiated cerium isotope mixture containing 1 or 2 mc of Ce^{144} dissolved in a 10 *M* HNO_3–1 *M* $NaBrO_3$ solution. The tetravalent cerium was extracted from the praseodymium-bearing aqueous phase with 15 successive portions of 0.75 *M* di(2-ethylhexyl)phosphoric acid in *n*-heptane, stirred for 2 min with each portion. The praseodymium was further purified by precipitation of the hydroxide with NaOH and NH_4OH, followed by precipitation as the fluoride and finally as the oxalate. The oxalate precipitate was washed into a porcelain Petri dish and dried. A mica end window G-M tube in a 64-scaler automatic absorption counter which had been calibrated with P^{32} was used to follow the decay of 5.9-hr Pr^{145} and to determine its beta energy. Successive absorption counts were taken for a period of ten Pr^{145} half lives. The Ce^{144} activity remaining in the praseodymium after complete decay of Pr^{145} was less than 10^{-4} of the Ce^{144} irradiated. The contribution of this activity was subtracted from the gross counts to determine the net Pr^{145}.

Results from these preliminary investigations indicate an effective neutron cross section for Ce^{144} of $(6 \pm 2) \times 10^{-24}$ cm^2/atom, which is approximately the same as that reported for the 33-hr Ce^{143}.

Work is now in progress to determine the thermal-neutron cross section and resonance integral of Ce^{144} by irradiation of cadmium-shielded and unshielded samples in the LITR. Samples of isotopically pure Ce^{140} are being placed in the MTR for long-time irradiation for Ce^{141} effective neutron absorption cross section determination.

THERMAL-NEUTRON FLUX DEPRESSION WITHIN AND NEAR CADMIUM FILTERS

R. W. Stoughton J. Halperin

Pertinent to studies involving the use of thermal-neutron filters, the flux depression within and near an infinite slab of cadmium was examined. The study was carried out using the SNG reactor code[14,15] on the IBM-704 computer. The code here used transport theory in an S (5) approximation. A 40-mil metallic cadmium filter was placed 0, 1, 2, and 3 cm from a plane source of one-speed (Maxwellian average for 20°C) isotropic neutrons. Liquid water was placed between the source and filter, and the flux distribution was determined. The flux level from the source plane to the filter dropped to 24, 33, and 48% for the 3-, 2-, and 1-cm distances respectively. The data for the 2-cm case are shown plotted in Fig. 7. The flux depression within the cadmium was substantially greater than an exponential decrease; this is consistent with what would be expected for the assumed angular dependence.

THE EFFECTIVE CROSS SECTION OF THE $Po^{210}(n,\gamma)Po^{211m}$ REACTION FOR THERMAL REACTOR NEUTRONS

J. Halperin J. H. Oliver R. W. Stoughton

The effective cross section of Po^{210} for thermal reactor neutrons for the production of the 25-sec isomer of Po^{211} has been found to be less than 0.1 barn. A gold-silicon surface barrier alpha

---

[14] B. G. Carlson, *Solution of the Transport Equation by the S_N Approximation*, LA-1891 (1955).

[15] The authors are indebted to V. E. Anderson of the ORGDP Central Data Processing Group for calculations made with this code.

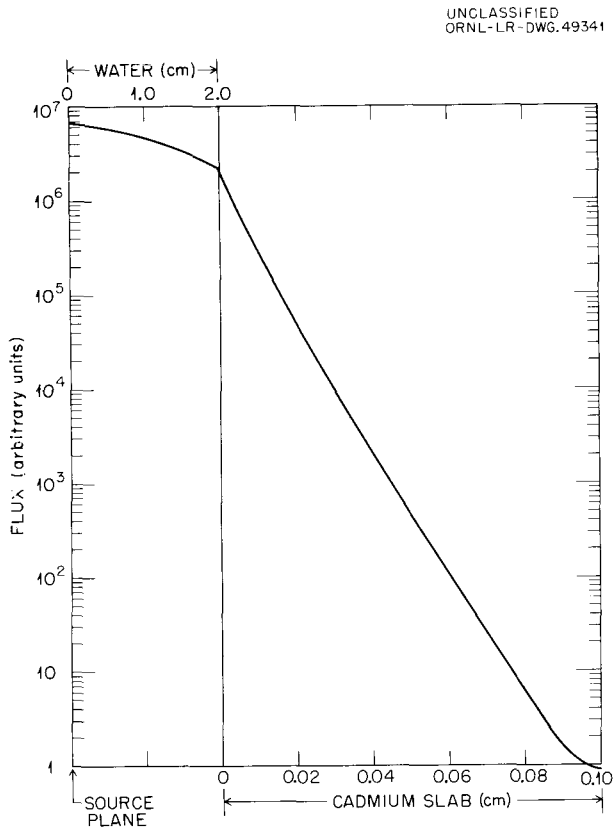

Fig. 7. Flux Depression in and near an Infinite Cadmium Slab.

detector[16] was used to discriminate between the 7.14–8.70 Mev alphas in the spectrum of Po^{211m} and the 5.30-Mev alphas of Po^{210}. Alterations in the amplifier and an increased neutron flux are expected to increase the sensitivity of the measurement some 100-fold or more, so that it may be possible in addition to look for the 7.44-Mev alphas of the 0.52-sec Po^{211}.

Since the Po^{210} has a closed shell of 126 neutrons and one pair of protons beyond the closed 82 shell, a low cross section for radiative capture is to be expected.

THE HALF LIFE OF Bi^{208}

J. Halperin R. E. Druschel R. W. Stoughton

A sample of Bi^{208}, which had been made by an $(n, 2n)$ reaction on bismuth[17] during a reactor irradiation and which had been further concentrated with respect to Bi^{209} by an electromagnetic separation,[18] was examined with an NaI scintillation spectrometer. Althought the spectrum analysis was complicated by the presence of the 28-year Bi^{207} and the 2.6×10^6 year Bi^{210}, the conclusions of Miller and co-workers[19] for the decay scheme were verified: namely, K capture followed by emission of a 2.6-Mev gamma ray. Mass spectrographic analysis[20] of the sample showed less than about 1 ppm of Bi^{208} in the sample, indicating a half life of less than about 7×10^5 years. Miller and co-workers have estimated about 7.5×10^5 years within a factor of 3 based upon cross-section systematics.

THE RESONANCE INTEGRAL FOR NEUTRON FISSION OF U^{233}

J. Halperin J. Oliver
R. W. Stoughton E. L. Blevins
F. J. Johnston

A measurement has been made of the resonance integral for fission of U^{233} using cadmium ratio techniques. The samples of U^{233} were irradiated in both the LITR and the ORR. Following the irradiation five fission products, 12.8-day Ba^{140}, 54-day Sr^{89}, 65-day Zr^{95}, 67-hr Mo^{99}, and 8.0-day I^{131}, were examined. In Table 1 are shown the fission resonance integrals computed on the basis

[16] The authors are indebted to J. L. Blankenship for making the detector available.

[17] The authors are indebted to B. C. Blanke for the irradiated material.

[18] The authors wish to express their appreciation to L. O. Love, W. A. Bell, and co-workers for the calutron separation.

[19] C. H. Miller, T. A. Eastwood, and J. C. Roy, *Can. J. Phys.* 37, 1126 (1959).

[20] Our thanks are due to A. E. Cameron for the mass analysis of the sample.

Table 1. Fission Resonance Integral of U^{233}

Based upon fission product analyses

Fission Product	$\int \sigma \, dE/E$ (barns)
Sr^{89}	855
Zr^{95}	992
Mo^{99}	877
I^{131}	1184
Ba^{140}	871

of energy-independent fission yields. The average resonance integral based upon Ba^{140}, Sr^{89}, and Mo^{99} is about 870 barns, which is in good agreement with the resonance integral estimated from the resonance data in BNL-325 of 900 barns and Terasawa's computation[21] of 820 barns. The higher values of the resonance integral based upon Zr^{95} and I^{131} suggest higher fission yields for the 95 and 131 chains for epithermal neutrons than for thermals. On this basis the ratios of fission yields for the 95 and 131 chains for the reactor epithermal to thermal spectra are 1.14 and 1.36 respectively.

The mass analysis of the U^{233} samples is under way to compare the value of α (i.e., σ capture/σ fission) for epithermal neutrons to that for thermal neutrons.

POLARIZATION OF BETA RAYS

A. R. Brosi B. H. Ketelle H. B. Willard[22]

In previously reported work, 1- to 3-curie sources of high-specific activity P^{32} were used to measure the polarization of 620-kev beta rays. A beam of beta particles was bent in an electric field to convert the polarization from longitudinal to transverse. The transverse polarization was then determined by measuring the asymmetry in single scattering from gold nuclei. Scattering from thin aluminum foils was used to measure the instrument asymmetry. The polarization of P^{32} beta particles was found to be $-v/c$ within a standard deviation of 2%.

Because of the requirement for high-specific-activity "point" sources of several curies, these measurements have not been extended to other beta emitters. Instead, some of the processes have been studied the occurrence of which in the polarization experiments makes corrections to the data necessary unless rigid requirements are met by the source and the scattering foil. Among these processes have been plural and multiple scattering in gold and aluminum foils. Depolarization of electrons by various elastic and inelastic scattering processes has also been studied. As a result of this work, measurements of good precision can be made with source intensities as much as a factor of 10 lower than those used in the P^{32} work.

Two major changes have been made in the experimental apparatus. A new multichannal analyzer will make the collection of data more efficient. The other change is in the scattering chamber, which now has five detectors instead of two. In addition to the two counters which measure the scattering asymmetry at an angle of 135° with respect to the electron beam, there are two at an angle of 30° which will be used to measure the instrument asymmetry. This change will reduce the data collection time by a factor of 2 and should essentially eliminate any contribution to the statistical error from the instrument asymmetry measurement. The fifth counter will monitor the undeflected beam when insulating baffles are used in some proposed plate scattering experiments.

[21] S. Terasawa, *The Effect of Epithermal Fission on Aqueous Homogeneous Reactors*, ORNL-2553 (Aug. 20, 1958).

[22] Physics Division.

ISOLATION AND CHEMICAL PROPERTIES OF SYNTHETIC ELEMENTS

CHEMISTRY OF TECHNETIUM

Solubility and Heat of Solution of Potassium Pertechnetate and Potassium Hexachlororhenate(IV)

R. H. Busey R. B. Bevan, Jr.

The solubility and standard heat of solution of $KTcO_4$ and K_2ReCl_6 have been measured. These data, in conjunction with the known entropies of the two salts, permit the calculation of the entropies of the two ions, TcO_4^- and $ReCl_6^{--}$.

Solubility. – The solubility of $KTcO_4$ in water was determined at 25.00 and 0°C. Equilibrium was approached from below and above saturation. The molal concentration of $KTcO_4$ in the saturated solution was determined by taking a weighed aliquot of the solution, carefully evaporating the water, and weighing the remaining dry salt. The solubility obtained was 0.1057 *m* at 25°C and 0.0344 *m* at 0°C. The solubility at 25°C calculated from the solubility measurements of Parker and Martin[1] of $KTcO_4$ in water at 7 and 27°C is 0.63 *m*. A serious counting error must have been made in their measurements.

The solubility of K_2ReCl_6 in 0.0100 *M* HCl was determined in a similar manner with the exception that the concentration of the K_2ReCl_6 in the saturated solution could not be determined by evaporation of the solvent since under those conditions the salt tends to hydrolyze to a slight extent. The concentration was determined spectrophotometrically utilizing the visible and near-infrared spectrum. The solubility data obtained were 0.1664 *m* at 25°C and 0.0832 *m* at 0°C. Rulfs and Meyer[2] obtained 0.175 *m* for the solubility at 25°C. These authors also determined the concentration of the salt spectrophotometrically. Their molar absorbancy indices of the $ReCl_6^{--}$ spectrum do not agree well with those of this research either in magnitude or wavelength, and are believed to be in error.

Heats of Solution. – The integral heats of solution of $KTcO_4$ in water and K_2ReCl_6 in 0.0100 *M* HCl were measured as a function of the concentration of the salt in the resulting solution. The solution calorimeter is an isothermal type utilizing a Dewar and a copper, platinum-encased, 100-ohm combination resistance thermometer–heater. The calorimeter has a measured sensitivity of 0.05 cal. The integral heats of solution of $KTcO_4$ in water in calories per mole as a function of the molal concentration of the resulting solution given in parentheses are: 12,735 (0.02592), 12,749 (0.02541), 12,777 (0.01572), 12,818 (0.00560), 12,746 (0.00476). Similarly, for K_2ReCl_6 in 0.0100 *M* HCl, the data are: 10,637 (0.02602), 10,627 (0.02471), 10,580 (0.01197), 10,535 (0.00514). Extrapolation of the results to infinite dilution using the Debye-Hückel limiting law gives the following standard heats of solution: $\Delta H^0_{25°C}(KTcO_4) = 12{,}765 \pm 15$ cal/mole and $\Delta H^0_{25°C}(K_2ReCl_6) = 10{,}397 \pm 15$ cal/mole.

Thermochemical Calculations; Entropies of $TcO_4^-(aq)$ and $ReCl_6^{--}(aq)$. – For the $KTcO_4$ solubility reaction the following thermochemical quantities at 25°C may be computed:

$$KTcO_4(c) = KTcO_4(aq) \ ;$$

$$m = 0.1057 \text{ mole per } 1000 \text{ g of } H_2O \ ,$$

$$\gamma_\pm = 0.74 \text{ (estimated from } KClO_4 \text{ and } NaClO_4 \text{ activity coefficient data)} \ ,$$

$$\Delta F^0 = -RT \ln (\gamma m)^2 = 3019 \text{ cal/mole} \ ,$$

$$\Delta S^0 = \frac{\Delta H^0 - \Delta F^0}{T} = 32.69 \text{ cal}\cdot\text{deg}^{-1}\cdot\text{mole}^{-1} \ .$$

Using 24.5 $\text{cal}\cdot\text{deg}^{-1}\cdot\text{mole}^{-1}$ for the entropy of $K^+(aq)$ and 39.74 $\text{cal}\cdot\text{deg}^{-1}\cdot\text{mole}^{-1}$ for the entropy[3] of $KTcO_4(c)$, the entropy of $TcO_4^-(aq)$ becomes:

$$S^0[TcO_4^-(aq)] = \Delta S^0 + S^0(KTcO_4) - S^0[K^+(aq)]$$

$$= 47.9 \pm 0.3 \text{ cal}\cdot\text{deg}^{-1}\cdot\text{mole}^{-1} \ .$$

The heat of formation[4] of $TcO_4^-(aq)$ is –173,000 cal/mole and the entropy of technetium has been

[1] G. W. Parker and W. S. Martin, *Chem. Quar. Prog. Rep. June 30, 1951*, ORNL-1116, p 26.

[2] C. L. Rulfs and R. J. Meyer, *J. Am. Chem. Soc.* **77**, 4505 (1955).

[3] R. H. Busey and Q. V. Larson, *Chem. Ann. Prog. Rep. June 20, 1957*, ORNL-2386, p 26.

[4] J. W. Cobble, W. T. Smith, Jr., and G. E. Boyd, *J. Am. Chem. Soc.* **75**, 5777 (1953).

estimated[4] to be 7.4 cal·deg^{-1}·mole^{-1}. By using the above value of 47.9 cal·deg^{-1}·mole^{-1} for the entropy of $TcO_4^-(aq)$, −73.2 cal·deg^{-1}·mole^{-1} is obtained for the entropy of formation and −151,200 cal/mole is obtained for the free energy of formation of $TcO_4^-(aq)$. From the last value the potential of the Tc-TcO_4^- couple is calculated to be −0.468 v.

For the K_2ReCl_6 solubility reaction the following thermochemical quantities at 25°C may be computed:

$$K_2ReCl_6(c) = K_2ReCl_6(aq) \ ;$$

$$m = 0.1664 \text{ mole per 1000 g of } H_2O \ ,$$

$$\gamma_{\pm} = 0.40 \text{ (estimate)} \ ,$$

$$\Delta F^0 = RT \ln [4(\gamma m)^3] = 3995 \text{ cal/mole} \ ,$$

$$\Delta S^0 = \frac{\Delta H^0 - \Delta F^0}{T} = 21.5 \text{ cal·deg}^{-1}\text{·mole}^{-1} \ .$$

Again using 24.5 cal·deg^{-1}·mole^{-1} for $S^0[K^+(aq)]$ and 87.0 cal·deg^{-1}·mole^{-1} for the entropy[5] of $K_2ReCl_6(c)$, the entropy of $ReCl_6^{--}(aq)$ becomes:

$$S^0[ReCl_6^{--}(aq)] = \Delta S^0 + S^0[K_2ReCl_6(c)] - 2S^0[K^+(aq)]$$

$$= 59.5 \pm 0.4 \text{ cal·deg}^{-1}\text{·mole}^{-1} \ .$$

Visible and Near-Infrared Spectrum of the $ReCl_6^{--}$ Ion and the Entropy of K_2ReCl_6

R. H. Busey

The spectrum of K_2ReCl_6 in 1 *M* HCl (Fig. 8) from 5500 to 12,000 A has been measured in the course of solubility studies. The unusual detail of vibrational fine structure superimposed on the electronic absorption bands prompted the measurement of the spectrum of the acid H_2ReCl_6 dissolved in cyclohexanone in hopes that the vibrational fine structure would be enhanced. The spectrum in cyclohexanone is given in Fig. 9. Measurement of the spectrum with cyclohexanone as solvent also permitted measurements to be extended to 15,100 A. No absorption bands were observed, however, from 12,000 to 15,100 A. The

[5]R. H. Busey, H. H. Dearman, and Q. V. Larson, *Chem. Ann. Prog. Rep. June 20, 1956*, ORNL-2159, p 11.

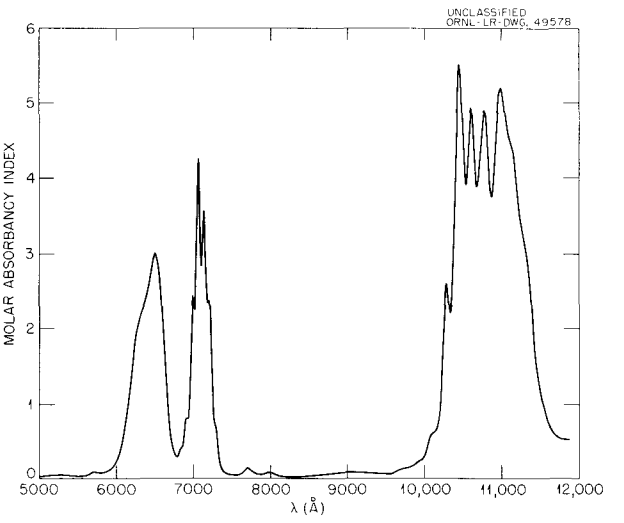

Fig. 8. Spectrum of K_2ReCl_6 in 1 *M* HCl.

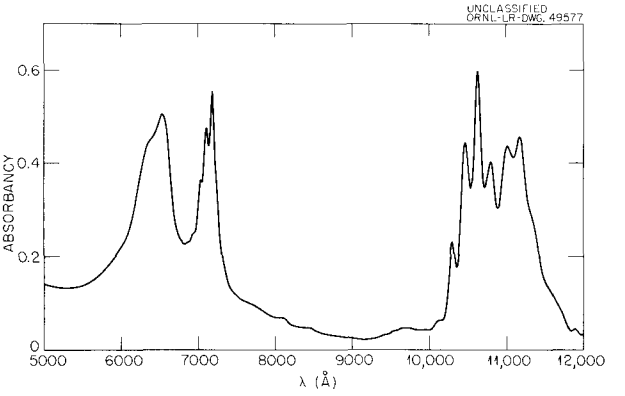

Fig. 9. Spectrum of H_2ReCl_6 (Approximately 0.1 *M*) in Cyclohexanone. 10-mm absorption cell.

concentration of the H_2ReCl_6 in the cyclohexanone was not known accurately but the molar absorbancy indices are not very different from those in 1 *M* HCl. The vibrational fine structure was not enhanced on the 7100-A band but was on the 10,800-A "band," clearly showing the latter to be an electronic doublet with maxima at approximately 10,600 and 11,100 A.

The point of interest is the narrow separation of the vibrational bands, indicating a low-energy vibrational state or states. For the 10,600- and 11,100-A electronic bands the average energy separation is 149 cm^{-1} in the 1 *M* HCl solution. In the cyclohexanone solution the vibrational bands appear to have an energy separation of 150 cm^{-1} on the 10,600-A electronic band and 127 cm^{-1} on the 11,100-A electronic band. The

separations of the vibrational bands on the 7100-A electronic band are not as constant as those above; they range in value from 120 to 180 cm^{-1} with an average separation of 150 cm^{-1}.

The entropy of K_2ReCl_6 at 25°C is 7.25 $cal \cdot deg^{-1} \cdot mole^{-1}$ in excess of that of the isomorphous, diamagnetic K_2PtCl_6 (ref 6). An entropy difference of $R \ln 4 = 2.75$ $cal \cdot deg^{-1} \cdot mole^{-1}$ is to be expected from the magnetic entropy of the rhenium compound. A portion, or perhaps all, of the remaining entropy of 4.50 $cal \cdot deg^{-1} \cdot mole^{-1}$ arises from the low-energy vibrational state or states. In general, vibrational bands observed in absorption represent a v' progression with $v'' = 0$;[7] however, in the present case a significant number of molecules are in higher vibrational states of the electronic ground state because of the small vibrational quanta observed. This would give rise to weak v' progressions with $v'' > 0$ which might complicate the interpretation of the vibrational fine structure.

If the 127- and 150-cm^{-1} vibrational quanta mentioned above represent separations of two different vibrational states of an upper electronic state, then the separations in the electronic ground state will be greater than this. In general the electronic ground-state vibrational level separations are approximately 30% greater than those of an excited state. Thus for the electronic ground state it is estimated the two above separations become 165 and 195 cm^{-1}. Two such low-energy vibrational levels would give rise to vibrational entropies at 25°C of 2.49 and 2.18 $cal \cdot deg^{-1} \cdot mole^{-1}$ respectively, or a total of 4.67 $cal \cdot deg^{-1} \cdot mole^{-1}$, which compares favorably with the 4.50 $cal \cdot deg^{-1} \cdot mole^{-1}$ mentioned above. The evidence for the 165-cm^{-1} vibrational state is not too strong, but the evidence for the 195-cm^{-1} vibrational state is good.

The spectrum of K_2ReBr_6 in hydrobromic acid is very similar to that of K_2ReCl_6. It gives the same electronic absorption bands, but the vibrational fine structure is not as distinct as in the chloride complex.

It will be of considerable interest to obtain the visible and near-infrared spectra of K_2TcCl_6 and K_2TcBr_6 for comparison. The corresponding fluoride complexes will be studied to complete the series.

[6] R. H. Busey, H. H. Dearman, and Q. V. Larson, *Chem. Ann. Prog. Rep. June 20, 1956*, ORNL-2159, p 11.

[7] G. Herzberg, *Molecular Spectra and Molecular Structure*, p 155, Van Nostrand, New York, 1950.

Technetium(III) in Hydrochloric Acid

R. H. Busey

Reduction of TcO_4^- in HCl solutions with zinc metal produces technetium(III), established by spectrophotometric titrations with $Ce(SO_4)_2$. Technetium(V)[8] and $TcCl_6^{--}$ are produced as intermediates. A species of technetium(III) produced in high acidities (3 to 6 *M* HCl) has an absorption maximum at 2650 A in its ultraviolet spectrum, but at lower acidities (0.5 to 2 *M* HCl) this maximum decreases and a second weak maximum at 4200 A develops. Titration shows that the technetium present is still technetium(III).

Considering that the technetium(III) with an absorption band at 2650 A is formed from $TcCl_6^{--}$ in 4–6 *M* HCl, and that rhenium(III) in HCl solutions forms the very stable $ReCl_4^-$ ion, it seems probable that this technetium(III) species is $TcCl_4^-$ and that the one formed in low acidities is a hydrolysis product of this ion. The Zn^{++} present in the solutions precludes the determination of the charge on the ion by the trioctylamine hydrochloride extraction method.

Evidence for the formula of the hydrolyzed technetium(III) species was obtained as follows. The equation for the hydrolysis may be written, assuming $TcCl_4^-$ as the unhydrolyzed species:

$$TcCl_4^- + H_2O = Tc(OH)Cl_3^- + HCl \ ;$$

$$K = \frac{[Tc(OH)Cl_3^-][HCl]}{[TcCl_4^-]} \ .$$

If C represents the total concentration of the technetium it is readily shown that

$$[TcCl_4^-] = \frac{C[HCl]}{K + [HCl]} = \frac{A_{2650}}{E} \ ,$$

where A_{2650} is the absorbancy at 2650 A due to $TcCl_4^-$ and E is the molar absorbancy index. This equation is rearranged to give:

$$\frac{A_{2650}}{C} = \frac{E[HCl]}{K + [HCl]} \ .$$

[8] R. H. Busey, *Chem. Ann. Prog. Rep. June 20, 1959*, ORNL-2782, p 13.

A series of spectra of technetium(III) in HCl were measured as a function of the HCl concentration, which ranged from 0.5 to 6 *M* HCl. The above equation was found to give a reasonable fit to the data plotted as A_{2650}/C vs [HCl]. A small correction was made for the absorbancy due to the $Tc(OH)Cl_3^-$ at 2650 A. The parameters were $K = 11$ and $E = 14{,}000$. The calculations lead to the result that approximately 25% of the technetium is present as $TcCl_4^-$ at 6 *M* HCl; at the lower acidities the technetium(III) is predominantly $Tc(OH)Cl_3^-$.

No fit of the data was obtained for the formation of $Tc(OH)_2Cl_2^-$, which requires that

$$\frac{A_{2650}}{C} = \frac{E[HCl]^2}{K + [HCl]^2} .$$

The $TcCl_4^-$ is only slowly oxidized by H^+ (approximately 1% per hour in 3 *M* HCl) and has been prepared in 8 *M* HCl. It is very rapidly oxidized by oxygen in the air to $TcCl_6^{--}$. This property is in marked contrast to $ReCl_4^-$, which is unaltered by bubbling pure oxygen into the solution of the ion.

CHEMICAL SEPARATION OF ISOTOPES

LITHIUM ISOTOPE SEPARATION BY ION EXCHANGE

D. A. Lee

The study of the influence of various parameters on separation factors for lithium isotopes in ion exchange systems has continued. Additional determinations have been made in ethylenediaminetetraacetate systems, in a formate system, and on ion exchangers containing phosphorus in the active sites. The previous work, together with the experimental procedures, has been described elsewhere.[1-3]

Ethylenediaminetetraacetic acid (EDTA) forms an anion complex with lithium ($LiEDTA^{---}$) at pH 10 to 11. Lithium isotope exchange studies were made in the following systems:

$$^{6}LiEDTA^{---}(aq) + R_3{}^{7}LiEDTA \rightleftharpoons {}^{7}LiEDTA^{---}(aq) + R_3{}^{6}LiEDTA$$

where R is an anion exchanger, Dowex 1-X10;

$$^{6}LiEDTA^{---}(aq) + {}^{7}LiR \rightleftharpoons {}^{7}LiEDTA^{---}(aq) + {}^{6}LiR$$

where R represents cation exchangers, Dowex 50-X2 and -X8;

$$^{6}Li^{+}(aq) + {}^{7}LiR \rightleftharpoons {}^{7}Li^{+}(aq) + {}^{6}LiR$$

where R is a cation exchanger containing iminodiacetate sites, Dowex chelating resin A-1.

For the Dowex 1 and the Dowex 50-X2 experiments, the eluants were 0.25 *M* KEDTA. For the Dowex 50-X8 experiment, the eluant was 0.1 *M* KEDTA. When NH_4EDTA solutions were used for eluants, two peaks were observed in the elution curve, indicating the presence of two $LiNH_4EDTA$ complexes. These two peaks were eliminated by using KEDTA as the eluting solution. For the experiment where the EDTA-type sites (iminodiacetate) were on the resin, 0.25 *N* NH_4Cl was used as an eluant. The experiments involving EDTA are summarized in Table 2. In these EDTA systems, ^{7}Li concentrates on the resin; in all other known systems involving lithium ions on ion exchange materials, ^{6}Li concentrates on the resin.

Previously there was reported the effect of various anions on the performance of certain cation exchange systems.[3] The effect of another anion, formate, in such systems has now been studied. Formate ion is a strong proton acceptor. It was chosen for study because it might have increased the separation factor as a result of localized hydrolysis of the lithium ion. However, the α was the same as that found for other potassium salt systems which do not affect the lithium ion species:

Anion	Formate
Resin	Dowex 50-X16
Mesh size	−200 +400
Column dimensions, ID × length (mm)	21.5 × 920
Flow rate (cm/sec)	1.52×10^{-3}
Number of theoretical plates	600
α	1.0028

Experiments were performed on three exchangers having phosphorus-containing groups as active sites. One of these was an inorganic exchanger of zirconium phosphate; the others were organic resins, one containing phosphonous acid groups (Bio-Rex 62) and the other containing phosphonic acid groups (Bio-Rex 63). These experiments are summarized in Table 3. The separation factors for lithium isotopes on these materials are somewhat lower than for sulfonic acid resins.

SEPARATION OF BORON ISOTOPES

A. A. Palko

The attempt to correlate single-stage boron isotopic separation factors with various properties of the BF_3-organic complexes has continued. The methods used in these studies have been described previously.[4,5]

[1] D. A. Lee and G. M. Begun, *J. Am. Chem. Soc.* **81**, 2332 (1959).

[2] D. A. Lee, *J. Phys. Chem.* **64**, 187 (1960).

[3] D. A. Lee, *Chem. Ann. Prog. Rep. June 20, 1959*, ORNL-2782, p 18.

[4] A. A. Palko, R. M. Healy, and L. Landau, *J. Chem. Phys.* **28**, 214 (1958).

[5] A. A. Palko, *J. Chem. Phys.* **30**, 1187 (1959).

Table 2. Summary of the Separation of Lithium Isotopes by Ion Exchange in the Presence of EDTA

Resin	Mesh Size	Column Dimensions, ID × Length (mm)	Flow Rate (cm/sec)	Number of Theoretical Plates	α
Dowex 1-X10	−400	26 × 1490	1.25×10^{-3}	190	0.9994
Dowex 50-X2	−200 +400	34 × 870	4.49×10^{-4}	240	0.9986
Dowex 50-X8	−100 +200	34 × 1150	7.07×10^{-4}	440	0.9977
Dowex chelating resin A-1	~50	26.5 × 1030	1.43×10^{-3}	140	0.9996

Table 3. Summary of the Separation of Lithium Isotopes on Phosphorus-Containing Exchangers

Exchanger	Mesh Size	Column Dimensions, ID × Length (mm)	Flow Rate (cm/sec)	Eluant	Number of Plates	α
$Zr_3(PO_4)_4$	30	34 × 1150	4.38×10^{-4}	0.25 *N* HCl	55	1.0016
Bio-Rex 62	−200 +400	21.5 × 1260	2.8×10^{-3}	0.25 *N* NH_4Cl	480	1.0006
Bio-Rex 63	−200 +400	21.5 × 1210	1.36×10^{-3}	0.25 *N* NH_4Cl	1000	1.0003

The vapor pressures of various mixtures of phenol and BF_3, methyl sulfide and BF_3, methyl selenide and BF_3, and triethylamine and BF_3 were measured as a function of temperature. Preliminary studies of the methyl sulfide–BF_3 system were contained in the last report of this series.[6] The vapor-pressure data were fitted by a method of least squares to the formula $\log p = a - b/T$. The constants calculated for these curves are shown in Tables 4–6. The freezing points were determined and the heats of reaction were estimated for the BF_3 complexes shown. These properties are given in Table 7.

Single-stage isotopic separation factors were determined for the phenol- and the triethylamine-BF_3 systems. These data along with the data obtained for systems previously studied were fitted to the equation $\log \alpha = b/T - a$. From the slopes of the curves obtained, ΔH for the isotopic exchange reaction was calculated; ΔF and ΔS were also calculated by using the relationships shown below:

$$\Delta H = \text{slope} \times 2.303R \ ,$$

$$\Delta F = -RT \ln \alpha = \Delta H - T\Delta S \ .$$

The values for a and b along with values of ΔH, ΔF, and ΔS at 30°C are shown in Table 8.

Measurements of the single-stage separation factors for the dimethyl selenide–BF_3 system are in progress.

ENRICHMENT OF C^{13}

D. Zucker

The exchange of CO between $CO(g)$ and $Fe(CO)_5$ was studied further. The previously reported[7] exchange half time of a few hours was found to be in error; new studies show that the exchange rate is immeasurably slow in the dark. The apparent exchange rate previously reported was due to a slight decomposition of the large quantity of $Fe(CO)_5$ used in the experiment. The CO liberated

[6] A. A. Palko, *Chem. Ann. Prog. Rep. June 20, 1959*, ORNL-2782, p 19.

[7] D. Zucker, *Chem. Ann. Prog. Rep. June 20, 1959*, ORNL-2782, p 21.

Table 4. Vapor Pressure of Methyl Sulfide–BF_3 Solutions from – 20 to +26°C

$\log p = a - b/T$

Composition of Solution (moles BF_3/mole sulfide)	a	b	ΔH of Reaction (kcal/mole) ($2.303Rb$)
0.303	7.837	1557	7.1
0.458	7.780	1556	7.1
0.537	7.819	1577	7.2
0.827	7.989	1665	7.6
0.850	8.377	1796	8.2
0.903	9.241	2056	9.4
0.961	9.982	2236	10.2
0.996	10.164	2209	10.1
Pure Me_2S	7.878	1546	7.1

Table 5. Vapor Pressure of Phenol-BF_3 Solutions from – 10 to +40°C

$\log p = a - b/T$

Composition of Solution (moles BF_3/mole phenol)	a	b	ΔH of Reaction (kcal/mole) ($2.303Rb$)
0.165	10.686	2999	13.723
0.205	10.753	2968	13.582
0.286	11.288	3037	13.897
0.309	11.075	2919	13.357
0.383	11.668	2989	13.678
0.489	11.294	2708	12.392
0.502	11.135	2626	12.017
0.587	10.419	2292	10.488
0.622	10.262	2204	10.086
0.783	9.703	1982	9.07
0.747	9.732	1912	8.75
0.792	9.858	1899	8.69
0.81*	9.936	1899	8.69

*Vapor-pressure measurements above 0.81 mole of BF_3 per mole of phenol are not feasible in the apparatus used for these studies because of the extremely high pressure of this system.

Table 6. Vapor Pressure of Dimethyl Selenide–BF_3 Solutions from −30 to +30°C

$\log p = a - b/T$

Composition of Solution (moles BF_3/mole selenide)	a	b	ΔH of Reaction (kcal/mole) ($2.303Rb$)
Pure selenide	7.861	1643	7.52
0.086	9.550	2013	9.21
0.356	10.376	2146	9.82
0.415	10.215	2084	9.54
0.933	10.440	1991	9.11
0.994	9.945	1824	8.35

Table 7. Melting Points and Heats of Reaction for Some BF_3-Organic Complexes

$BF_3(g) + \text{organic}(l) \rightarrow BF_3 \cdot \text{organic}(l)$

Complex	Melting Point (°C)	ΔH of Reaction (Estimated) (kcal/mole)
$(CH_3)_2S \cdot BF_3$	−19.6	−10.1
$(CH_3)_2Se \cdot BF_3$	−43	−8.6
$(CH_3CH_2)_3N \cdot BF_3$	+29.6	*
$(C_6H_5OH)_2 \cdot BF_3$	~−5**	−13.6
$C_6H_5OH \cdot BF_3$	~−15**	−8.7

*The vapor pressures for the triethyl amine were so low over the temperature range studied that a reliable estimate of ΔH could not be made.

**The phenol-BF_3 system supercools so readily that reproducible mp's are difficult to obtain.

Table 8. Single-Stage Separation Factors and Thermodynamic Functions at 30°C for the Isotopic Exchange for Various BF_3-Organic Systems

$BF_3(g) \rightleftharpoons BF_3\text{-Organic Complex}(l)$

$\log \alpha = b/T - a$

Complex	a	b	$-\Delta H$ (cal/mole)	$-\Delta F$ (cal/mole)	$-\Delta S$ (cal·mole^{-1}·deg^{-1})	α at 30°C
$(CH_3)_2S \cdot BF_3$	16.9	0.0440	+77.3	17.1	0.194 ~~+0.311~~	1.029
$(C_4H_9)_2S \cdot BF_3$	15.870	0.04007	+72.7	17.2	0.183 ~~+0.297~~	1.029
$C_6H_5OCH_3 \cdot BF_3$	12.156	0.02814	+55.7	16.4	0.130 ~~+0.238~~	1.028
$C_6H_5OH \cdot BF_3$	10.315	0.02433	+47.2	13.7	0.111 ~~+0.201~~	1.023
$(C_2H_5)_3N \cdot BF_3$	11.105	0.02694	+50.8	13.5	0.123 ~~+0.212~~	1.023

as a result of this decomposition diluted the small quantity of labeled C*O present, giving the appearance of exchange.

The isotope effect in the decomposition of $Fe(CO)_5$ according to the reactions

$$Fe(CO)_5 + I_2 \longrightarrow Fe(CO)_4 I_2 + CO$$

$$Fe(CO)_4 I_2 \xrightarrow{\text{heat}} FeI_2 + 4CO$$

in 1,1,2,2-tetrabromoethane was measured. These reactions are essentially quantitative. In the first reaction, C^{13} was depleted in the gas evolved by a factor of 1.025 ± 0.003. Enrichment of C^{13} in the $Fe(CO)_4 I_2$ should then have been 1.006; actual assay of the CO from the second reaction gave 1.008 ± 0.003. A similar result was obtained by photodecomposition and thermal decomposition of $Fe(CO)_5$.

Consideration of exchange reactions involving chromium, molybdenum, and tungsten carbonyls (ref 7) was dropped when $Mo(CO)_6$ showed no detectable exchange with C*O in 18 hr in $CHCl_3$ solution. The absence of rapid exchange was to be expected from the relatively great stability of these compounds, compared with other carbonyls.

In using the cuprous ammonium lactate–CO system for C^{13} enrichment, reflux difficulties are encountered. As previously reported,[7] use of monoethanolamine in place of NH_3 leads to excessive decomposition. Two organic bases showed promise as ammonia substitutes. Pyridine and *sec*-butylamine were less volatile and produced stable solutions. Isoamylamine caused slow precipitation of metallic copper, though not nearly as rapidly as monoethanolamine. In addition to the above compounds, two other materials, glycine and ethylenediamine, yield solutions with CO solubility comparable to that in ammoniacal solutions. However, in both cases disproportionation and precipitation of the copper occurs very rapidly. With glycine this occurred with or without the presence of lactate, and with or without addition of NaOH.

Bases whose solutions would not dissolve appreciable CO include piperidine, piperazine, diethanolamine, di-*n*-butylamine, and 2-aminopyridine. In general, it appears that substitution of an organic moiety for one hydrogen of ammonia produces a compound which, with cuprous ion, dissolves CO; substitution in a second place on the NH_3 molecule destroys this ability. The effect may be steric.

Formic, acetic, and propionic acids may be substituted for lactic acid in cuprous solutions with pyridine or *sec*-butylamine.

NITROGEN ISOTOPE SEPARATION STUDIES

Distillation of NO for Enrichment of N^{15} and O^{18}

L. L. Brown L. B. Yeatts, Jr.

At the close of the last report period, a 10-mm-ID × 200-cm-long column had been constructed for the distillation of NO, and preliminary runs had been made. Simultaneously, a search was begun for a good method of isotopically analyzing the oxygen contained in NO, which itself cannot be used because mass 32 is contaminated by O_2 produced from the ionized sample.

Two sample preparation techniques are now available. In the first technique the oxygen of the sample is converted to CO_2 by treating the NO with $Hg(CN)_2$ in the presence of $HgCl_2$. The reaction is not quantitative, however, and the usefulness of the method is limited to samples obtained from multistage equilibrations in which relatively large amounts of isotopic enrichment have occurred. The second sample preparation technique was devised by Taylor[8] and consists in dissociating NO into N_2 and O_2 by means of a high-voltage arc. The distinct advantage of this method is that both elements are processed at the same time. The ratio of isotope ratios between two samples is good to ± 0.002 for both nitrogen and oxygen. The conversion is 99% complete for sample pressures of about 1.5 cm.

With the sparking technique available for better sample analysis, a shorter distillation column was built. It was a modified Clusius[9] type 10 mm ID and 40 cm long, packed with Helipak No. 3012. Several runs have been completed with different temperatures and boilup rates. The nitrogen and oxygen isotope separations were determined for each set of conditions. The number of stages of separation obtained was calculated from the total separation across 40 cm of packing

[8] T. I. Taylor, personal communication; *Separation of Isotopes Annual Report*, NYO-7763 (1959).

[9] K. Clusius and K. Schleich, *Helv. Chim. Acta* **42**, 232 (1959).

by using the single-stage factors of Clusius.[10] The column data are included in Table 9 for runs made at total reflux. The best results were obtained for low temperatures and low boilup rates.

Nitrogen Isotope Fractionation Between NH_3 Gas and Concentrated Aqueous LiCl + NH_3 Solution

A. C. Rutenberg

An experiment was performed to determine whether the nitrogen separation factor between NH_3 gas and aqueous NH_3 was enhanced by the presence of LiCl. It was hoped that this approach might yield some data on the interaction of Li^+ with NH_3.

Ammonia gas was equilibrated for 4.5 hr at 25°C with an aqueous solution of the composition $LiCl \cdot 2.7NH_3 \cdot 3.1H_2O$. The apparatus used was similar to that described by Brown and Begun.[11] After equilibration the NH_3 from both phases was converted to N_2 which was analyzed on an isotope ratio mass spectrometer. The measured separation factor, $(N^{15}/N^{14})_{liq}/(N^{15}/N^{14})_{gas}$, was 1.0054 ± 0.0015 (95% confidence interval), which was essentially the same as the value obtained by Kirshenbaum *et al.*[12] in the absence of LiCl. The Raman spectrum of a solution similar to the liquid phase showed no lines which could be attributed to an Li-NH_3 vibration.

Production of N^{15}

W. M. Jackson

Operation of the Nitrox facility[13] was continuous during the year except for 35 days down time to clean and repair the equipment. A total of 214.5 g of N^{15} was produced, of which 203 g had an isotopic purity of 94.5 to 97.9%, and 11.5 g a purity greater than 87%.

Rate of NH_3 Exchange Between Aqueous Ammonia and $Co(NH_3)_6Cl_3$

A. C. Rutenberg

This cobalt amine rate study was initiated to determine whether the measurement of isotopic equilibrium constants involving cobalt complexes was practical. It was soon obvious that the exchange rates were too slow for this purpose, but the experiment was continued long enough to obtain kinetic data on the system.

A solution 0.17 *M* in $Co(NH_3)_6Cl_3$ and 0.41 *M* in $N^{15}H_4OH$ (~83% N^{15}) was placed in a constant-temperature bath at 35°C and sampled periodically. The uncomplexed NH_3 in the samples was removed by vacuum distillation at room temperature. The

[10] K. Clusius and K. Schleich, *Helv. Chim. Acta* 41, 1342 (1958).

[11] L. L. Brown and G. M. Begun, *J. Chem. Phys.* 30, 1206 (1959).

[12] I. Kirshenbaum *et al.*, *J. Chem. Phys.* 15, 440 (1947).

[13] G. M. Begun *et al.*, *Chemical and Isotopic Studies of the Nitrox System for N^{15} Enrichment*, ORNL-2291 (June 6, 1957).

Table 9. Isotope Separation and Stages Observed in Distillation of NO in a Packed Column

Heat (w)	Pressure (cm)	S_N*	S_O*	N_N**	N_O**	Note
2.1	38	1.275	1.408	8.20	8.52	Equilibrium (?)
	54	1.184	1.217	5.87	6.25	Equilibrium (?)
3.2	36	1.252	1.383	7.47	7.96	Equilibrium
9.0	70	1.099	1.142	3.41	3.68	Equilibrium
9.2	74	1.147	1.212	4.98	5.27	Equilibrium
9.45	71	1.086	1.122	2.65	3.17	Equilibrium
9.70	69	1.128	1.230	4.32	5.54	Approached from condition of high separation; equilibrium (?)

*$S_N = (N^{14}/N^{15})_{top}/(N^{14}/N^{15})_{pot}$; $S_O = (O^{16}/O^{18})_{top}/(O^{16}/O^{18})_{pot}$.

**N_N, N_O: theoretical stages for nitrogen and oxygen, respectively, in 40 cm of packing.

complexed NH_3 was isolated by using the usual Kjeldahl analytical procedure for nitrogen analysis. The NH_3 was oxidized to N_2 and analyzed mass spectrometrically. The isotopic composition of the samples as a function of time is given below:

Time (days)	Complexed NH_3 (% N^{15})	Uncomplexed NH_3 (% N^{15})
0	0.44	83.4
16	2.24	77.8
51	3.84	73.7
98	5.34	69.9

The first sample of complexed NH_3 was found to contain a little more N^{15} than the normal isotopic composition of 0.37%, indicating that a small amount of exchange occurs in the course of the separation. The rate of exchange during the initial sampling period was much more rapid than the subsequent rate; therefore the half times of exchange were calculated with the omission of the zero time samples which did not lie on the first-order exchange curve. A half time of 420 days was obtained by using the isotopic data from the complexed NH_3. The free NH_4OH data yielded a half time of 360 days. This value is presumed to be lower because of some exchange of H_2O for complexed NH_3. A small loss of NH_3 from the complex was observed during the course of the experiment. The 420-day half time should correspond to the rate of NH_3 exchange at 35°C at the described concentrations.

Nitrogen Exchange in the Alkaline Hypobromite Oxidation of Urea

A. C. Rutenberg

A study was made of the alkaline hypobromite oxidation of urea to determine whether exchange of nitrogen atoms occurs between urea molecules during the following reaction:

$$CO(NH_2)_2 + 3NaOBr + 2NaOH \longrightarrow N_2 + 3NaBr + Na_2CO_3 + 3H_2O$$

Urea which contained a high percentage of the species $H_2N^{15}CON^{14}H_2$ was synthesized by the reaction[14] of $N^{15}H_4Cl$ with normal AgOCN. The hypobromite oxidation was performed by using (1) the above synthesized urea, (2) normal urea, and (3) a mixture of normal urea with the synthesized enriched urea. The N_2 obtained in each case was analyzed mass spectrometrically to determine the percentage of N_2^{14}, N_2^{15}, and $N^{14}N^{15}$ for the various starting materials (see Table 10).

Table 10. Isotopic Distribution of N_2 from the Oxidation of Urea (% of total N_2)

Mass No.	Enriched Urea	Normal Urea	Mixture* Enriched + Normal Urea
28	26.02	99.24	62.28
29	73.41	0.74	37.49
30	0.57	0.02	0.23

*50.5% enriched urea.

The data indicate that random mixing of nitrogen atoms does not occur, since under those conditions the mass-30 peak from the enriched urea would comprise 13.9% of the total N_2. A composition can be calculated which exactly fits the observed isotopic data for enriched urea. In this case one position would contain 0.77% N^{15} and the other position 73.78% N^{15}. It is not unexpected to find a slight enrichment of the "normal" nitrogen position, since the synthesis and purification involved long periods of heating during which some nitrogen exchange could occur.

The oxidation of a mixture of normal and enriched urea gave additional information on the isotopic composition of the synthesized enriched urea and made it possible to detect a small amount of isotopic exchange. The mixture was found to yield slightly less of mass 30 than would be expected from the mass-30 content of the two constituents, indicating that a very small amount of nitrogen exchange could have occurred. It may be concluded that in the alkaline hypobromite oxidation of urea little or no exchange of nitrogen occurs in the course of the reaction, and that both nitrogen atoms in the N_2 molecule are derived from the same urea molecule.

[14] A. Murray III and D. L. Williams, *Organic Synthesis with Isotopes, Part II*, p 1856, Interscience, New York, 1958.

OXYGEN ISOTOPE FRACTIONATION STUDIES

Cobalt Di(salicylal)ethylenediimine Oxygen Complex

L. L. Brown

The single-stage separation factor (α) for O^{16}/O^{18} in the system $O_2(g)$ vs cobalt di(salicylal)ethylenediimine·O_2 was measured and was reported[15] previously as 1.013 ± 0.002 at 1 atm pressure and 21°C. Recently, Panchenkov *et al.*[16] published the value 1.032 ± 0.02 for a single-stage equilibration and the range 1.024–1.030 from multistage contacting at 0.5 atm pressure and 26°C. Since these results differed appreciably from those measured earlier in this laboratory, new measurements of the value of α were undertaken.

Our new experiment was done at room temperature and 0.5 atm pressure in a spherical, rather than the previous cylindrical, reactor. The oxygen inventory was distributed between the phases as $O_2(g)/O_2(s) = 1.38$. Isotopic samples were prepared for the mass spectrometer from both phases and the feed oxygen (see Table 11).

Table 11. Isotope Ratios and Separation Factor for the System O_2 vs Cobalt Di(salicylal)ethylenediimine·O_2

	Ratio O_2^{34}/O_2^{32}	α^*
Gas/solid	1.0050	1.0124
Feed/solid	1.0074	
Gas/solid-I		1.0129
Gas/solid-II		1.0113
	Av	1.0122

*$\alpha = (O^{18}/O^{16})_{gas}/(O^{18}/O^{16})_{solid}$.

The heavy oxygen isotope enriched in the gas phase. The new value of α is in agreement with our earlier one. Since the three experiments under consideration all measured the same fractionation factor in different manners, the lower value appears to be correct. In any event, the system does not seem potentially useful for enrichment of O^{18} in quantity.

Isotope Fractionation Factors for the Carbon Dioxide–Dipropylamine Carbamate System

L. L. Brown

Carbon dioxide can be distilled from dipropylamine carbamate [$R_2NCOON(H)_2R_2$, where R is C_3H_7] below the boiling point of the pure amine. This feature makes possible a thermally refluxed, gas-liquid isotope separation system employing CO_2 gas and liquid dipropylamine carbamate. The pure amine boils at 110°C, while CO_2 comes out of the carbamate at about 65°C.

The isotope fractionation factors for C^{12}/C^{13} and O^{16}/O^{18} have been determined at 25, 38, and 60°C. The heavy-carbon and light-oxygen isotopes enrich in the liquid phase. Carbon enrichment becomes smaller with increasing temperature and, conversely, oxygen enrichment becomes larger. The data are shown in Table 12.

Table 12. Isotope Separation Factors for CO_2–Dipropylamine Carbamate System

Temperature (°C)	α_C*	α_O**
25	1.0059	1.0081
28	1.0046	1.0090
60	1.0028	1.0096

*$\alpha_C = (C^{12}/C^{13})_{gas}/(C^{12}/C^{13})_{liq}$.

**$\alpha_O = (O^{16}/O^{18})_{liq}/(O^{16}/O^{18})_{gas}$.

Enrichment of O^{18} by Distillation of Aliphatic Amine Carbamates

L. B. Yeatts, Jr.

The determination of the fractionation of the stable oxygen isotopes between the vapor and liquid phases of several aliphatic amine carbamates has continued. Estimates of the separation factors previously reported[17] have been revised upward, in the light of new data. The single-stage fractionation factors last reported were based upon

[15] L. L. Brown, *Chemical Separation of Isotopes Section Semiannual Report Dec. 31, 1955*, ORNL-2097, p 35.

[16] G. M. Panchenkov, A. M. Tolmachev, and V. B. Kondratova, *Zhur. Fiz. Khim.* 33, 734 (1959).

[17] L. B. Yeatts, Jr., *Chem. Ann. Prog. Rep. June 20, 1959*, ORNL-2782, p 23.

Holmberg's[18] values for O^{18} and C^{13} enrichment upon distilling diethylamine carbamate at 62°C. With his values of α of 1.007 for O^{18} and 1.002 for C^{13}, the number of theoretical plates in a small packed column was calculated, after distilling diethylamine carbamate, from the relationship

$$S = \alpha^n ,$$

where

S = total isotopic separation,

α = single-stage separation factor,

n = number of theoretical plates.

After measuring the total isotopic separation upon distilling another amine carbamate in this same column and assuming that the number of theoretical plates remained constant, this same relationship was used to determine the single-stage fractionation factors. Subsequently, single-stage experiments with diethylamine carbamate at 62°C have shown an O^{16}/O^{18} α of 1.0105 ± 0.0004 at the 95% confidence interval. The higher revised values based on this measurement are found in Table 13.

[18]K. E. Holmberg, p 202 in *Proceedings of the International Symposium on Isotope Separation*, North Holland Publishing Co., Amsterdam, 1958.

Table 13. Oxygen-18 Distillation Fractionation Factors* for Aliphatic Amine Carbamates

Amine Carbamate	Boiling Point (°C)	$\alpha^{O^{18}/O^{16}}$
Primary Amine Carbamates		
Ethyl	Decomposes	
n-Propyl	82	1.0040
Isopropyl	Decomposes	
n-Butyl	92	1.0069
n-Butyl	92	1.0061**
sec-Butyl	76	1.0064**
t-Butyl	Decomposes	
Isobutyl	86	1.0060**
Secondary Amine Carbamates		
Dimethyl	59	1.0060
Methylethyl	60	1.0049
Diethyl	62	1.0105**
Di-*n*-propyl	Decomposes	
Diisopropyl	Decomposes	

*$\alpha = (O^{18}/O^{16})/(O^{18}/O^{16})$.

**Single-stage equilibration.

Additional experimental results show that *n*-propylamine carbamate possesses a much larger separation factor than first reported.

In order to test the validity of the assumption that the number of theoretical plates in the distilling column does not change as one distills different carbamates, both single-stage and multistage experiments were made with *n*-butylamine carbamate. The results given in Table 13 indicate that there may have been one additional theoretical plate operating when *n*-butylamine carbamate was used in place of diethylamine carbamate.

Our most recent studies have shown that at least some of these carbamates are dissociated in the vapor phase. Additional experiments are planned wherein the degree of dissociation will be determined.

Cascade for the Production of High-Purity O^{17}

J. S. Drury

A cascade to produce 50% O^{17} and 98% O^{18} has been designed and fabricated. It is presently being installed in Building 4501. The cascade consists of two interconnected units, a water distillation cascade and a thermal diffusion cascade. Oxygen gas will be employed in the latter unit.

The water distillation cascade was designed to produce daily 1.6 g of water containing 3.5% O^{17} and 2.5 g of water containing 98% O^{18}. The oxygen contained in this water will be separated from the hydrogen by electrolysis and fed into the thermal diffusion unit. The thermal diffusion cascade was designed to produce daily 70 mg of oxygen having a 50% O^{17} content and 700 mg of oxygen having a 98% O^{18} content. Operation of the equipment is expected to begin during October.

Product Withdrawal for the O^{17} Facility

D. A. Lee

The product withdrawal from the water distillation cascade and the thermal diffusion cascade in the O^{17} facility should be continuous for optimum operation. The withdrawal rates were designed to be 1.6 ml of H_2O per 24 hr for the water distillation unit and 35 ml of O_2 (STP) per 24 hr for each thermal diffusion unit. Special nonclogging leaks have been developed to accommodate these small flow rates. It has been demonstrated that the

required flow may be obtained by the use of porous porcelain and alumina thimbles with a pressure drop of 1 atm across the wall of the thimble. These thimbles have leaked steam continuously for a period of one month at a constant rate. The porcelain thimbles may be sealed directly to Pyrex, while the alumina thimbles are sealed by means of rubber or neoprene gaskets in Swagelok fittings.

SEPARATION OF CALCIUM ISOTOPES

D. Zucker

The separation of calcium isotopes by chemical exchange between aqueous calcium and calcium amalgam is being investigated. The stability of the amalgam phase in such a system varies greatly, depending upon the ions present in the aqueous phase. The presence of chloride, bromide, iodide, nitrate, perchlorate, cacodylate, acetate, butyrate, or isobutyrate caused rapid decomposition of the amalgam. The amalgam phase was found to be most stable in the presence of calcium hydroxide solutions. However, the limited solubility of the hydroxide precluded its use in a system of this type. The most attractive salts from the standpoint of solubility and amalgam compatability were calcium formate and propionate. The former was selected for use in the following experiments.

The rate of exchange of calcium between the two phases of the system was measured with the aid of Ca^{45}. The exchange half time was found to be about 7 sec or less.

The isotopic fractionation factor was measured by means of a multistage batch equilibration of the two phases. After the initial equilibration, one half of the calcium in the amalgam phase was converted to an aqueous calcium formate solution which was then equilibrated with the remaining calcium amalgam. This process was continued through six equilibrations after which all of the calcium remaining in the amalgam was collected for mass analysis. In a similar manner successive equilibrations were performed on the aqueous phase. In this case calcium amalgam was prepared from the aqueous solution by electrolysis. After six such equilibrations the calcium contained in the last aqueous phase was collected for mass analysis. The ratio of 48/42 ratios of the two samples was found to be about 1.050. This degree of fractionation is equivalent to a separation factor of ~ 1.001 per stage per unit mass difference, with the heavy isotope concentrating in the aqueous phase. A great deal of difficulty was experienced in the mass analysis of the experimental samples. The result, therefore, must be regarded as tentative until further refinements can be made in the mass analysis of such samples.

SPECTROSCOPIC INVESTIGATIONS OF ISOTOPIC MOLECULES

Infrared and Raman Spectra of N_2O_4 and $BF_3 \cdot (CH_3)_2O$

G. M. Begun W. H. Fletcher

The observation and interpretation of the Raman and infrared spectra of $N_2^{15}O_4$ and $N_2^{14}O_4$ have been completed and published.[19] Accurate isotopic partition function ratios for nitrogen-containing molecules (N_2, N_2O, NO, NOCl, NO_2, NO_2^-, NO_3^-, and N_2O_4) have been calculated. All available isotopic and anharmonic data including many isotopic frequencies observed in this laboratory have been used in these calculations. Values of the isotopic partition function ratios (Q^{15}/Q^{14}) have been tabulated for various temperatures from 100 to 600°K. Isotopic equilibrium constants between these molecules and ions can be calculated from these tabulations. This material has been assembled and submitted for publication.

The theoretical investigation of the various boron isotope separation systems involving the exchange of BF_3 between gaseous BF_3 and a liquid complex $BF_3 \cdot X$ is of considerable interest, since, contrary to most predictions, the B^{11} isotope is found experimentally to concentrate in the gaseous BF_3. Many isotopic separation factors have been measured, but no theoretical calculations have been made, since the vibrational spectra of these compounds are rather complex. Investigations are being made at present on the infrared and Raman spectra of $BF_3 \cdot (CH_3)_2O$. Separate samples of the dimethyl ether complex have been prepared with highly enriched B^{10} and B^{11}.

The observation of the Raman spectra of both the B^{10} and B^{11} complexes has been completed, and very satisfactory data have been obtained. These data are summarized in Table 14.

---

[19] G. M. Begun and W. H. Fletcher, *J. Mol. Spectroscopy* 4, 388 (1960).

Table 14. Raman Spectra (cm^{-1}) of Liquid $BF_3 \cdot (CH_3)_2O$

Intensity	$B^{11}F_3 \cdot (CH_3)_2O$, 98.4% B^{11}	$B^{10}F_3 \cdot (CH_3)_2O$, 94.8% B^{10}	Δ (cm^{-1})	Polarization
m	322	322	0	P
m	344	344	0	D
s	499	500	1	P
s	661	672	11	P
s	804	809	5	P
s	918	925	7	P
s	1020	1020	0	D
w	1150	1150	0	
w	1264	1264	0	
vs	1459	1459	0	D
m	2850	2850	0	P
m	2889	2889	0	P
vs	2979	2979	0	P
m	3036	3036	0	D
m	3069	3069	0	D

Infrared spectra of the complexes are being obtained, and it is expected that a complete vibrational frequency assignment can then be made which will enable a calculation of the boron isotopic partition function ratio.

Raman Spectra of Zinc Ammonia Bromides

L. Landau

The Raman spectra of

$$Zn(N^{15}H_3)_4Br_2\,, \quad Zn(ND_3)_4Br_2\,, \quad Zn(NH_3)_4Br_2$$

were observed in the 400-cm^{-1} region, and the symmetric Zn-N stretching frequencies were compared. The observed frequencies are nearly in the ratio of

$$\frac{1}{\sqrt{18}} : \frac{1}{\sqrt{20}} : \frac{1}{\sqrt{17}}\,,$$

which is to be expected if the assumption is made that the NH_3 groups act as single particles for these vibrations:

Compound	Observed Frequency (cm^{-1})	Frequencies (cm^{-1}) Calculated To Be in the Ratio $\frac{1}{\sqrt{17}} : \frac{1}{\sqrt{18}} : \frac{1}{\sqrt{20}}$
$Zn(NH_3)_4Br_2$	424.9	425.6
$Zn(N^{15}H_3)_4Br_2$	413.1	413.6
$Zn(ND_3)_4Br_2$	393.6	392.4

The Raman spectra of the compounds $Zn(NH_3)_4Br_2$ and $Zn(ND_3)_4Br_2$ were previously observed and compared in this laboratory.[20,21]

Isotopic Mass Spectral Research

G. M. Begun L. Landau

A mass spectral study of the cracking patterns of the isotopic nitrous oxides has been made.

[20] A. C. Rutenberg and L. Landau, *Chem. Ann. Prog. Rep. June 20, 1958*, ORNL-2584, p 17.

[21] A. C. Rutenberg, *Chem. Ann. Prog. Rep. June 20, 1959*, ORNL-2782, p 25.

The molecules studied were the linear molecules $N^{14}N^{14}O$, $N^{14}N^{15}O$, $N^{15}N^{14}O$, and $N^{15}N^{15}O$. These molecules were synthesized from highly enriched N^{15} produced by chemical exchange in the Nitrox pilot plant. The cracking pattern data when corrected and normalized can be interpreted in terms of seven elementary processes which take place upon electron impact. These are illustrated for the molecule $N^{15}N^{14}O$ as follows:

$$N^{15}N^{14}O \longrightarrow (N^{15}N^{14}O)^+ + e^- \quad (1)$$

$$N^{15}N^{14}O \longrightarrow N^{15} + (N^{14}O)^+ + e^- \quad (2)$$

$$N^{15}N^{14}O \longrightarrow (N^{15}N^{14})^+ + O + e^- \quad (3)$$

$$N^{15}N^{14}O \longrightarrow (N^{15}O)^+ + N^{14} + e^- \quad (4)$$

$$N^{15}N^{14}O \longrightarrow N^{15}N^{14} + (O)^+ + e^- \quad (5)$$

$$N^{15}N^{14}O \longrightarrow (N^{15})^+ + N^{14}O + e^- \quad (6)$$

$$N^{15}N^{14}O \longrightarrow N^{15}O + (N^{14})^+ + e^- \quad (7)$$

By the use of the isotopic nitrogen atoms, it has been established that these reactions are quite possibly the ones involved. The neutral species, of course, are not observed, but the charged ions are observed, and the fact that $(O)^+$, $(N^{14})^+$, and $(N^{15})^+$ are observed in almost equal quantities leads one to believe that reactions (5), (6), and (7) may involve a triangular intermediate or complete dissociation into atoms. Table 15 lists the normalized results of the cracking pattern study for all four isotopic molecules in terms of the seven postulated reactions listed above. Each set has been normalized to make the formation of the parent ion equal to 100.

Table 15. Summary of Cracking Pattern Data for Isotopic Nitrous Oxides

Process	Relative Peak Height			
	$N^{14}N^{14}O$	$N^{14}N^{15}O$	$N^{15}N^{14}O$	$N^{15}N^{15}O$
1	100.0	100.0	100.0	100.0
2	20.4	21.6	18.9	21.7
3	8.10	8.49	7.63	8.99
4	2.01	2.05	1.96	2.15
5	2.13	2.50	2.04	2.46
6	1.99	2.31	1.90	2.36
7	1.99	2.35	1.83	2.36

It is interesting to note that process (4) has been shown to occur. The formation of an activated complex with a triangular or ring structure would account for this reaction very satisfactorily. The data are being considered further, and an attempt to calculate a cracking pattern from theoretical considerations is being made.

In the course of the mass spectral studies of nitrous oxide, several diffuse peaks were noted at nonintegral mass positions in the spectra. Diffuse peaks have been reported in the literature for polyatomic ions. These peaks are due to delayed decomposition of the ions which occurs in the field-free region between the source and the analyzing magnet of the mass spectrometer. The decomposition of the ions may be either spontaneous or induced by collision with gas molecules. Melton, Bretscher, and Baldock[22] have observed a spontaneous metastable transition in acetylene, but none have been reported for such a simple molecule as N_2O. For this reason a study of the pressure dependence of the transitions was made, and the observations were repeated on the various isotopic species. Figure 10 shows a typical recorder trace for $N^{15}N^{14}O$. The peaks at masses 17 and 18 are from residual water in the mass spectrometer, while the peak at 22.5 results from the doubly charged ion $(N^{15}N^{14}O)^{++}$. Three metastable peaks may be observed at masses 18.8, 20.0, and 21.5. The apparent mass M observed from a metastable transition may be calculated from the formula

$$M = \frac{(M_f)^2}{M_p} ,$$

where M_f is the mass of the charged fragment and M_p is the mass of the parent ion. By use of this formula the metastable transitions producing these three peaks are found to be:

$$(N^{15}N^{14}O)^+ \longrightarrow (N^{15}N^{14})^+ + O \quad (1)$$
(apparent M = 18.7)

$$(N^{15}N^{14}O)^+ \longrightarrow (N^{14}O)^+ + N^{15} \quad (2)$$
(apparent M = 20.0)

[22] C. E. Melton, M. M. Bretscher, and C. R. Baldock, *J. Chem. Phys.* **26**, 1302 (1957).

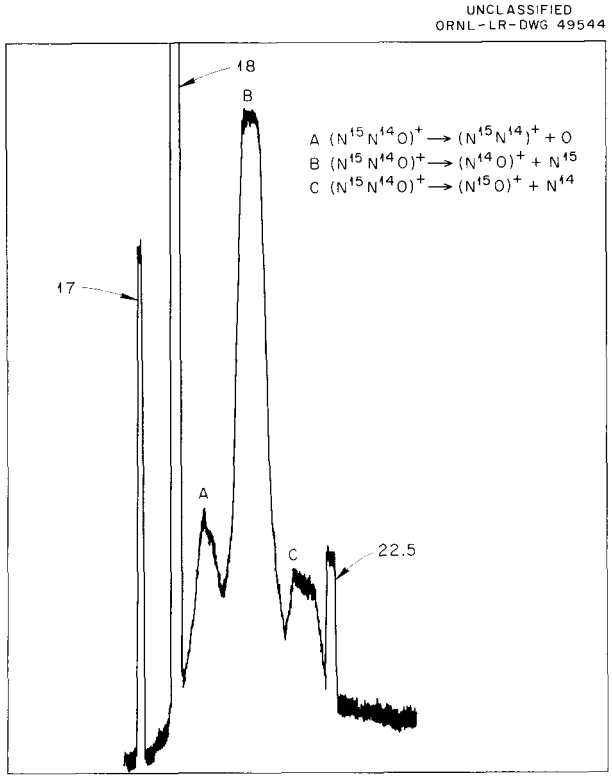

Fig. 10. Mass Spectra of $N^{15}N^{14}O$.

$$(N^{15}N^{14}O)^+ \longrightarrow (N^{15}O)^+ + N^{14} \qquad (3)$$
(apparent $M = 21.4$)

It is interesting to note that reaction (3) must result from the triangular or ring activated complex proposed above to account for the cracking pattern data. Similar patterns were observed for the other three isotopic molecules, with the peaks appearing at the calculated positions. In order to determine whether these metastable transitions were collision-induced or spontaneous, pressure-dependence studies were made. Figure 11 shows the results of one such study with $N^{14}N^{14}O$. It can be seen that the relative intensity of the metastable peak increases somewhat with pressure, indicating some collision-induced transitions. However, the increase is not as the square of the pressure nor does the curve extrapolate to zero pressure as would be expected for a purely collision-induced transition. Thus we conclude that the spontaneous metastable transitions have been observed corresponding to reactions (1), (2), and (3) above. Considering the small number of atoms in nitrous oxide, delayed decomposition is very interesting.

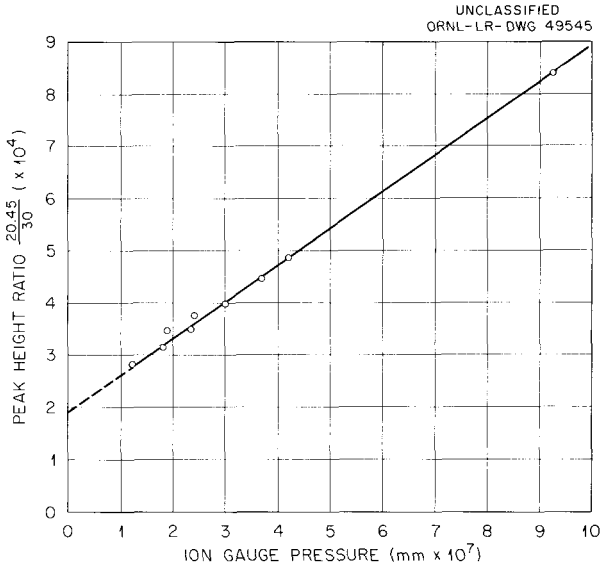

Fig. 11. $N^{14}N^{14}O$ Mass Spectra – Relative Abundance of Peak 20.45/Peak 30 vs Analyzer Ion Gage Pressure.

The data are being assembled and will be submitted for publication.

MASS SPECTROSCOPIC ANALYSES

L. Landau

Routine isotopic mass analyses have been performed on samples of NO, $N^{15}O$, N_2, O_2, CO, CO_2, and BF_3, using a dual-collector, ratio mass spectrometer from Nuclide Analysis Associates.

The NO samples analyzed well for nitrogen isotope ratios, or mass 31/30, but not so well for oxygen isotope ratios, or mass 32/30, because there was always a small O_2 contamination or background at mass 32 which made 32/30 ratios unsatisfactory. By using highly enriched $N^{15}O$ for exchange experiments, the oxygen ratios could be measured very well because they now became the ratios of 33/31, both of which are very clean mass positions. It was subsequently found that NO samples could be analyzed well for both nitrogen and oxygen by sparking the samples at low pressure and converting them to mixtures of N_2 and O_2, which could be analyzed separately.[23]

[23] T. I. Taylor, personal communication; *Separation of Isotopes Annual Report*, NYO-7763 (1959).

The NO, $N^{15}O$, N_2, O_2, CO, and CO_2 samples could all be analyzed by dual collection, simultaneously collecting the heavy isotopic species and the light one and comparing them electronically. Separation factors by this method could generally be reproduced to better than ±0.001.

All of the BF_3 separation factors were obtained by B^{10} and B^{11} peak-height measurements of individual samples. It was not feasible to use dual-collection techniques because of memory effects. The separation factors for BF_3 were generally reproducible to ±0.002.

RADIATION CHEMISTRY

EFFECT OF IONIZING RADIATION ON CATALYSTS

Metals and Elemental Semiconductors

G. E. Moore E. H. Taylor

In contrast to the large changes in catalytic activity produced by high-energy irradiation of inorganic compounds, considerably less effect has been shown by metals, probably because metals cannot store energy through ionization or electronic excitation but only through atomic displacements. Pure copper (99.999%) has been irradiated in the ORR at fast-neutron (>0.75 Mev) doses of about 10^{18}–10^{19} *nvt*, which theoretically should have produced at least 0.05% atomic displacements. Such treatment has produced no detectable alteration in the catalytic activity for the H_2-D_2 exchange. Recently, the catalytic decomposition of formic acid vapor has been used as a probe of surface activity; no alteration in the catalytic activity for this reaction as a result of atomic displacements in the solid has been conclusively demonstrated. It is possible that the perturbations of crystal structure created by fast-neutron bombardment do not detectably influence the surface activity, or that these changes are destroyed before they can be detected by the assaying method, by poisoning, for example.

The relationship between semiconductivity and catalysis has been investigated by studying the kinetics of both the H_2-D_2 exchange and the decomposition of formic acid vapor on intrinsic and on highly doped (*ca.* 10^{20} impurity atoms/cc) germanium. Both intrinsic and *p*-type germanium are more active than *n*-type germanium for the heterogeneous H_2-D_2 exchange (by 10^1–10^4 times over the range 100–350°C) and also for the total rate of decomposition of formic acid vapor (by 10–100 times over the range 100–200°C). Although both CO and CO_2 are decomposition products of formic acid on intrinsic and *p*-type germanium, apparently only CO is produced on *n*-type germanium.

Nonmetals

H. W. Kohn E. H. Taylor

Studies of the effects of ionizing radiations on the catalytic properties of silica gels have been continued, with increasing emphasis on the effects of comparatively low-energy radiations, measurements of *o-p* H_2 conversion (as well as H_2-D_2 exchange and ethylene hydrogenation), studies of exchanges with constituents of the catalyst itself, and the observation of physical changes upon irradiation.

The principal effort still centers about the catalytic activity of silica gel. Neutron-irradiated samples, after annealing at temperatures above 500°C, retain some enhanced activity for H_2-D_2 exchange and extremely rapid activity for *o-p* H_2 conversion, but no activity for ethylene hydrogenation. Samples irradiated with ultraviolet light, as well as with 50- and 250-kv x rays, show enhanced H_2-D_2 exchange activity. Both initial activity and radiation enhancement for H_2-D_2 exchange are related to aluminum impurity content.

The behavior of silica gel during Co^{60} gamma irradiation has been investigated using principally tracer techniques on samples exchanged with D_2O^{18}. Exchange of oxygen gas with oxygen in the gel occurs only during the irradiation, and is very minor. After an irradiation *in vacuo*, small amounts of silanol deuterium will slowly exchange with gaseous hydrogen. Samples irradiated *in vacuo* and then decolorized by the adsorption of deuterium show a rapid exchange of a small amount (~1%) of this deuterium with gaseous hydrogen. The yield for these three processes is small, about 10^{-2} molecule exchanged per 100 ev absorbed by the solid. In contrast to these reactions, if hydrogen is present during the irradiation of a gel deuterated with D_2O, comparatively large amounts of the heavy isotope, corresponding to a yield of 2 molecules exchanged or released per 100 ev absorbed by the gel, are found in the gas phase, and this value increases to about 5 with continued irradiation. The disproportionate amount of D_2 relative to HD found in the gas when poisoned gels are so irradiated indicates a release of molecular deuterium from the gel itself. Gels irradiated *in vacuo* have also shown oxidizing properties towards I^- and Fe^{++} solutions, and reducing properties for Ce^{4+} solutions.

The adsorption of hydrogen by silica gel irradiated *in vacuo* has been followed out to large dosages. The initial yield of hydrogen adsorption sites is 1 H_2 adsorbed per 100 ev absorbed by the gel; the yield drops gradually to a value of ~0.1.

Evacuation experiments have shown that a small amount (~15%) of the hydrogen is adsorbed reversibly. Oxygen adsorption is also observed in irradiated silica gel, not differing greatly in amount and rate from that of hydrogen. For either gas, the observed yield is approximately doubled if the adsorbed gas is present during irradiation instead of being added after the irradiation is done.

The adsorption of gas also affects the physical species produced by the radiation in silica gel, and aids in their identification. Thus the disappearance of color in irradiated impure silica gel during hydrogen adsorption indicates that the color centers are electron acceptors, probably positive holes trapped at impurity centers. Decolorization is also accompanied by a white luminescence, although, since its intensity and spectrum have not been measured, it is not yet clear that this really corresponds to a measure of the energy of adsorption. Similarly, a sharp paramagnetic resonance at $g = 2.0005 \pm 0.0005$ formed by the radiation *in vacuo* is destroyed by the adsorption of oxygen, implying that it is caused by an electron trapped at an oxygen vacancy or at a surface defect. Both color centers and the sharp paramagnetic resonance are destroyed by illumination with ultraviolet light. This seems to be a recombination reaction of positive holes with trapped electrons due to their excitation by the ultraviolet. The fact that ultraviolet not only fails to destroy radiation-enhanced catalytic activity but can also produce catalytic sites in unirradiated gels indicates that there are other point defects as yet undetected which can be responsible for catalytic activity.

RADIATION ENERGY TRANSFER IN MIXTURES OF SOLIDS

A. R. Jones

Energy transfer resulting in chemical change in solid systems has been a difficult subject to approach experimentally. A procedure which exploits the convenience and specificity of infrared absorption techniques has been used to investigate such transfer. It is based upon the facts that alkali halides when exposed to high-energy radiation remain completely transparent over the ordinary analytical region of the infrared, even though they acquire complex absorption spectra in the visible and ultraviolet regions, and that transfer of energy actually occurs to substances suspended in the alkali halides.[1] Thus the pressed alkali halide disk method for the identification and quantitative determination of organic and inorganic solids has become a tool for study of the effect of variation of structure of the receiver on the transfer of energy primarily absorbed by the alkali halide and the effect of various alkali halides on energy transfer to a given receiver.[1] Dibasic acids, $HOOC-(CH_2)_n-COOH$, have been used as chemical indicators in the first case, and nitrate ion in the second.

The rate of the zero-order disappearance of the dibasic acids (as indicated by the decrease in absorption characteristic of the carboxyl group) appeared to be independent of chain length beyond adipic. The shorter members of the series showed behavior characteristic of two opposing effects, with succinic acid appearing as the most stable and glutaric as the least stable homolog. Relative decarboxylation yields for n = 1, 2, 3, 4, 8 are 1.0, 0.64, 1.64, 1.10, 1.10.

In a study of the kinetics of the decomposition of nitrate ion in potassium bromide matrix, it has been found that the effect of adsorbed water on the system becomes negligible for concentrations below 0.001 wt %. The product of the radiolysis of nitrate ion was nitrite ion, which itself underwent decomposition with G values ranging from 0.03 for 0.001 wt % to an apparently constant value of 0.7 for >0.04 wt % KNO_2.

RADIATION CHEMISTRY OF SULFURIC ACID SOLUTIONS

J. W. Boyle

Sulfuric acid is often present in aqueous solutions used in radiation chemistry. Two examples, each a common dosimeter solution, are air-saturated Ce(IV) in 0.4 *M* H_2SO_4 and air-saturated Fe(II) in 0.4 *M* H_2SO_4. The present report deals with yields of the irradiation products from Ce(IV) and Fe(II) solutions as functions of the H_2SO_4 concentration, from 0.4 to 17 *M*. From this study information was obtained about the radiation chemistry of H_2O and H_2SO_4 and about strongly hydrogen-bonded systems in general.

Even though the electron fraction of H_2SO_4 present in 0.4 *M* solutions is as high as 0.037,

[1] A. R. Jones, *Chem. Ann. Prog. Rep. June 20, 1957*, ORNL-2386, p 37–38.

the classical explanation of the 100-ev Ce(III) and Fe(III) yields assumes the only chemical intermediates present are from H_2O:

$$H_2O \rightsquigarrow H,\ OH,\ H_2,\ H_2O_2\ ; \qquad (1)$$

$$G[Ce(III)] = 2G_{H_2O_2} + G_H - G_{OH} = 2.4\ , \qquad (2)$$

$$G[Fe(III)] = 2G_{H_2O_2} + 3G_H + G_{OH} = 15.6\ . \qquad (3)$$

The present study showed that H_2SO_4 also plays a part in the mechanism. In 0.4 M H_2SO_4–Ce(IV) solution there is a small amount of H_2SO_5 present after irradiation which does not react with Ce(IV). In irradiated Fe(II) solutions, H_2SO_5 is not present because H_2SO_5 and Fe(II) react.

Chemical intermediates present in H_2SO_4 solutions under irradiation arise from H_2O and also from H_2SO_4 [Eqs. (1), (4), and (5)]:

$$H_2SO_4 \rightsquigarrow H,\ HSO_4,\ H_2,\ H_2S_2O_8\ , \qquad (4)$$

$$OH + HSO_4 \longrightarrow H_2SO_5\ . \qquad (5)$$

The Ce(III) and Fe(III) yields are then described by Eqs. (6) and (7):

$$G[Ce(III)] = 2G_{H_2O_2} + G_H - G_{OH} - G_{HSO_4}\ , \qquad (6)$$

$$G[Fe(III)] = 2G_{H_2O_2} + 3G_H + G_{OH} + G_{HSO_4} + 2G_{H_2S_2O_8} + 2G_{H_2SO_5}\ . \qquad (7)$$

Peroxysulfuric acids have been shown to be present in low steady-state concentrations in irradiated H_2SO_4.[2] In Ce(IV) solutions, H_2SO_5 and $H_2S_2O_8$ together with molecular H_2 increase linearly with dose because they do not react with Ce(IV) or Ce(III) and are protected from radical attack by the Ce(IV) and Ce(III). In concentrated H_2SO_4 solutions the peroxy acids are produced in appreciable yields. For example in 4.0 M H_2SO_4–Ce(IV) solutions the 100-ev H_2SO_5 yield is approximately 0.4 and the $H_2S_2O_8$ yield is about 0.1.

The results already obtained indicate that molecular products arising from a change in the solvent are probably produced by combination of free radicals supposedly in regions of high ionization density. The products H_2, H_2O_2, and $H_2S_2O_8$ result from combination of like radicals and H_2O, H_2SO_4, and H_2SO_5 from the combination of unlike radicals. The amount of H_2O and H_2SO_4 re-formed cannot be determined, but the H_2SO_5 can be measured and may give an indication as to the amount of "unlike" combinations. It should be possible when this study is completed to evaluate the yields of all the important chemical intermediates over a wide acid range.

RADIOLYSIS OF AQUEOUS METHANE SOLUTIONS

H. Sakurai[3] J. W. Boyle C. J. Hochanadel

Radiolysis of aqueous methane solutions, and also methane solutions with added ceric sulfate or ferric sulfate, indicated that methane reacts readily with OH but not with H. Irradiation of methane solution with gamma rays produced hydrogen with a yield of $G \approx 1$. Methane was depleted with about the same yield, and little or no ethane or hydrogen peroxide was observed. Analysis for other products in solution was not made. Results for radiolysis of aqueous solutions can be interpreted on the basis of initial decomposition of water into H, OH, H_2, and H_2O_2, and the 100-ev yields for gamma irradiation are 2.71, 2.23, 0.45, and 0.71 in neutral solution and 3.63, 2.95, 0.45, and 0.79 in 0.4 M H_2SO_4 solution. The measured hydrogen yield is intermediate between the yield of molecular hydrogen, $G_{H_2} = 0.45$, and the sum $G_{H_2} + G_H \approx 3.2$, the value predicted assuming additional hydrogen is produced by reaction of H atoms with methane. The low hydrogen yield and the very low yield of ethane indicate that the H atom abstraction reaction is unimportant. Scavenging of OH by methane protects H_2 from further reaction. Hydrogen peroxide is removed by reaction either with CH_3 or with H.

In 2×10^{-4} M ceric sulfate solution containing 10^{-3} M methane, ceric ion is completely reduced. The yield remains nearly constant with increased dose. For a solution with no methane present, Ce(IV) is reduced by H and H_2O_2 and the Ce(III) is reoxidized by OH, giving a yield for ceric reduction of 2.36, which is equivalent to $G_H - G_{OH} + 2G_{H_2O_2}$. With added methane the yield is increased to 5.25 in 0.05 M sulfuric acid and

[2] M. Daniels, J. Lyon, and J. Weiss, *J. Chem. Soc.* 1957, 4388.

[3] Guest scientist, December 1958 to July 1959, from Osaka University, Osaka, Japan.

4.15 in 0.4 M acid. Methane reacts with OH to give CH_3, which reduces ceric ion, leading to a maximum yield $G[Ce(III)] = G_H + G_{OH} + 2G_{H_2O_2}$. The low values and the dependence on acid concentration indicate a mechanism similar to the Ce(IV)-H_2 system.[4] The acid competes with CH_4 for OH radicals to give HSO_4, which reacts with Ce(III) but not with CH_4. On this basis the ratios of rate constants for reaction with OH are estimated to be

$$H_2SO_4:H_2:CH_4:Ce(III) = 1:100:350:650 \ .$$

In sulfuric acid solution at pH 2 containing 5×10^{-4} M ferric sulfate and 10^{-3} M methane, Fe(III) is reduced with an initial yield of 2.1 to 4.3. With increased dose a steady state is eventually reached. In absence of methane, no reduction is observed. Again methane reacts with OH to give CH_3, which reduces Fe(III). Iron(III) is also reduced by H, and Fe(II) is reoxidized by H_2O_2. Reaction of Fe(II) with OH is the principal competing reaction leading to a steady state. On the basis of this mechanism the maximum predicted yield is $G[Fe(II)] = G_H + G_{OH} = 4.9$.

THE OH RADICAL YIELD IN THE Co^{60} RADIOLYSIS OF AQUEOUS $NaNO_3$ SOLUTIONS

H. A. Mahlman

The reduction of Ce^{4+} in an 0.8 N H_2SO_4 solution during Co^{60} irradiation has been determined to be equal to

$$2G(H_2O_2) + G_H - G_{OH} + [0.45 - G(H_2)]$$

(see refs 5 and 6), while in the presence of thallous ion,[7]

$$G(Ce^{+++}) = 2G(H_2O_2) + G_H + G_{OH} + [0.45 - G(H_2)] \ .$$

The difference in the cerous yields is equal to $2G_{OH}$. The "direct action effect"[8] upon the added solute, $NaNO_3$, should manifest itself by increasing the $G(Ce^{+++})$ the same amount in both the Ce^{4+}-acid-$NaNO_3$ and Ce^{4+}-acid-$NaNO_3$-Tl^+ systems. Therefore, the difference between the cerous yields should continue to monitor $2G_{OH}$. The G_{OH} was found to be constant and equal to 2.86 in the $NaNO_3$ concentration range 0.1 to 5.0 M. A constant G_{OH} indicates that the total energy absorbed by the solution is effective in decomposing the water solvent. Proposed reactions of OH radical with NO_3^- yield products that reduce Ce^{4+} (HO_2, H_2O_2, and NO_2) (ref 9) and would predict a decreasing G_{OH}. However, a constant G_{OH} indicates that the OH radical does not react with nitrate ion.

HYDROGEN FORMATION IN THE RADIATION CHEMISTRY OF WATER

H. A. Mahlman

Previous studies of Co^{60}-irradiated aqueous sodium nitrate solutions indicated that the NO_3^- lowered the hydrogen yield,[10] $G(H_2)$, and that the $G(H_2)$ observed from solutions less than 1.0 m are a linear function of the $NaNO_3$ thermodynamic activity.[11] As shown in Fig. 12, an extension of these data to 9.1 m indicated two mechanisms of molecular hydrogen formation, as evidenced by two scavenging efficiencies for H atoms – the assumed precursors of molecular hydrogen. One process, designated E_1, is readily affected by scavenging, the interpretation being that the scavenged H atoms originate from the decomposition of excited water molecules (the Samuel-Magee model[12]). The second process, designated E_2, is not readily affected by scavenging; in this case the scavenged H atoms are thought to be originating from electrons reacting with water molecules (the Lea-Gray-Platzman model[13]). Similar results for D_2O solvent are shown in Fig. 12. The $G(H_2)$ from the E_1 process

---

[4] J. W. Boyle and C. J. Hochanadel, *Chem. Ann. Prog. Rep. June 20, 1959*, ORNL-2782, p 28.

[5] A. O. Allen, *Radiation Research* 1, 87 (1954).

[6] H. A. Mahlman, *J. Am. Chem. Soc.* 81, 3203 (1959).

[7] T. J. Sworski, *Radiation Research* 4, 483 (1956).

[8] T. J. Sworski, *J. Am. Chem. Soc.* 77, 4689 (1955).

[9] G. E. Challenger and B. J. Masters, *J. Am. Chem. Soc.* 77, 1063 (1955).

[10] H. A. Mahlman and J. W. Boyle, *J. Chem. Phys.* 27, 1434 (1957).

[11] H. A. Mahlman, *J. Chem. Phys.* 31, 993 (1959).

[12] A. H. Samuel and J. L. Magee, *J. Chem. Phys.* 21, 1080 (1953).

[13] D. E. Lea, *Actions of Radiations on Living Cells*, 2d ed., Cambridge University Press, London, 1955; L. H. Gray, *J. chim. phys.* 48, 172 (1951); H. Fröhlich and R. L. Platzman, *Phys. Rev.* 92, 1152 (1953).

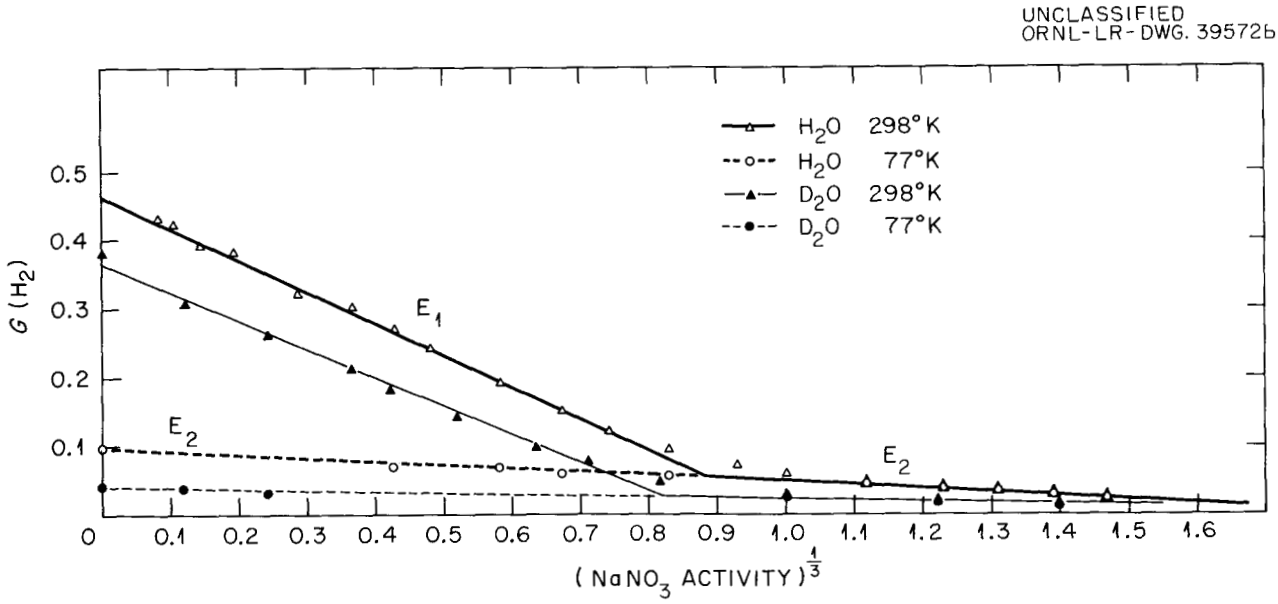

Fig. 12. Hydrogen Yields as a Function of $NaNO_3$ Activity.

is the difference between the total observed $G(H_2)$ and the $G(H_2)$ derived from the E_2 process. The similarity of the $G(H_2)$ by the E_1 processes, 0.36 and 0.33, from H_2O and D_2O, is consistent with the Samuel-Magee model, while the difference in $G(H_2)$ by the E_2 processes, 0.10 and 0.06, from H_2O and D_2O, is consistent with the Lea-Gray-Platzman model.

Figure 12 also presents the $G(H_2)$ observed from the 77°K irradiation of these solutions. The data show that the E_1 process may be eliminated at 298°K by $NaNO_3$ concentrations greater than 1.3 *m* as well as by irradiation at 77°K. Elimination of the E_1 process by irradiation at 77°K probably occurs by the caging effect of the ice matrix, which promotes the back reaction to reform water: $H + OH \rightarrow H_2O$.

KINETICS OF THE ALPHA RADIOLYSIS OF CARBON MONOXIDE[14]

P. S. Rudolph S. C. Lind

The radiolytic decomposition of CO induced by alpha particles appears to be initiated by two reactive species, CO^+ and CO*. Carbon dioxide formed during the reaction depletes the CO^+ by charge transfer. Thus when CO_2 pressure becomes sufficiently high, it is the CO* only which initiates reaction. Figure 13 shows the experimental evidence for these conclusions. Curve *A* (CO only) has a steep initial slope due to both reactive species but levels off to a limiting slope due to CO* only. Line *B* (CO in presence of Ascarite) has the high initial slope of curve *A*, since the CO_2 formed is removed from the reaction field by the Ascarite and, thus, both reactive species continue to react. Line *C* ($CO + CO_2$) has the final limiting slope of curve *A*, since there was added initially sufficient CO_2 to remove all the reactive CO^+ by charge transfer, leaving only CO* to react.

The reaction mechanism suggested is consistent with ionization and photochemical studies in the CO system.

[14] An abstract of a paper to be published in *J. Chem. Phys.* (August 1960).

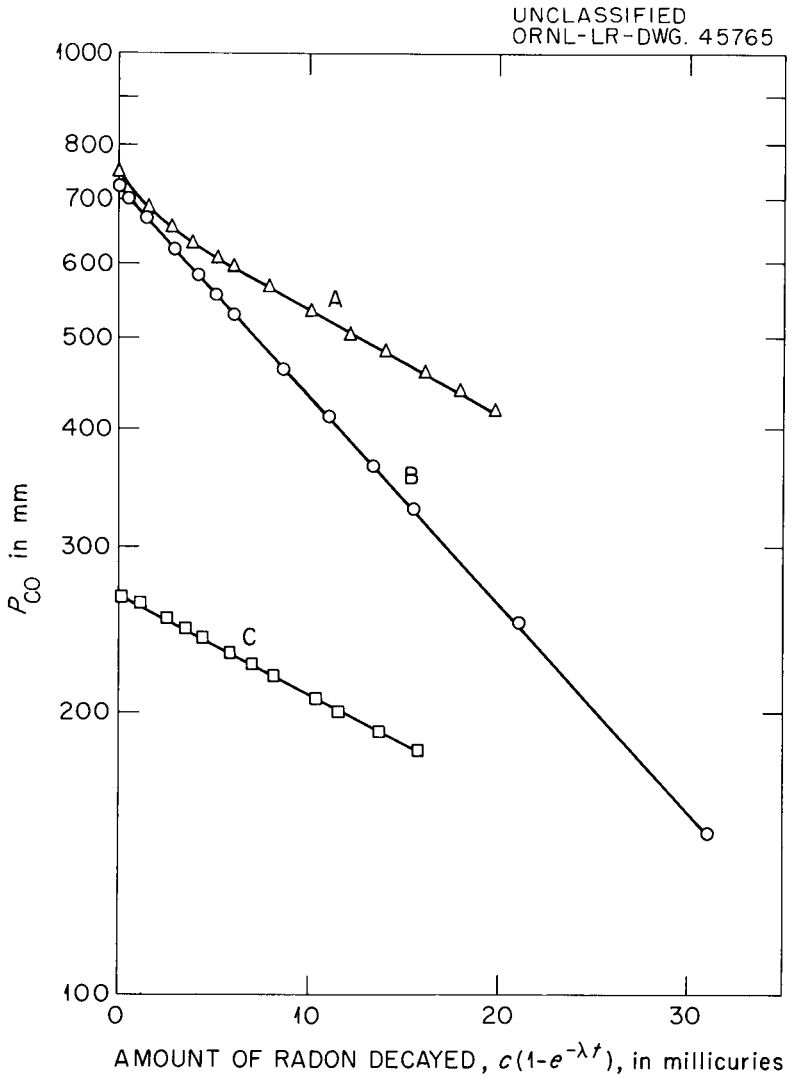

Curve	P^0_{CO} (mm)	$P^0_{CO_2}$ (mm)	Volume (cc)	Initial Radon (mc)		Slope
				Actual, E_0	Normalized, c	
A	748	0	8.43	79.2	21.6	25.1 initial, 11.5 final
*B**	723	0	7.89	160.8	45.8	22.1
C	265	88	7.51	160.0	47.1	10.6

*In the presence of Ascarite.

Fig. 13. The Dependence of CO Pressure on the Amount of Radon Decayed Normalized to a 2-cm-dia Sphere.

ORGANIC CHEMISTRY

THE STEREOCHEMISTRY AND RADIOCHEMISTRY OF THE DEAMINATION REACTION

B. M. Benjamin C. J. Collins

The deamination of stereospecifically phenyl-labeled (+)-1,1-diphenyl-2-amino-1-propanol (I) has previously been examined.[1,2] The radiochemical results were as shown in Chart 1, through which it was demonstrated that whereas the labeled phenyl approached the migration terminus with inversion, yielding (–)-II in approximately 88% yield, the unlabeled phenyl approached the migration terminus with retention, yielding (+)-II in approximately 12% yield. The foregoing results foreshadowed additional experiments concerning the nature of the carbonium ion intermediates in deamination reactions. In particular it appeared possible to gain information with respect to the relative importance of neighboring group participation[3] during these deaminations.

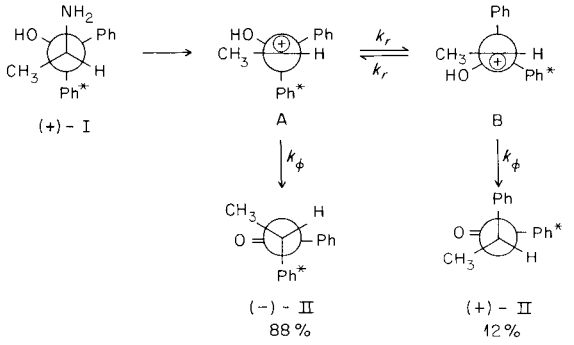

Chart 1

We therefore undertook the stereochemical-radiochemical investigation of (*a*) (+)- and (–)-*erythro*-1,2-diphenyl-1-amino-2-propanol (IV), labeled with C^{14} in the 1-position, and (*b*) (+)-1,1-diphenyl-2-aminopropane (VII) stereoselectively labeled in one of the two phenyls. The syntheses of (–)-IV and of (+)- and (–)-VII are shown in Chart 2.

Because there existed no a priori method of ensuring the total stereoselectivity of the reaction sequence given in Chart 2, we carried

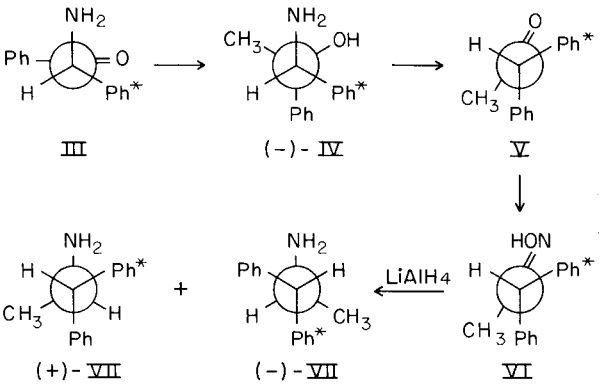

Chart 2

out the experiments illustrated in Chart 3, in order to determine whether or not it would be possible to oximinate the model compound benzhydryl-$^2H_1$ phenyl ketone-C^{14} (XI) and then reduce the oxime (XII) to the amine hydrochloride (XIII) without loss of deuterium. It was reasoned that if the deuterium label of structure XI could survive the reaction sequence XI → XII → XIII, then in all probability the reaction sequence V → VI → VII could also be carried out without racemization of the labeled phenyl. The numbers under the structures of Chart 3 refer to the C^{14} contents of the compounds expressed as relative

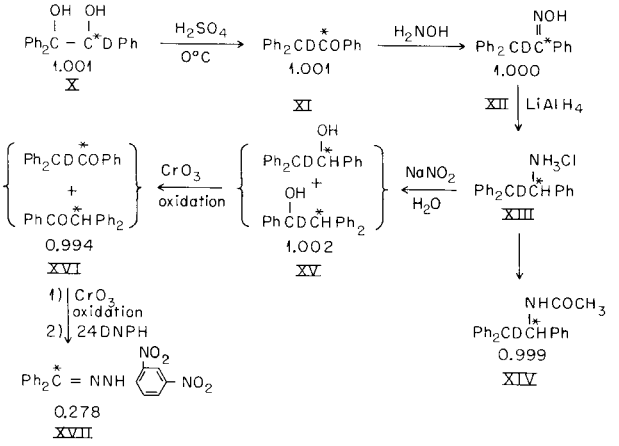

Chart 3

[1] A. McKenzie, R. Roger, and G. O. Wills, *J. Chem. Soc.* **1926**, 779.

[2] B. M. Benjamin, H. J. Schaeffer, and C. J. Collins, *J. Am. Chem. Soc.* **79**, 6160 (1957).

[3] S. Winstein *et al.*, *J. Am. Chem. Soc.* **74**, 1113 (1952).

molar radioactivities. This series of reactions was carried out twice.

In the first run the oximination XI → XIII was performed in very low yield under mild conditions. Infrared analyses of ketones XI and XVI indicated ketone XI to be devoid of hydrogen in the benzhydryl position, whereas ketone XVI contained approximately 26% hydrogen in the benzhydryl position. This is a very good check with the C^{14} data shown in Chart 3, and indicates that no deuterium was lost during the sequence X → XI → XII → XIII → XIV. In the second experiment, higher temperature and higher concentration of base were used during oximination in order to increase the yield of XII. Results of infrared analyses indicated considerable loss of deuterium from XVI (about 55%) in excess of the 28% to be expected on the basis of the C^{14} data. Nuclear magnetic resonance spectra[4] of all of the samples of Chart 3 except XIII indicated approximately 40% loss of deuterium during oximination, but no loss of deuterium during the transformations XII → XIII → XIV. From the NMR data it could be calculated that approximately 25% rearrangement had taken place during the deamination XIII → XV, again in very good agreement with the radiochemical data of Chart 3. We therefore concluded that under sufficiently mild conditions the oximination V → VI should take place without interchange of Ph and Ph*, and that the lithium aluminum hydride reduction VI → VII could be performed also with maintenance of the optical integrity of the benzhydryl position.

Erythro-(+)-IV, *erythro*-(–)-IV, and their corresponding hydrochlorides were synthesized through the action of methylmagnesium iodide upon C^{14}-labeled, racemic aminodesoxybenzoin (+–III), followed by resolution through the (+)-tartrate and (+)-10-camphorsulfonate salts. Through deamination, under conditions previously reported,[2] followed by oximination and reduction (Chart 2), the two enantiomers were converted to the isotope position isomers of (±)-1,1-diphenyl-2-aminopropane (VII) illustrated in Chart 4. From the two racemic mixtures of VII produced, it was possible to isolate α-(+)-VII and β-(+)-VII by resolution through their salts with (+)-camphoric and (+)-camphorsulfonic acids.

[4]Performed by Varian Associates, Inc., Pasadena, Calif.

The absolute configurations of *erythro*-(+)- and *erythro*-(–)-IV were demonstrated through the reactions shown in Chart 5, L-(–)-2-amino-1,1,2-triphenylethanol having previously been related to L-(+)-phenylglycine.[5] The configuration of L-(+)-glycine has been reported by Ingold *et al.*[6] and is confirmed by the present work when considered in conjunction with the findings of other investigators.[5,7] The configurations of (+)- and (–)-1,1-diphenyl-2-aminopropane (VII) are deduced from the conversions of α-(+)-VII and of β-(+)-VII,

[5]A. McKenzie and A. C. Richardson, *J. Chem. Soc.* **123**, 79 (1923); A. McKenzie and G. O. Wills, *J. Chem. Soc.* **127**, 283 (1925).

[6]B. C. Hibbin, E. D. Hughes, and C. K. Ingold, *Chem. & Ind.* (London) **1954**, 933.

[7]G. Drefahl and H. Crahmer, *Chem. Ber.* **91**, 745–50 (1958).

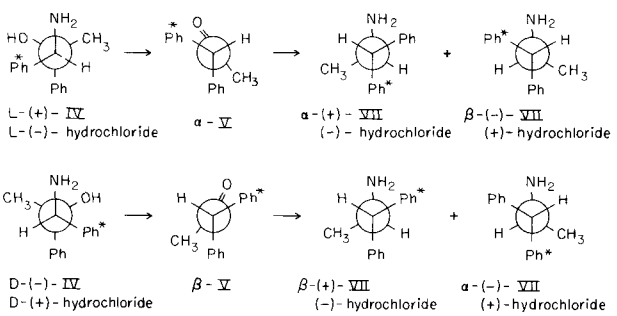

Chart 4

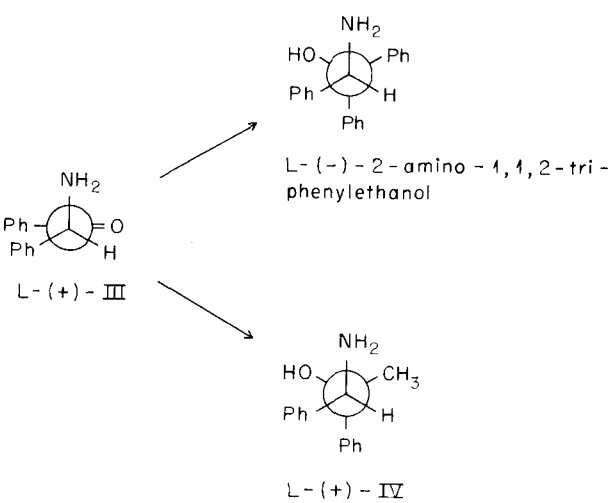

Chart 5

upon deamination, to *threo*- and *erythro*-1,2-diphenylpropanol-1 (VIII) of known configuration[8] (see Chart 6). The conditions for deamination were those previously[2] employed.

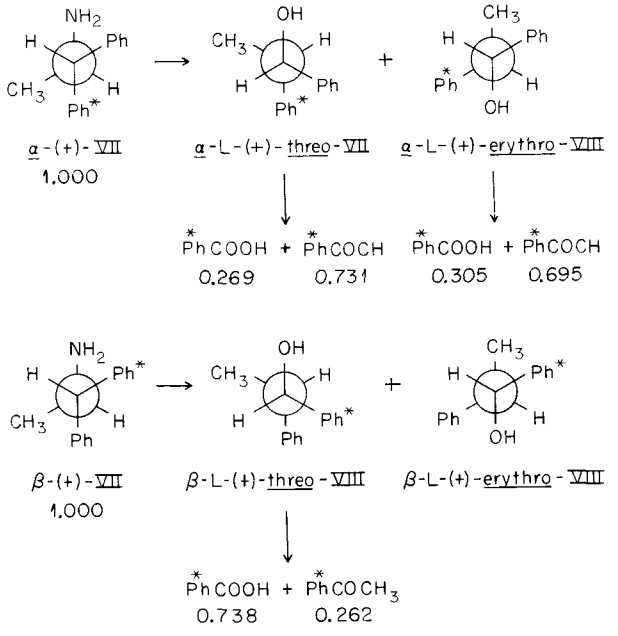

Chart 6

The positions of radioactivity in the enantiomers of VII are deduced from the experimental results shown in Chart 6, in which the molal radioactivities of reactants and degradation products are shown under the appropriate structures. The isotope-dilution method was employed to determine that (+)-VII upon deamination yielded (+)-*threo*-VIII and (+)-*erythro*-VIII in combined yield of 65%, and in the ratio of 5.2:1. Further, there was not more than 1% of racemic *threo*-VIII formed during the deamination, as shown also by the isotope-dilution method. Determination of racemic *erythro*-VIII failed because of the limited yield of the *erythro*-isomer. The degradative studies of Chart 6 indicate, however, that the (+) forms of *threo*- and *erythro*-VIII obtained upon deamination of α-(+)-VII possess almost the same C^{14} distributions, and we deduce therefrom that in all likelihood no significant amount of racemic *erythro*-VIII was formed upon deamination of α-(+)-VII.

Next, *threo*- and *erythro*-1-amino-1-phenyl-2-*p*-tolylpropanol-2 (IX) were synthesized through the action of *p*-tolylmagnesium bromide and methylmagnesium bromide, respectively, upon the appropriate α-aminoketones. Each racemic mixture was resolved through its salt with (+)-tartaric, (+)-10-camphorsulfonic, or (+)-camphoric acid. The configurations of (+)- and (–)-*erythro*-IX and (+)- and (–)-*threo*-IX were related to D-(–)-phenylglycine as shown in Chart 7. The two enantiomers of *erythro*-IX were then subjected to deaminating conditions, and the isotope-dilution method was employed to determine the relative yields of (+)- and (–)-*p*-methylbenzhydryl phenyl ketone (XVII). The results are given in Table 16, and were calculated from the experimental data by the method of Berson and Ben-Efraim.[9]

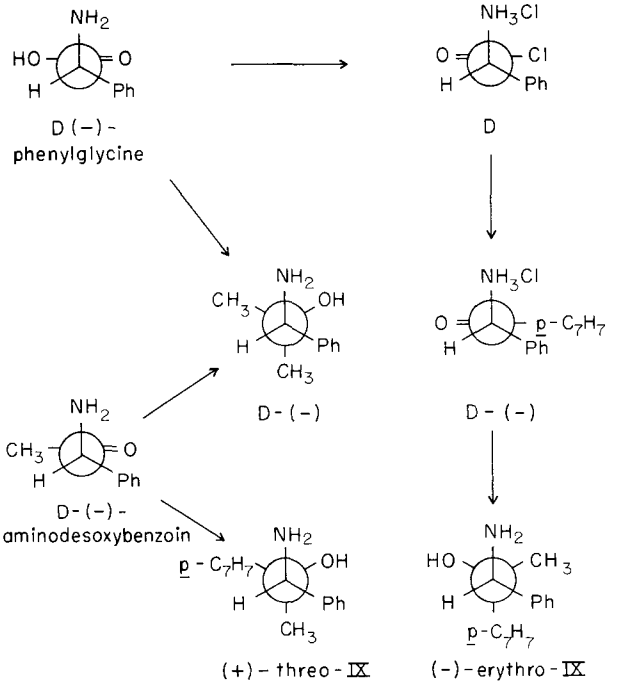

Chart 7

Finally, in one experiment, (+)-*threo*-IX was also subjected to conditions of deamination. The combined yield of (+)- and (–)-XVIII was 83%. From the specific rotation of the oily material it was calculated that, after separation from approximately 20% hydroxylic material, the

[8] F. A. Abd Elhafez and D. J. Cram, *J. Am. Chem. Soc.* **74**, 5849 (1952).

[9] J. Berson and D. A. Ben-Efraim, *J. Am. Chem. Soc.* **81**, 4084 (1959).

Table 16. Determination of Per Cent Racemization During the Deamination of (+)- or (–)-IX

Experiment No.	Reactant	Yield of Product (%)	
		(+)-XVIII	(–)-XVIII
1	(+)-IX [(–)-hydrochloride]*	70.4	29.6
2	(+)-IX [(–)-hydrochloride]*	76.5	23.5
3	(–)-IX [(+)-hydrochloride]**	25.5	74.5
4	(–)-IX [(+)-hydrochloride]**	25.4	75.6
	Average inversion	74.3 ± 2.0	
	Average retention	25.7 ± 2.0	

*Reactants radioactive; combined yields of (+)- and (–)-XVIII, 80%.

**Diluents radioactive.

ketonic fraction consisted of approximately 58% (+)-IV and 42% (–)-IX.

The ketonic products of all deaminations reported in this paper were shown to be resistant to further racemization under the conditions of deamination employed.

The present data allow the following conclusions:

1. The data of Chart 3 indicate that in all probability the reaction sequence V → VI → VII should proceed without racemization, or "scrambling" of the labeled and unlabeled phenyls. Since the per cent racemization of the *p*-methylbenzhydryl methyl ketone (XVIII) produced upon deamination of optically active *erythro*-1-amino-1-phenyl-2-*p*-tolylpropanol-2 (IX) (Table 16) is experimentally identical with the C^{14} distributions shown in the degradative sequences of Chart 6, we consider these data as excellent evidence that *erythro*-(+)-IV and *erythro*-(–)-IV suffer deamination to yield ketone V in which the C^{14} is distributed between the two phenyls in the ratio 73:27 (see Charts 4 and 6). This means that whereas during the deaminations of α-(+)-VII and β-(+)-VII, phenyl migration takes place *only* with inversion and only through *trans* transition states, the deaminations of L-(+)-IV, D-(–)-IV, and (–)-*erythro*-IX proceed with aryl migration in which the relative importance of *trans* and *cis* transition states are in the ratio of about 3:1.

2. The close agreement between the radiochemical distributions in α-L-(+)-*threo*-VIII and α-L-(+)-*erythro*-VIII (Chart 6) demands the presence of open carbonium ions in the deamination of VII. This statement follows, for since the *threo* and *erythro* products possess the same radiochemical distribution, they must therefore have arisen from a common ionic precursor, whose carbonium center was capable of being attacked from either side. If bridged ions were the sole intermediates, no *erythro*-VIII should be produced.

3. The deaminations of the *erythro* isomers of IV and IX have been shown to proceed through both *trans* and *cis* transition states, with the *trans* transition state favored by an approximately threefold margin. One would expect the *trans* transition state to be of lower potential energy than the *cis*, even without participation.[3] Since the *cis* transition state is further hindered by the requirement that its migrating aryl group proceed to the same side of the migration terminus originally bonded to nitrogen, it thus follows that during the deaminations of IV and IX neighboring group participation[3] in the scission of the carbon-nitrogen bond cannot be of great importance.

4. Finally, the data cited concerning the deamination of (+)-*threo*-IX seem to indicate retention of configuration through a mechanism in which the *p*-tolyl group migrates to the same side of the migration terminus which was originally bonded to nitrogen. Since the configurations of the No. 1 carbons (bonded to the amino groups) of (+)-*threo*-IX and (–)-*erythro*-IX are identical (see Chart 7), both aminoalcohols should yield upon deamination *p*-methylbenzhydryl methyl ketone (XVIII) of the same sign of rotation, providing the *p*-tolyl group in both cases migrates

with predominant inversion. Since IX yields (+)-ketone, whereas (+)-*threo*-IX yields (–)-ketone, it is presumed that *threo*-IX yields predominantly that product whose configuration with respect to the No. 1 carbon of the reactant is unchanged.

THE SECONDARY C^{14}-C^{12} ISOTOPE EFFECT

V. F. Raaen A. K. Tsiomis[10]
C. J. Collins

We wish to report the direct measurement of a secondary isotope effect k^*/k of 1.008 ± 0.001 in the formation, at 0°C, of the 2,4-dinitrophenylhydrazone of (aceto-2-C^{14})-phenone. An expression,

$$\ln x = \left(\frac{k^*}{k} - 1\right) \ln(1 - f) + \ln \frac{k^*}{k} \quad , \qquad (1)$$

relating the ratio x of the differentials of the fractions of labeled to unlabeled molecules as a function of the isotope effect k^*/k and the fraction of reaction, f, was derived by Downes[11] for homocompetitive first-order reactions, and was recently employed[12] in this laboratory to provide plots for several values of k^*/k. Some years ago one of us[13] obtained presumptive evidence for small secondary C^{14} isotope effects during reactions in which the C^{14} label was apparently not in a position involved in the primary bond-making or bond-breaking process. Since the precision of the radioactivity measurements was very close to the magnitude of the suspected isotope effects, however, it was not possible to state with assurance that these effects were real. From the plots[12] previously mentioned it seemed possible to study such small secondary isotope effects, provided quantitative reactions could be carried out in such a way as to allow removal of small aliquots (1–2%) of reaction at known fractions f of completion. Such a reaction is the formation, at 0°, of acetophenone-2,4-dinitrophenylhydrazone:

The reaction was carried out by the addition of successive aliquots of standardized 2,4-dinitrophenylhydrazine hydrogen sulfate solutions, cooled to 0°C, to a cooled alcoholic solution containing a carefully weighed quantity of methyl-labeled acetophenone. After each addition sufficient time was allowed to ensure complete precipitation of the derivative. The precipitate was filtered, and to the filtrate was added the next aliquot of reagent solution. The process was repeated until all of the acetophenone had undergone reaction. Each fraction was crystallized four to six times from tetrahydrofuran-ethanol mixtures and then dried *in vacuo*; all had constant melting points of 250°C. Given in Table 17 are the pertinent data, including radioactivity assays[14] of each sample. The reaction was shown to be nonreversible under the conditions employed. The data have been programmed for the IBM-704 computer through a nonlinear least-squares code[15] which will be used to find the best fit for Eq. (1). For the present a graphical integration of the data have given a value for the isotope effect k^*/k of 1.008 ± 0.001.

SUBSTITUTED TETRAHYDROPYRANS

B. M. Benjamin J. B. Christie[16]

The Grignard reaction between allylmagnesium bromide and benzaldehyde gives principally

[10] International Cooperation Agency participant from Thessaloniki, Greece.

[11] A. M. Downes, *Australian J. Sci. Research* **5A**, 521 (1952).

[12] C. J. Collins and M. H. Lietzke, *J. Am. Chem. Soc.* 81, 5379 (1959).

[13] V. F. Raaen, unpublished work.

[14] The method employed was the dry-combustion method of B. M. Tolbert, *Chemistry Division Quarterly Report [for] June, July, and August, 1956*, UCRL-3595, p 12.

[15] We are indebted to M. H. Lietzke for writing the code and for analyzing the data with the IBM-704 computer.

[16] Oak Ridge Institute of Nuclear Studies.

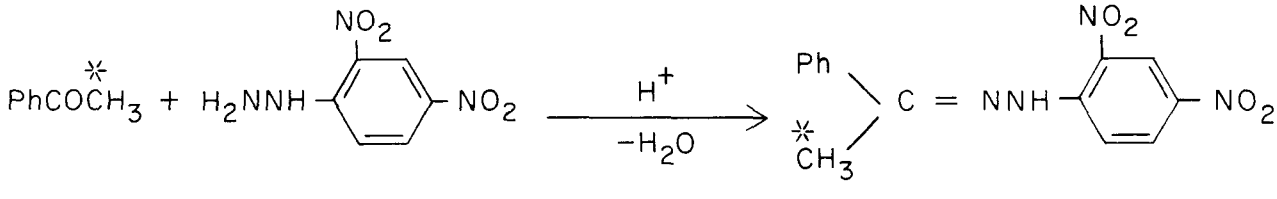

Table 17. Radioactivity Assays of (Aceto-2-C^{14})-phenone-2,4-dinitrophenylhydrazone Fractions Taken During Successive States of Reaction

Fraction Taken	f (midpoint)	Molar Radioactivity (mc/mole)
$\times 10^{-2}$		
0–2.05	0.0103	5.711 ± 0.006
2.05–63.72	0.324	5.710 ± 0.010
63.72–65.85	0.6479	5.641 ± 0.019
65.85–86.38		
86.38–88.50	0.8744	5.620 ± 0.000
88.50–94.62		
94.62–99.66	0.9564	5.582 ± 0.012
96.66–98.16	0.9741	5.549 ± 0.010
98.16–99.20	0.9868	5.517 ± 0.036
99.20–99.82	0.9951	5.477 ± 0.001
99.82–100.00	0.9991	5.350 ± 0.019

allylphenylcarbinol.[17] During a study of the reaction it was found that when the reaction complex was hydrolyzed with ammonium chloride a small amount of high-boiling residue was obtained in addition to the expected carbinol. When hydrolysis was done with strong sulfuric acid a solid melting at 118°C was obtained. This compound was identified as a bromo derivative of 2,6-diphenyltetrahydropyran (I) which results from the addition of two molecules of benzaldehyde to the original allylic system. The reaction was repeated under various conditions but the results were not consistent. It was shown in the following way that the principal product, allylphenylcarbinol, was reacting with a second molecule of excess benzaldehyde during acid hydrolysis. An equimolar mixture of pure allylphenylcarbinol and benzaldehyde was treated with hydrobromic acid to produce an excellent yield of I. Furthermore, the latter reaction occurs with a variety of acid catalysts, and the nucleophilic portion of the catalyst mixture adds to the tetrahydropyran ring. The catalytic conditions used and the products obtained are listed in Table 18.

Proof of the structure of one of the products, compound II, obtained with sulfuric acid catalyst, was accomplished by independent synthesis. Thus *cis*-2,6-diphenyltetrahydro-1,4-pyrone was prepared[18] and reduced with lithium aluminum hydride to give a carbinol identical with II. Oxidation of II gave *cis*-2,6-diphenyltetrahydro-1,4-pyrone. Therefore compound II was shown to be 4-hydroxy-2,6-diphenyltetrahydropyran with the phenyls *cis* to each other. Since no trace of the compound with the phenyls *trans* to each other was found, it is assumed that the acid-catalyzed reaction between allylphenylcarbinol and benzaldehyde takes place stereospecifically.

An analogous reaction[19] involving the addition of two molecules of aldehyde to benzylmagnesium bromide was studied in more detail by Siegel,[20] who explained the double addition product as a consequence of an abnormal Grignard reaction. The normal addition product is phenylbenzylcarbinol and the "abnormal" product is substituted isochromane (a benzene ring fused to a dihydropyran ring). Since the benzyl system sometimes has chemical properties similar to the allyl system it seemed likely that the second molecule of aldehyde could add to phenylbenzylcarbinol by an acid-catalyzed mechanism. This possibility was investigated by treating a mixture of phenylbenzylcarbinol and benzaldehyde with 9 *M* sulfuric acid. The reaction product melted at 130°C and was not identical with Siegel's abnormal product[20] of melting point 110°. When the latter reaction was catalyzed by acetic acid containing sulfuric acid, an unidentified oily product resulted. The reaction is currently under further investigation.

[17] D. Klimenko, *J. Russ. Phys.-Chem. Soc.* **43**, 212 (1911).

[18] R. Cornubert and P. Robinet, *Bull. soc. chim. France* [5]1, 90 (1934).

[19] H. Rupe, *Ann. Chem., Liebigs*, **402**, 161 (1913); J. Schmidlin and A. Garcia-Banus, *Ber. deut. chem. Ges.* **45**, 3193 (1912).

[20] W. G. Young and S. Siegel, *J. Am. Chem. Soc.* **66**, 356 (1944); S. Siegel, W. M. Boyer, and R. R. Jay, *J. Am. Chem. Soc.* **73**, 3237 (1951); S. Siegel, S. K. Coleman, and D. R. Levering, *J. Am. Chem. Soc.* **73**, 3163 (1951).

Table 18. Products of the Acid-Catalyzed Reactions of Allylphenylcarbinol and Benzaldehyde

Reaction No.	Catalyst	Product	Melting Point (°C)
1	9 *M* H_2SO_4 + $MgBr_2$*	(I) 4-Bromo-2,6-diphenyl-tetrahydropyran	118
2	37% aqueous HBr		
3	Gaseous HBr		
4	9 *M* H_2SO_4	(II) 4-Hydroxy-2,6-diphenyl-tetrahydropyran	112
		(III) **	150 with decomposition
5	85% H_3PO_4	(IV) **	140 with decomposition
6	37% aqueous HCl	(V) 4-Chloro-2,6-diphenyl-tetrahydropyran	110
7	47% aqueous HI	(VI) 4-Iodo-2,6-diphenyl-tetrahydropyran	130
8	CH_3COOH and H_2SO_4	(VII) 4-Acetoxy-2,6-diphenyl-tetrahydropyran	90
		(III) **	150 with decomposition

*Equimolar quantities of allylphenylcarbinol and benzaldehyde were dissolved in a little ether and mixed with the acid catalyst. After 30 min to an hour the product was extracted with ether and worked up with the appropriate solvent.

**The products have not been completely identified.

THE RELATIVE IONIZATION CONSTANTS OF FORMIC ACID AND FORMIC-*d* ACID AT 24.0 ± 0.5°C

G. A. Ropp

Because of the recent interest in secondary deuterium isotope effects,[21] the ratio of the ionization constant of formic acid to that of formic-*d* acid in aqueous solution at 24.0 ± 0.5°C was measured.

Halevi and Nussim[22] reported that the two deuterium atoms in α,α-dideuterophenylacetic acid, $C_6H_5CD_2COOH$, lowered the ionization constant of phenylacetic acid about 12% at 25°; the ionization constant of α-deuterophenylacetic acid, $C_6H_5CHDCOOH$, should therefore be about 6% smaller than that of phenylacetic acid. Halevi[23] suggested that the measured effect of deuterium on the ionization constant is due to a greater *inductive electron release* of a deuterium atom on the electron displacement toward the oxygen atoms of the carboxyl group as compared with a hydrogen atom. The *inductive effect* of a substituent (in this case a deuterium atom) is well known to increase markedly as the substituent is moved closer to the reaction center.[24] Since the deuterium atom in formic-*d* acid is one atom closer to the oxygen atoms than is the deuterium atom in α-deuterophenylacetic acid, a greater lowering of the ionization constant by deuterium substitution would accordingly be expected for formic-*d* acid than for α-deuterophenylacetic acid. From the 6% lowering of the ionization constant in the latter acid, a lowering of the ionization constant of formic-*d* acid of at least 15% would be predicted[24] if the influence of deuterium in each acid were exerted *solely through an inductive mechanism.*

[21]Symposium on Hyperconjugation, University of Indiana, June 1958.

[22]E. A. Halevi and M. Nussim, *Bull. Research Council Israel* 5A, 263 (1956).

[23]E. A. Halevi, *Tetrahedron* 2, 175 (1957).

[24]G. Branch and M. Calvin, *The Theory of Organic Chemistry*, p 203, Prentice-Hall, New York, 1941.

Experimental

Formic-*d* Acid. – Formic-*d* acid samples of >95% purity were synthesized by deuterolysis of sodium cyanide. Formic acid, cp 98–100%, was used in three titrations. In two titrations formic acid of >95% purity, prepared by hydrolysis of sodium cyanide, was used. Since the hydrolysis and the deuterolysis were carried out in the same way, the formic acid prepared from cyanide served as a control to demonstrate that the observed difference between the ionization constant of formic acid and that of formic-*d* acid was not due to a difference in methods of preparing the two acids.

Titrations. – For each determination a 10-λ sample of acid was dissolved in 15 ml of freshly boiled distilled water and titrated with *N*/100 sodium hydroxide in a laboratory where the temperature was maintained at 24.0 ± 0.5°C. The Beckman model M pH meter used was checked at frequent intervals against a standard buffer solution of pH = 4.00. The pH at 50% neutralization from the complete titration curve was taken to be equal to pK_a (ref 25). This method does not give a highly accurate estimate of either ionization constant individually. However, it is reasonable to assume that most of the error inherent in the method should cancel in the calculation of the ratio of the ionization constants of formic acid and formic-*d* acids for two reasons. First, care was taken to treat both acids in identically the same manner experimentally; second, formic acid and formic-*d* acid are very nearly identical in many of their physical and chemical properties.

Table 19 presents the measured pH values, their means, and the 95% confidence intervals of the means.

[25]This method was suggested by G. H. Cartledge.

Results and Discussion

From the data of Table 19,

$$\log K_a(\mathrm{H}) - \log K_a(\mathrm{D}) = 0.025 \pm 0.012 \text{ (95\% C.I.)}$$

and

$$\frac{K_a(\mathrm{H})}{K_a(\mathrm{D})} = 1.06 \pm 0.03 \ .$$

The difference between the free energies of ionization for the two isotopic species is

$$\Delta F(\mathrm{H}) - \Delta F(\mathrm{D}) = -2.303\,RT\,(0.025 \pm 0.012)$$

$$= -34 \pm 16 \text{ cal/mole} \ .$$

Since the deuterium in formic-*d* acid lowers the ionization constant only about 6%, the isotope effect is hardly greater than the isotope effect due

Table 19. pH Values of Formic Acid and Formic-*d* Acid at Half-Neutralization Point at 24.0 ± 0.5°C

Source of Acid	pH	
	HCOOH	DCOOH
From hydrolysis of NaCN	3.715	
Batch 1 from deuterolysis of NaCN		3.725
98% cp chemical	3.70	
Batch 2 from deuterolysis of NaCN		3.745
98% cp chemical	3.71	
Batch 2 from deuterolysis of NaCN		3.73
From hydrolysis of NaCN	3.70	
Batch 2 from deuterolysis of NaCN		3.72
98% cp chemical	3.71	
Batch 3 from deuterolysis of NaCN		3.74
Mean values and 95% C.I.	3.707 ± 0.006	3.732 ± 0.010

to the substitution of one deuterium atom on the alpha carbon in phenylacetic acid. It is therefore reasonable to conclude that the anomalously large effect of deuterium substitution in phenylacetic acid[22] *is exerted mainly through some mechanism other than the inductive mechanism* proposed by Halevi. It may be that deuterium substitution on the alpha carbon atom of phenylacetic acid exerts its effect on the ionization constant by a direct interaction through space between the deuterium atom and the oxygen atoms of the carboxyl group. Hyperconjugation involving the deuterium atom may also play a part. Assuming either of these mechanisms or a combination of both, the results reported by Halevi and Nussim[22] are not inconsistent with the results reported here.

DEUTERIUM ISOTOPE EFFECTS IN PHOTOCHEMICAL REACTIONS OF FORMIC-*d* ACID BY USE OF C^{14}

G. A. Ropp W. A. Guillory[26]

The usefulness of measured values of primary and secondary deuterium kinetic isotope effect ratios in the study of organic reactions is well known. However, measurement of such ratios by direct methods is sometimes difficult. An indirect method which can be used to circumvent difficulties in some cases is illustrated by the determination of the primary deuterium isotope effects in the following vapor-phase reactions:

$$HCOOH + Cl_2 \xrightarrow[\text{light}]{\text{visible}} 2HCl + CO_2 \qquad (1)$$

and

$$HCOOH + Br_2 \xrightarrow[\text{light}]{\text{visible}} 2HBr + CO_2 \qquad (2)$$

For the evaluation of k_D/k_H, the ratio of specific rate constants for reaction of formic-*d* acid and formic acid, a 50:50 mixture of DCOOH and $HC^{14}OOH$ was added to enough chlorine (or bromine) to effect reaction of approximately 5% of the mixture of acids. The carbon-14 dioxide produced was precipitated as barium carbonate-C^{14}, the specific activity S_5 of which was then determined by radioassay of the gas released when a sample was acidified. The specific activity S_{100} of the barium carbonate-C^{14} representing 100% reaction of a portion of the 50:50 mixture of DCOOH and $HC^{14}OOH$ with excess chlorine was also determined.

The equation

$$\frac{k_D}{k_H} = (R + 1)\frac{S_{100}}{S_5} - R \ , \qquad (3)$$

where R is the molar ratio of $HC^{14}OOH$ to DCOOH in the mixture of acids used, was derived making the reasonable assumption that the C^{14} isotope effects in reactions (1) and (2) are negligibly small in comparison with the deuterium isotope effects. Using Eq. (3), k_H/k_D values, 2.0 and 2.7, were calculated for reactions (1) and (2) respectively.

An earlier study[27] showed that reaction (1) was accompanied by a much smaller C^{13} kinetic isotope effect than reaction (2). This was taken as an indication that the carbon-hydrogen bond is stretched more in the transition state for reaction (2) than for reaction (1). The presently reported difference between the corresponding deuterium isotope effects is less pronounced, though in the same direction as the difference between the C^{13} effects. A reasonable conclusion is that bromine-hydrogen bonds formed in the transition state for reaction (2) largely compensate the stretching of the carbon-hydrogen bond.

MASS SPECTROMETRIC TEST FOR AN INTERMEDIATE IN A PHOTOCHEMICAL REACTION INVOLVING CHLORINE

G. A. Ropp C. E. Melton
P. S. Rudolph

During the course of studies aimed at developing techniques of direct application of a research mass spectrometer to problems in chemistry and radiation chemistry, a brief investigation was made of the photochemical reaction[27,28] of formic acid with chlorine:

$$\text{Monomer: } HCOOH + Cl_2 \xrightarrow[\text{light}]{\text{visible}} 2HCl + CO_2$$

$$\text{Dimer: } \tfrac{1}{2}(HCOOH)_2 + Cl_2 \xrightarrow[\text{light}]{\text{visible}} 2HCl + CO_2$$

[26]Research apprentice, summer 1959, from Dillard University, New Orleans, La.

[27]G. A. Ropp, C. J. Danby, and D. A. Dominey, *J. Am. Chem. Soc.* **79**, 4944 (1957).

[28]H. L. West and G. K. Rollefson, *J. Am. Chem. Soc.* **58**, 2140 (1936).

The technique used was similar to that employed by Zemeny and Burton[29] and by Kistiakowsky and Kydd.[30] The earlier investigators[28] had reported evidence for the presence of measurable quantities of a reaction intermediate which, they suggested, was probably chloroformic acid, ClCOOH. However, chloroformic acid is known to be highly unstable, presumably because its structure includes a chlorine atom and a hydroxyl group attached to the same carbon atom. For this reason it seemed improbable to the present investigators that chloroformic acid could have been present as an intermediate in sufficient concentration to explain the experimental data of West and Rollefson.[28]

The reaction was therefore carried out in a 25-ml reaction chamber just before the gold foil leak leading into the ionization chamber of a research mass spectrometer.[31] The expansion bulb and the exit tube leading to the reaction chamber were always kept dark. With the light on, the progress of the reaction was readily followed by the changes in the mass spectrometric peaks corresponding to reactants and products.[32] Mass spectrometric peaks corresponding to chloroformic acid might have been expected if that compound had been formed during the reaction. Although chloroformic acid has not been isolated, a structurally similar chlorine compound, phosgene, yields the positive ion $(COCl_2)^+$ upon electron bombardment in the mass spectrometer.[33] However, no measurable concentration of the ions [$(Cl^{35}COOH)^+$ and $(Cl^{37}COOH)^+$, masses 80 and 82; $(Cl^{35}COO)^-$ and $(Cl^{37}COO)^-$, masses 79 and 81] that would be expected, on the basis of previous studies of the positive spectrum of phosgene[33] and the positive and negative spectra of formic acid,[34] to arise from chloroformic acid was found. Instead a series of ions including

$(Cl^{35}HCOOH)^-$ and $(Cl^{37}HCOOH)^-$,
masses 81 and 83

$(Cl^{35}Cl^{35}HCOOH)^-$ and $(Cl^{35}Cl^{37}HCOOH)^-$,
masses 116 and 118

$[Cl^{35}Cl^{35}(HCOOH)_2]^-$ and $[Cl^{35}Cl^{37}(HCOOH)_2]^-$,
masses 162 and 164

were observed with the light either on or off. These ions were very probably produced by negative-ion–molecule reactions[35] between ionized chlorine and monomeric and dimeric formic acid molecules.

The extreme sensitivity of the research mass spectrometer and its adaptability for studying both positive and negative ions make it highly unlikely that an intermediate that could be detected by the methods employed by West and Rollefson would be overlooked in the study described here.

The presently described technique could be useful in examining other photochemical reactions for intermediates. The only proviso is that the intermediate being looked for be capable of passing through the gold foil leak and yielding, under electron bombardment, representative positive or negative ions stable enough to reach the collector. Any species detected *only with the light on* could reasonably be attributed to some molecule or radical resulting from a photochemical process. Since natural chlorine contains 75% Cl^{35} and 25% Cl^{37}, an ion containing one atom of chlorine can be identified readily because it gives rise to twin peaks, two mass units apart, with heights in 3:1 ratio. A similar characteristic pattern is observed if the ion contains two or more chlorine atoms or if it contains one or more bromine atoms.[31] Ions containing hydrogen can often be identified with the help of deuterium labeling.

---

[29] P. D. Zemeny and M. Burton, *J. Phys. & Colloid Chem.* **55**, 949 (1951).

[30] G. B. Kistiakowsky and P. H. Kydd, *J. Am. Chem. Soc.* **79**, 4825 (1957).

[31] C. E. Melton, G. A. Ropp, and P. S. Rudolph, *J. Chem. Phys.* **29**, 968 (1958).

[32] Under controlled conditions relative reaction rates have been estimated by this method with sufficient precision to permit calculation of deuterium isotope effect ratios, k_H/k_D, when samples of formic acid and formic-*d* acid were used alternately. Details were presented in *Chem. Ann. Prog. Rep. June 20, 1959*, ORNL-2782, p 78.

[33] J. D. Morrison and A. J. C. Nicholson, *J. Chem. Phys.* **20**, 1021 (1952).

[34] G. A. Ropp and C. E. Melton, *J. Am. Chem. Soc.* **80**, 3509 (1958).

[35] C. E. Melton and G. A. Ropp, *J. Am. Chem. Soc.* **80**, 5573 (1958).

The present method can also be applied in tests for intermediates in other types of reactions than those induced by visible light. The source of visible light can, for example, be replaced by a source of ultraviolet light, by a source of ionizing radiation, by a hot filament, or by a catalytic surface in the reaction chamber, etc., with minor alterations of the apparatus. However, recent work with a modified ion source has demonstrated that *the research mass spectrometer can be operated with the pressure as high as 1 mm inside the ionization chamber.*[36] With such a modified ion source, it should be possible to carry out a photochemically induced reaction *inside the ionization chamber* by using a light pipe. With this arrangement it should be possible to detect intermediates such as free radicals that might be too unstable to pass through the gold foil leak of an ordinary mass spectrometer.

CATIONIC COMPLEXES OF DIBUTYLPHOSPHORIC ACID

W. H. Baldwin

Dibutylphosphoric acid is a product that is formed during many of the reactions of tributyl phosphate. Dibutylphosphoric acid forms complexes with cations in solvent extraction processes. Many of these complexes have a high solubility in the organic phase, while others have low solubilities and may stabilize emulsions at water-organic interfaces.

Smith[37] has reported the infrared spectra of a number of these cationic complexes without giving analytical data or physical properties. We have prepared several of the complexes from P^{32}-labeled dibutylphosphoric acid. The radioactive phosphorus was useful in the analysis of the compounds and in following the fragments from the compounds. The compounds CuA_2, UO_2A_2, FeA_3, YA_3, LaA_3, AlA_3, and ThA_4 (where A is dibutylphosphate anion) were obtained in analytical purity. The compound CuA_2 melted at 118–119°C; the others decomposed when heated. The molecular weights of CuA_2 and UO_2A_2, determined cryoscopically in biphenyl, exceeded 10,000, while the others were too insoluble to measure. Aqueous sodium hydroxide or sodium carbonate solutions, by metathesis, removed the anion as the water-soluble sodium salt. The residue (if any) from metathesis was completely soluble in nitric acid. The practical significance of the ease of metathesis may be found in the decontamination of organic solvents and of equipment where the insoluble complexes have been deposited.

REFRACTOMETRIC DETERMINATION OF THE MUTUAL SOLUBILITY OF TRIBUTYLPHOSPHINE OXIDE AND WATER AS A FUNCTION OF TEMPERATURE[38]

C. E. Higgins W. H. Baldwin

Tributylphosphine oxide has been shown to form stronger coordination complexes with electrolytes than does tributyl phosphate. The high solubility of tributylphosphine oxide in water has been the limiting factor in the usefulness of tributylphosphine oxide in solvent extraction. The solubility of tributylphosphine oxide, which has not previously been reported as a function of temperature, is sufficiently high so that it can be measured refractometrically.

Tributylphosphine oxide and water are completely miscible at 13.0°C. At 25°C the two phases that are in equilibrium contain 55.7 g of tributylphosphine oxide per kilogram of aqueous solution and 375 g of water per kilogram of tributylphosphine oxide solution.

The distribution coefficient of tributylphosphine oxide between carbon tetrachloride and water is a function of the tributylphosphine oxide concentration. Furthermore, the number of moles of water per mole of tributylphosphine oxide in the carbon tetrachloride phase is also a function of the concentration of the tributylphosphine oxide (reaching a maximum of 2.3 moles of water per mole of tributylphosphine oxide at a concentration of 440 g of tributylphosphine oxide per liter of carbon tetrachloride solution).

THERMALLY INDUCED REACTIONS OF TRIBUTYL PHOSPHATE

C. E. Higgins W. H. Baldwin

Tributyl phosphate is the active solvent that has been extensively used for solvent extraction purification of many electrolytes, including source and fissionable elements. The heating of pure tributyl phosphate *in vacuo* or in an inert atmosphere

[36] C. E. Melton and P. S. Rudolph, *J. Chem. Phys.* 30, 848 (1959).

[37] T. D. Smith, *J. Inorg. & Nuclear Chem.* 9, 150 (1959).

[38] Abstract of paper published in *Anal. Chem.* 32, 233 (1960).

produces butenes and dibutylphosphoric acid in high yields along with lesser yields of butanol, dibutyl ether, and tetrabutyl pyrophosphate. The reaction rate increases with time as the acid product in the residue increases. The reaction is first order at the beginning (up to 3% dibutylphosphoric acid), and the specific reaction rates were 0.39×10^{-7} sec^{-1} at 178°C, 3.3×10^{-7} at 198°C, 27.1×10^{-7} at 223°C, and 132×10^{-7} at 240°C.

The reaction rates that were measured on the series of compounds tributyl phosphate, dibutyl butylphosphonate, and butyl dibutylphosphinate (where the number of C-O-P bonds decreased in the order 3, 2, and 1) indicated greater stability than could be accounted for by the mere statistical availability of C-O-P bonds for cleavage.

DIFFERENTIAL THERMAL ANALYSIS IN THE QUALITATIVE STUDY OF REACTIONS BETWEEN NITRATES AND TRIBUTYL PHOSPHATE

W. H. Baldwin

Differential thermal analysis was developed as a technique for the study of physical and chemical reactions at elevated temperature. It has only recently been employed for the study of physical and chemical reactions in organic systems. A major advantage for differential thermal analysis is the small size sample that is required. This was particularly important for our application, where exothermic reactions were expected. Nitric acid and nitrate salts (Li, Na, Al, UO_2, Th, Fe) were dissolved in tributyl phosphate; 0.5-ml aliquots of the resulting solutions were examined by the differential thermal analysis technique. Endothermic reactions were observed at lower temperatures in some of the solutions. Exothermic reactions were observed with nitric acid and tributyl phosphate at 147°C and with lithium nitrate at 197°C. The other salts were observed to react exothermally at temperatures between the two extremes.[39]

Practical application of the method can be made to organic-nitrate systems to define safe operating conditions. Methods have been developed for the synthesis of butyl nitrate from tributyl phosphate and nitric acid or lithium nitrate by operating below the temperature for exothermic reactions. Purity of the butyl nitrate product was found by gas-liquid chromatography to exceed 99%.

THE REACTION OF AMSCO 125-82 WITH SULFURIC ACID

W. H. Baldwin

Amsco 125-82 is a mixture of branched, saturated aliphatic hydrocarbons that has been used to dilute tributyl phosphate in the pilot-plant solvent extraction activities of the Laboratory. It has been found here that the Amsco reacts with 95% sulfuric acid at 25°C to produce at least nine hydrocarbons that boil lower than the original mixture. The reaction of saturated hydrocarbons with sulfuric acid has been studied by others using a number of techniques. The recent development of gas-liquid chromatography permits a more detailed examination than was possible previously. The gas-liquid chromatographic technique was used here to show the presence of the nine low-boiling products and a change in the ratio of the major, original components without the complete removal of any one component. The practical significance of this reaction lies in the fact that after treatment with sulfuric acid the diluent gives better decontamination in the solvent extraction process. Reactive components of the original Amsco are among the first to react with sulfuric acid and are thus altered to more stable compounds. It is assumed that the same compounds would be the most reactive in the solvent extraction process. The details have been summarized to be issued in a CF memo.

[39] W. H. Baldwin, *Differential Thermal Analysis: Qualitative Study of Nitrate–Butyl Phosphate Systems*, ORNL CF-60-1-99 (Jan. 25, 1960).

CHEMISTRY OF AQUEOUS SYSTEMS

HIGH-TEMPERATURE SPECTROPHOTOMETRIC STUDIES ON UO_2SO_4-$CuSO_4$-D_2SO_4-D_2O SOLUTIONS

W. C. Waggener A. J. Weinberger
R. W. Stoughton

A 0.017 *m* UO_2SO_4 solution in 0.01 *m* D_2SO_4-D_2O (98.5 at. % D) was examined spectrophotometrically from 0.34 to 0.80 μ over a period of 43 days and over a temperature range from 25 to 251°C. The 0.42-μ band (which exhibits characteristic vibrational structure) showed a monotonic increase in absorptivity with temperature to 1.74 times the room-temperature value at 251°C.

The data indicate that the spectra observed throughout were due solely to hexavalent uranium species; there was no turbidity or indication of soluble lower valence species which absorb in the visible region. Further, while there was no evidence of solution instability at the lower temperatures, the data show a slow, steady loss of uranium to a total (loss) of 9.8% in 98 hr at 251°C. Analyses to date indicate that most of this loss was associated with a solute transfer to the reservoir above the cell, which was maintained about 8°C above the cell temperature.

An aqueous solution composed of UO_2SO_4 (0.0123 *m*), $CuSO_4$ (0.0085 *m*), and D_2SO_4 (0.0072 *m*) in D_2O (98.5 at. % D) was examined spectrophotometrically from 0.34 to 1.2 μ over a period of 50 days and over a temperature range from 4 to 280°C.

The 0.42-μ band of U(VI) and the 0.82-μ band of Cu(II) do not overlap and could be studied independently. The bands showed a monotonic increase in molar absorptivity with temperature from 4 to 280°C by a factor of 2.3 and 2.0 respectively for U(VI) and Cu(II). At 280°C the half-intensity band width of U(VI) was 2330 cm^{-1} (6% narrowed from 25°C) while that of Cu(II) was 5480 cm^{-1} (3% broadened from 25°C).

In contrast to the earlier study of 0.017 *m* UO_2SO_4 in 0.01 *m* D_2SO_4, in which there was no indication of soluble lower valence species, the data of the solution containing $CuSO_4$ after a heating cycle indicate the presence of U(IV) at lower temperatures beginning with an estimated 0.05% (just detectable) at 50°C and increasing to 1.5% at 4°C. This appearance and disappearance of U(IV) was observed in four successive thermal cyclings.

THE STANDARD POTENTIAL OF THE Ag-AgBr ELECTRODE AND THE MEAN IONIC ACTIVITY COEFFICIENT OF HYDROBROMIC ACID

M. B. Towns[1] R. S. Greeley
M. H. Lietzke

The emf of the cell Pt-$H_2(p)$ | HBr(*m*) | AgBr-Ag was measured from 25 to 200°C using hydrogen pressures of about 1 atm and HBr concentrations from 0.005 to 0.5 *m* (using the convention that the standard potential of the hydrogen electrode is zero at all temperatures). Additional measurements were made on 1.0 *m* HBr from 25 to 150°C. The standard potential of the cell was determined and found to fit the equation

$$E^\circ = 0.08289 - 4.0647 \times 10^{-4} t - 2.3986 \times 10^{-6} t^2 \text{ v} ,$$

with a standard error of fit of 1.1 mv. The mean ionic activity coefficients of HBr were calculated for several concentrations from an extended Debye-Hückel equation, the linear (B) parameter of which was obtained from a least squares treatment of the emf data. All results have been submitted for publication.[2]

The values of E° obtained at 25 and 60°C agree with those of Harned, Keston, and Donelson[3] within 0.3 and 0.5 mv respectively, while the activity coefficient values agree within 1%.

THE STANDARD ELECTRODE POTENTIAL OF THE QUINHYDRONE ELECTRODE FROM 25 TO 55°C

J. C. Hayes[4] M. H. Lietzke

In the present work the standard electrode potentials of the quinhydrone electrode were measured from 25 to 55°C at 5° intervals, using an

[1]Research participant, summer, 1959, from Tennessee A. and I. College, Nashville.

[2]M. B. Towns, R. S. Greeley, and M. H. Lietzke, *J. Phys. Chem.*, in press.

[3]H. S. Harned, A. S. Keston, and J. G. Donelson, *J. Am. Chem. Soc.* 58, 989 (1936).

[4]Research participant, summer, 1959, from Hamline University, St. Paul, Minn.

Ag-AgCl reference electrode. The establishment of standard electrode potentials allows the direct calculation of activity coefficients at these temperatures. In carrying out the calculations, values of

$$E^{\circ\prime\prime} = E_T - \frac{2RT}{F} \ln m + \frac{2RT}{F} \frac{\mathring{a}_T \sqrt{I}}{1 + A\sqrt{I}} \qquad (1)$$

were computed at each concentration of HCl, m, at 5° intervals from 25 to 55°C. Then the values of E° for the electrode system at each temperature can be determined by extrapolating the $E^{\circ\prime\prime}$ values to zero ionic strength using the equation:

$$E^{\circ\prime\prime} = E^\circ + \left(\frac{2RT}{F} B\right) I \ . \qquad (2)$$

In this work, however, the parameters A and B and the values of E° were determined by a non-linear least squares method on a high-speed computer (the Oracle).

The values of E° for one Ag, AgCl, HCl, quinhydrone cell from 25 to 55°C, as well as the mean ionic activity coefficients of HCl calculated therefrom, have been published.[5] The values agree closely with those obtained by other investigators.[6] Hence it appears that the quinhydrone electrode may be used in activity coefficient measurements in a manner similar to the hydrogen electrode.

ACTIVITY COEFFICIENT MEASUREMENTS IN HYDROBROMIC ACID SOLUTIONS USING THE BECKMAN AMBER GLASS ELECTRODE

M. H. Lietzke J. V. Vaughen[7]

An attempt has been made to measure the activity coefficients of HBr solutions to 100°C using the Beckman amber glass electrode in conjunction with either an Ag, AgBr or an Hg, Hg_2Br_2 reference electrode. The upper limit of 100°C was adopted in this work because it has been shown that the amber glass electrode cannot be cycled between 25 and 150°C more than two or three times without losing its correct pH response. Measurements were made in HBr solutions over the concentration range 0.001 to 0.1 m.

In calculating the activity coefficients values of

$$E^{\circ\prime\prime} = E_T + \frac{2RT}{F} \ln m - \frac{2RT}{F} \frac{\mathring{a}_T \sqrt{m}}{1 + 1.5\sqrt{m}}$$

were computed at 5° intervals from 20 to 100°C for each concentration of HBr. In all the calculations the constant value 1.5 was used in the denominator of the Debye-Hückel term, since plots of $E^{\circ\prime\prime}$ vs m showed sufficient scatter to make a statistical determination of this quantity unwarranted. Hence the values of E° for the electrode system were calculated at each temperature by the method of least squares using the equation

$$E^{\circ\prime\prime} = E^\circ - cm \ ,$$

where $c = (2RT/F)\ B$, and B is the coefficient of the linear term in the extended Debye-Hückel expression for the log of the activity coefficient. From the values of c (and hence of B) the values of the activity coefficient of HBr were computed at even concentrations and temperatures using the expression

$$\ln \gamma = \frac{\mathring{a}_T \sqrt{m}}{1 + 1.5\sqrt{m}} + Bm \ .$$

At 0.001 m the activity coefficient of HBr measured with the glass electrode agrees with the hydrogen electrode values obtained by Harned,[8] while at 0.01 m the value becomes at 60°C as much as 1.7% low. The deviations at higher acid concentrations are negative and consistent with the acid error mentioned by Bates.[9] The acid error increases as the temperature increases, becoming 16% in the activity coefficient at 0.1 m and 60°C. Hence it appears that the useful range of the amber glass electrode for activity coefficient measurements in acid solutions is restricted to the millimolal region and below.

The results of this work have been presented in greater detail in another report.[10]

---

[5] J. C. Hayes and M. H. Lietzke, *J. Phys. Chem.* **64**, 374 (1960).

[6] H. S. Harned and R. W. Ehlers, *J. Am. Chem. Soc.* 55, 2179 (1933).

[7] Stetson University, Deland, Fla.

[8] H. S. Harned, A. S. Keston, and J. G. Donelson, *J. Am. Chem. Soc.* **58**, 989 (1936).

[9] R. G. Bates, *Electrometric pH Determinations*, p 241, Wiley, New York, 1954.

[10] M. H. Lietzke and J. V. Vaughen, *Activity Coefficient Measurements in Acid Solution Using the Beckman Amber Glass Electrode: The Activity Coefficient of HBr Solutions*, ORNL CF-59-10-106 (Oct. 29, 1959).

THE SOLUBILITY OF SILVER SULFATE IN ELECTROLYTE SOLUTIONS

M. H. Lietzke R. W. Stoughton

In a series of previous papers[11] describing the solubility of Ag_2SO_4 in KNO_3, K_2SO_4, H_2SO_4, HNO_3, and $MgSO_4$ solutions it was shown that the experimental solubility values are in good agreement with those calculated on the basis of the solubility of Ag_2SO_4 in pure water and on the assumption that the activity coefficient of Ag_2SO_4 can be expressed as a single-parameter Debye-Hückel expression. The single parameter was found to be essentially independent of temperature to about 200°C, although it did show some variation with concentration of supporting electrolyte in certain cases. In the cases not involving acid media complete dissociation was assumed for both Ag_2SO_4 and the supporting electrolyte. In the cases involving acidic media the incomplete dissociation of HSO_4^- and HNO_3 was taken into account. The values of the acid constants for these species vs temperature were obtained from Young,[12] while the variation of the acid quotients with ionic strength was assumed to be given by single-parameter Debye-Hückel equations.

In a recent paper[13] the concentrations of the various species present in 0.1, 0.5, and 1.0 *m* solutions of H_2SO_4 and HNO_3 saturated with respect to Ag_2SO_4 have been discussed as a function of temperature. Also the values of the solubility product, of the standard enthalpy and entropy of solution, and of the standard partial molal entropy of the solute Ag_2SO_4 are given vs temperature to 200°C. The fact that the entropy of solution decreases from −7 to −44 e.u. and the partial molal entropy decreases from 40 to 20 e.u. in going from 25 to 200°C indicates that the presence of the solute Ag_2SO_4 increases the amount of "structure" shown by the solvent water and that this enhancement of structure is greater the higher the temperature.

The solubility of Ag_2SO_4 has also been measured in 0.100, 0.409, 0.622, 1.060, and 1.348 *m* UO_2SO_4 solutions[14] to as high a temperature as possible without precipitation of a second solid. The upper limit of temperature varied from about 140° to 200°C depending on the UO_2SO_4 concentration. The agreement between calculated and observed solubilities was good when hydrolytic and complexing reactions of the uranyl ion were taken into account. The concentrations of all assumed species have been calculated as functions of UO_2SO_4 concentration and temperature, and it has been shown that the relative stability of the neutral species UO_2SO_4 compared to UO_2^{++} and $UO_2(SO_4)_2^{--}$ increases with temperature. The standard enthalpy and entropy for the reaction

$$UO_2^{++} + SO_4^{--} = UO_2SO_4$$

increase from about 4 to 55 kcal and from about 25 to 155 e.u., respectively, in going from 25 to 200°C, indicating that a large degradation of solute-solvent (or solvent-solvent) "structure" occurs when UO_2^{++} and SO_4^{--} ions associate to form the neutral species UO_2SO_4.

Using the values of the complexing and hydrolysis constants for UO_2SO_4 determined in the study of the solubility of Ag_2SO_4 in UO_2SO_4 solutions, the concentrations of the species UO_2^{++}, UO_2SO_4, $UO_2(SO_4)_2^{--}$, $U_2O_5^{++}$, H^+, HSO_4^-, and SO_4^{--} have been calculated as a function of temperature to 225°C for aqueous solutions containing various concentrations of uranyl sulfate and in most cases also containing one or more of the following electrolytes: H_2SO_4, a 1-2 sulfate M_2SO_4, and a 2-2 sulfate MSO_4.[15]

ULTRACENTRIFUGATION AND LIGHT SCATTERING OF AQUEOUS SOLUTIONS

E. W. Anacker[16] K. A. Kraus
J. S. Johnson, Jr. R. M. Rush

Ultracentrifugation and Light Scattering of Silicotungstic Acid Solutions

The study[17] of the light scattering of two-component solutions of $H_4SiW_{12}O_{40}$ was completed

[11] M. H. Lietzke and R. W. Stoughton, *J. Phys. Chem.* 63, 1183, 1186, 1188, 1190, and 1984 (1959).

[12] T. F. Young, private communication; also T. F. Young, L. F. Maranville, and H. M. Smith, chap. 4 of *The Structure of Electrolytic Solutions*, ed. by W. J. Hamer, Wiley, New York, 1959.

[13] R. W. Stoughton and M. H. Lietzke, *J. Phys. Chem.* 64, 133 (1960).

[14] M. H. Lietzke and R. W. Stoughton, *J. Phys. Chem.*, in press.

[15] M. H. Lietzke and R. W. Stoughton, *Concentrations of Species in Aqueous UO_2SO_4 Solutions as a Function of Temperature*, ORNL CF-60-2-102 (February 1960).

[16] Summer employee, 1959, from Montana State College, Bozeman.

[17] J. S. Johnson, E. W. Anacker, and K. A. Kraus, *Chem. Ann. Prog. Rep. June 20, 1958*, ORNL-2584, p 56–58.

with an independent determination of the activity coefficients of this solute by ultracentrifugation. The activity coefficients in the concentration range covered (0.0004–0.04 mole/liter) were found to be in satisfactory agreement with the Debye-Hückel equation for a 1-4 electrolyte,

$$-\log \gamma_{\pm} = \frac{4(0.5097)\sqrt{\mu}}{1 + a'\sqrt{\mu}},$$

with a distance of closest approach parameter $a' = 2.50$, that is, $\mathring{a}$ *ca.* 7.6 A.

With the activity coefficients, turbidities of silicotungstic acid solutions can be computed, and the results of a comparison are given in Fig. 14. The agreement of computed with our experimental values is good, but there is poor agreement with some recently published results of Kronman and Timasheff.[18] Origin of the discrepancy is not clear.

Kronman and Timasheff invoke Kirkwood-Mazur ordering (an effect arising from repulsion of the multicharged negative ions, which would be somewhat surprising in the present case) to explain the fact that their turbidities are much less than they expect. Our experimental turbidities are even lower than theirs, and would, therefore, require even greater ordering. The agreement between our ultracentrifugation and light-scattering measurements indicates that there is no ordering other than implied by Debye-Hückel considerations. Their expectation of greater scattering seems to arise from their failure to consider in their equations the number of moles of ions per mole of solute, here 5; as we have discussed, consideration of this quantity leads (in the ideal case of constant mean ionic activity coefficients) to a

[18] M. J. Kronman and S. N. Timasheff, *J. Phys. Chem.* 63, 629 (1959).

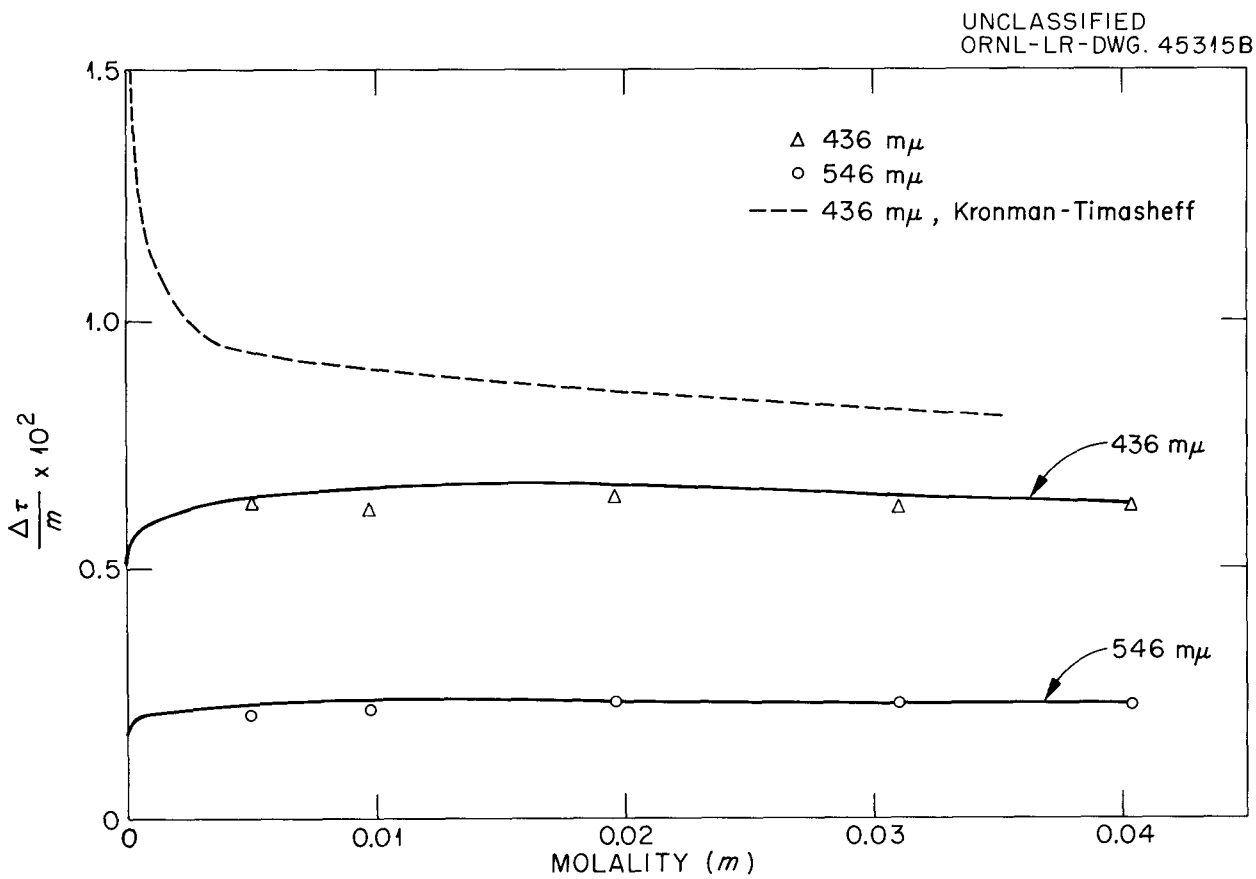

Fig. 14. Comparison of Turbidities of Silicotungstic Acid Solutions Determined by Light Scattering with Values Computed from Activity Coefficients (Solid Curve).

predicted turbidity of only $\frac{1}{5}$ of the value for un-ionized $H_4SiW_{12}O_{40}$ species.

Kronman and Timasheff report a large increase in turbidity per mole at low concentrations. Although one would expect such a rise to occur in extremely dilute solutions, where the restriction of electroneutrality in volumes of the order of the wavelength of light breaks down, and the ions, therefore, scatter independently, the concentration at which the effect is observed here is much higher than predicted by the treatment of Hermans.[19]

Ultracentrifugation and Light Scattering of Soap Solutions

The micelles formed by soaps seem in many ways analogous to species formed by amine extractants. We have carried out equilibrium ultracentrifugations and turbidity measurements on solutions of an anionic soap, sodium lauryl sulfate (NaLS), and on a cationic soap, dodecyltrimethylammonium bromide (DTAB). With respect to NaLS, our results in 0.1 and 0.4 *M* NaCl confirm the statement frequently made that the micelles are predominantly monodisperse at a given salt concentration. The ultracentrifugal values for the number of soap molecules per micelle (*ca.* 80 in 0.1 *M* NaCl and *ca.* 125 in 0.4 *M* NaCl) and the charge (*ca.* 0.2 per monomer unit) agree fairly well with our light-scattering measurements, as well as with the recent ones of Mysels and Princen.[20] In 0.5 *M* NaCl, indications of polydispersity were found.

The distribution of DTAB in 0.1 *M* NaBr also appears to be monodisperse, but polydispersity is strongly apparent in 2 *M* NaBr. The evaluation of molecular weight by ultracentrifugation is more difficult in this case, since the specific volume of the solute, 0.96, is very close to that of the solvent; the light-scattering values (*ca.* 70 monomers per micelle) are probably more reliable here.

A strange sedimentation behavior was observed with some solutions of NaLS. It was found that at speeds which should have given substantial sedimentation, no sedimentation, or only sedimentation at the high radial end of the cell, was found, even after periods of a week or more. The phenomenon was not altogether reproducible – some soap preparations never exhibited it, and others ceased showing it after aging of the solutions or of the solids from which the solutions were made. Equilibrium distributions could always be obtained by centrifuging at higher speeds for a few hours, and then reducing speed. There was no significant difference in molecular weights between those solutions which originally gave the strange pattern, and those which did not. No satisfactory explanation has been found. Neither convection currents in the centrifuge cell nor impurities seem to be the cause, although these possibilities are difficult to exclude completely.

ANION EXCHANGE STUDIES

F. Nelson K. A. Kraus D. C. Michelson

Studies of the properties of anion exchange resins and their utilization for separations continued, though with reduced emphasis. Typical results are summarized below.

Adsorption of HF by Anion and Cation Exchangers

Strong adsorption of HF by anion exchangers in the F^- form was reported earlier.[21] At low HF concentrations, uptake is largely determined by the reaction $HF + F^-_{(r)} \rightleftharpoons HF_2^-{}_{(r)}$. While some ambiguity exists regarding the magnitude of the various equilibrium and exchange constants at high HF concentration because of uncertainties in the activity coefficients and species in the aqueous phase, this ambiguity is eliminated by extrapolation to zero HF concentration. Under these conditions, the selectivity coefficient

$$K^{()} = \frac{(HF_2^-)_{(r)}(F^-)}{(HF_2^-)(F^-)_{(r)}} = 11.5$$

was determined. Thus, compared with F^- the HF_2^- ion is very strongly adsorbed by the exchanger.

The distribution coefficient D_{HF} of the species HF was found to differ widely for anion exchangers and cation exchangers containing the same polystyrene-divinylbenzene network. Thus for the anion exchanger Dowex-1 X10 in the HF_2^- form,

[19] J. J. Hermans, *Rec. trav. chim.* 68, 859 (1949).

[20] K. J. Mysels and L. H. Princen, *J. Phys. Chem.* 63, 1699 (1959).

[21] F. Nelson *et al.*, *Chem. Ann. Prog. Rep. June 20, 1957*, ORNL-2386, p 98–99.

D_{HF} is *ca.* 3 and varies only slowly with HF concentration ($D_{HF} \approx 3$ for $m_{HF} \leq 1$, $D_{HF} = 2.5$ in concentrated HF). For the same anion exchanger in the chloride form D_{HF} = *ca.* 4.4 at $m_{HF} = 0.1$, that is, it is only slightly larger than for the HF_2^- form. However, for Dowex-50 X10 in the hydrogen form, D_{HF} is substantially less than unity ($D_{HF} = 0.42$ for $m_{HF} = 0.5$, $D_{HF} = 0.63$ for $m_{HF} = 47.6$). The reason for the pronounced differences in selectivity of anion and cation exchange resins for (molecular) HF is not clear.

Volume of Anion Exchangers in Electrolyte Solutions

Volume changes of quaternary amine polystyrene-divinylbenzene anion exchange resins were determined in HCl and LiCl solutions as a function of electrolyte concentration by measuring (microscopically) the diameter of single beads. In both media, volume first decreases with increasing concentration of electrolyte and then increases. A volume minimum is located near 1 *M* Cl^-. The effect, while slight for 10% divinylbenzene exchangers, is very marked for the 2% resins. This behavior may be contrasted with that of cation exchangers of the polystyrene-divinylbenzene type, for which minima are not usually observed and for which the volume decreases in a monotone fashion with increasing electrolyte concentration.

Additivity of apparent molar volumes for various quaternary amine solutions in three-component systems had earlier been established,[22] and thus adherence of the exchangers to this additivity rule was tested. Since the additivity rules relate to mixtures of constant total ionic strength, it was necessary to assume invariance with concentration of the apparent molar volume of the resin and, in some cases, to extrapolate the apparent volumes of HCl and LiCl in two-component systems. However, even with these restrictions and assumptions, the observed volumes for three-component systems were in good agreement with those calculated from simple additivity relationships.

Elution of Anions by Complexing with Cations; Application to SCN^- Analysis

Thiocyanate belongs to a group of anions which are strongly adsorbed by the usual anion exchange resins. Its possible rapid removal from anion exchange columns through complexing with appropriate metal ions was investigated. In this case, one would expect acceleration of band movement in proportion to the fraction of the anion complexed in the aqueous phase. Using moderately concentrated Fe(III) solutions (in nitric acid), SCN^- was found to be rapidly removed from columns, as expected from idealized theoretical considerations. Thus, on the addition of a solution containing Fe(III) (*ca.* 0.2 *M*) to the column, the characteristically red-colored $FeSCN^{++}$ complex forms, which within one to two column volumes can be removed from the bed. Removal of SCN^- was found to be essentially quantitative. The resulting solution may be used directly for the colorimetric analysis of SCN^-.

Adsorption of Positively Charged Complexes by Anion Exchangers

Adsorption of certain types of anions by cation exchangers had earlier been reported.[23] The corollary adsorption of cations by anion exchangers has now been demonstrated. The effect was first observed during attempts to accelerate the elution of bromide ions from anion exchangers through complexing with Hg(II). Distribution coefficients of the order of 10 were found under conditions where the values computed with the assumption of negligible adsorption of the complex formed should have been of the order of 10^{-7}. From the available complex constants for the Hg(II)-Br^- system, one concludes that under the experimental conditions only the species $HgBr^+$ occurs in significant concentrations. The slow elution thus presumably is caused by adsorption of this positively charged complex by the anion exchanger. Confirmation of this effect was obtained by studying adsorbability of Br^- in the presence of excess Hg(II) as a function of supporting electrolyte concentration. Adsorption increased with supporting electrolyte concentration, as expected from theoretical considerations; had a negatively charged species been involved, the reverse, of course, should have been the case.

---

[22] F. Nelson *et al.*, *Chem. Ann. Prog. Rep. June 20, 1959*, ORNL-2782, p 47.

[23] K. A. Kraus, D. C. Michelson, and F. Nelson, *J. Am. Chem. Soc.* 81, 3204 (1959).

ADSORPTION ON INORGANIC MATERIALS

H. O. Phillips K. A. Kraus

Studies of properties of essentially amorphous inorganic materials and their application to separations were continued during the past year. The studies included a search for new ion exchange active materials; further evaluation of materials previously shown to have exchange properties, particularly insoluble phosphates; high-temperature studies; and search for optimum conditions for special separations.

Preparation of Zirconium Phosphate

The ion exchange properties of Zr(IV) phosphates prepared by use of various alkali and ammonium phosphates or phosphoric acid were studied as a function of phosphate-zirconium ratio. At the same phosphate-zirconium ratio, only minor differences were observed. Trisodium phosphate was found, however, to be unsuitable since the phosphate content of the precipitated materials was usually very low. Presumably, this is caused by the high basicity of the solutions, which prevents retention of phosphate by the underlying oxide matrix.

Separation of Cs^+ and Rb^+ with Zirconium Phosphate

Distribution coefficients (D) of Rb^+ and Cs^+ on zirconium phosphate had earlier been shown to be very much larger in HCl solutions than in salt solutions of the same concentration. In an attempt to search for optimum conditions for the separation of these ions, their selectivity coefficients and their separabilities were studied over a wide range of acid and salt (NH_4Cl) concentrations. The separation factor (D_{Cs}/D_{Rb}) in HCl was found to be *ca.* 8 in 0.1 *M* HCl, *ca.* 4 in 6 *M* HCl, and *ca.* 2.5 in NH_4Cl solutions in this concentration range. In NH_4Cl-HCl mixtures, the separation factors seem to be intermediate.

Stability of Zirconium Phosphate at High Temperatures

Using the high-temperature ion exchange column, the stability of zirconium phosphate was studied at 200°C. Phosphate loss was negligible in acid solutions and, surprisingly, even in 0.1 *M* NaOH, where at room temperature most of the phosphate is removed. Cesium uptake at 200°C was approximately the same as at 25°C and the separation factors between alkali metals were also approximately the same. Attempted separations of the higher alkali metals at 200°C were not significantly improved over those at room temperature; rather there is some indication that operation at the higher temperatures causes an unexpected increase in tailing.

Properties of Titanium Phosphate

Titanium phosphate had earlier been shown to have interesting cation exchange properties. A somewhat more detailed study of the ion exchange and stability properties of Ti(IV) phosphate was carried out. Material was prepared by mixing solutions of $TiCl_3$ and H_3PO_4, adding ammonia, and permitting air oxidation. Studies were carried out on this material after drying it at various temperatures between 25 and 1000°C. The water content, which is *ca.* 20 moles/kg at 25°C, decreases to *ca.* 4 moles/kg after drying at 300°C. Above 500°C drying temperature, the water content is less than 1 mole/kg. After drying at 400°C, the phosphate content is approximately 9 moles/kg, essentially as expected for the pyrophosphate, TiP_2O_7. Capacity and adsorption properties of the material are not very different from those of zirconium phosphate. However, the stability both to acid and base was considerably lower. The difference is particularly striking at 200°C, where titanium phosphate loses rapidly an appreciable fraction of its phosphate content on washing with 1 *M* NH_4NO_3 while, as discussed in the previous section, zirconium phosphate at 200°C does not lose phosphate significantly even in moderately concentrated base.

Properties of Tantalum Phosphate

Tantalum phosphate was prepared from potassium tantalate, phosphate, and excess acid. Cation exchange capacity as measured by cesium uptake in acidic solutions was approximately 0.6 mole per kg of solid, if dried at 25°C. Material dried at 200°C had essentially negligible capacity. The separation factor between Cs^+ and Rb^+ in 1 *M* HCl was *ca.* 10 for material dried at 25°C. As with zirconium phosphate, the separation factor is substantially lower from NH_4Cl solutions. Alkaline earths and rare earths were strongly adsorbed from 0.1 *M* HCl.

While phosphate loss from the material is negligible in acidic solutions, severe loss occurs

in basic solutions, although complete removal of phosphate from the solid is difficult to achieve even in strongly basic solutions.

Separation of Ba^{137} from Cs^{137}

As described previously, Cs^{+} is strongly adsorbed by zirconium phosphate from acidic solutions. Under the same conditions, Ba^{++} is not adsorbed. Hence, separation of these two elements can readily be achieved in, for example, 0.5 *M* HCl. It is, therefore, very simple to separate the short-lived Ba^{137} daughter from the Cs^{137} parent by a semicontinuous "milking" procedure. The rates are very favorable; when acid is pumped over a zirconium phosphate bed containing Cs^{137}, the counting rate of Ba^{137} decreases within a few seconds to essentially a steady-state value.

Since the adsorbent presumably is stable at high radiation levels, this "milking" arrangement should be suitable even for large quantities of Cs^{137}-Ba^{137} mixtures. If the eluted Ba^{137} can be readsorbed on a material which has low selectivity for Cs^{137}, a mobile radiation source should become feasible. Barium sulfate was found to have sufficient ability to hold Ba^{137} tracer from a rapidly pumped solution, although difficulties were encountered in the preparation of barium sulfate beds of suitable flow characteristics. A mixed precipitate of $BaSO_4$ and hydrous tantalum oxide, on the other hand, could be obtained in suitable particle size while still retaining rapid adsorptive capacity for the tracer and low selectivity for Cs^{137}.

PHYSICAL CHEMISTRY OF ION EXCHANGERS

Calorimetric Measurements of the Zinc-Sodium Ion Exchange Reaction

F. Vaslow G. E. Boyd

The heats of the ion exchange reaction

$$2NaR + Zn(NO_3)_2 \longrightarrow 2NaNO_3 + ZnR$$

were measured with nominal 2, 4, 8, 16, and 24% divinylbenzene (DVB) Dowex 50 resins for a series of ionic compositions. The final compositions and selectivities were obtained either directly or from the selectivity measurements of Lindenbaum.[24]

[24]Reported in part in *Chem. Semiann. Prog. Rep. Dec. 20, 1955*, ORNL-2046, p 53.

The estimated standard free energy changes for the reaction (uncorrected for the activity coefficients in aqueous solution) increased from −550 cal/equiv in the 2% resin to −750 cal/equiv in the 8% resin and then decreased to −400 cal in the 24% resin. The standard heats, however, increased monotonically from +600 cal/equiv for the 2% to +1900 cal in the 24% DVB resin. The differential heat of exchange varied from +1500 (at $x_{Zn^{++}} = 0$) to +3400 cal/equiv in the 24% resin, with smaller variations in the more lightly cross-linked resins.

In this system the more strongly hydrated ion is preferentially bound, in contrast to the ion exchange reactions with the alkali-metal cations. Furthermore, the binding resulted from the increase in entropy of the system rather than from a decrease in ΔH° (i.e., the potential energy).

The extent to which the entropy can increase is limited, however, and, as the heat of exchange grows larger in the higher cross-linked exchangers, the affinity of zinc ion for the resin decreases. With the 24% DVB resin, in fact, the free energy changes sign and becomes positive when $x_{Zn^{++}} = 1.0$.

Thermodynamic Calculations of Anion Exchange Selectivities

G. E. Boyd S. Lindenbaum

A rigorous thermodynamic computation of the equilibrium selectivity coefficients for the exchange of bromide with chloride, iodide, or fluoride ions present in dilute aqueous solutions was performed for a series of cross-linked strong-base anion exchangers (polystyrene quaternary ammonium type) using the Gibbs-Donnan equation. Swelling pressures, P, and activity coefficient ratios, $\log (\gamma_{X^-}/\gamma_{Br^-})_r$, were evaluated from weight swelling measurements conducted in isopiestic vapor pressure experiments on virtually un-cross-linked and on cross-linked exchangers. Partial molar volume differences, $(\bar{v}_{X^-} - \bar{v}_{Br^-})$, needed for the swelling free energy estimate were derived from density measurements on a weakly cross-linked exchanger.

The calculated selectivity coefficients were in satisfactory agreement with independently measured experimental values except with the most highly cross-linked exchanger. When the

values for the latter were corrected for their lower exchange capacities, good agreement with theory was obtained. The thermodynamic treatment reported has led to the important generalization that, at constant temperature in the absence of specific interactions in the aqueous electrolyte phase, the selectivity coefficient, D_1^2, is a function solely of the weight swelling of the exchanger; whatever changes the swelling, be it the exchanger cross-linking, ionic composition, or external electrolyte concentration, also will change D_1^2 in a manner that may be estimated from the Gibbs-Donnan equation.

Estimation of Partial Molal Volume Difference of Resin Halides. – Equivalent volume, V_e, measurements on various salt forms of a weakly cross-linked anion exchanger in the dry state and with varying equivalent water content, x_w, were conducted pycnometrically using n-octane as a displacement liquid. The data were fitted to equations of the form[25]

$$V_e = V_a + \phi_w x_w \quad , \tag{1}$$

$$\phi_w = \frac{\phi_w^0 x_w}{b + x_w} \quad , \tag{2}$$

which lead to

$$V_e = V_a + \frac{\phi_w^0 x_w^2}{b + x_w} \quad , \tag{3}$$

where V_a is the equivalent volume of the anhydrous exchanger salt and ϕ_w is the apparent molar volume of water in the exchanger. In general, ϕ_w is not equal to ϕ_w^0, the molar volume of pure water (18.069 ml), but must be a function of the (exchanger) weight normality N_m (or x_w) as with ordinary aqueous electrolyte solutions. It is necessary, however, that ϕ_w approach ϕ_w^0 at infinite dilution. Values of V_a and b derived from the volume measurements are listed in Table 20 together with corresponding values for the partial molar volume of the exchanger salt at infinite dilution, $\bar{v}_a^0$. The magnitude of the difference $(V_a - \bar{v}_a^0)$ may be a measure of the electrostriction experienced by water on entering the dry exchanger. Interestingly, the fractional molar electrostriction, $(V_a - \bar{v}_a^0)/\phi_w^0$, appears to be the same numerically as the empirical constant, b, in Eq. (2).

Values for the partial molal volume of water in the exchanger were found by differentiating Eq. (1), $\bar{v}_w = (\partial V_e/\partial x_w)_{x_2}$, and are shown in Fig. 15 as a function of the weight normality. For a given N_m, the partial molal volume of water is smallest for the fluoride and largest for the

[25] In earlier treatment of these data (cf. *Chem. Semiann. Prog. Rep. June 20, 1956*, ORNL-2159, p 43) an exponential equation in x_w was employed, which now is believed to have been inadequate theoretically.

Table 20. Terms in Eq. (3) for the Equivalent Volumes (ml/equiv) of Anion Exchanger Salt Forms

Salt Form	Terms				
	V_a	$\bar{v}_a^0$	b	$V_a - \bar{v}_a^0$	$(V_a - \bar{v}_a^0)/\phi_w^0$
Fluoride	210.9	199.3	0.648	11.6	0.642
Chloride	225.3	218.5	0.378	6.8	0.376
Bromide	231.8	226.5	0.292	5.3	0.293
Iodide	242.2	238.9	0.181	3.3	0.183
Fluoride-Bromide*	220.2	213.7	0.361	6.5	0.360
Chloride-Bromide*	228.5	222.0	0.359	6.5	0.360
Iodide-Bromide*	238.3	233.3	0.276	5.0	0.277

*Equimolar mixture, $x_{Br^-} = 0.5$.

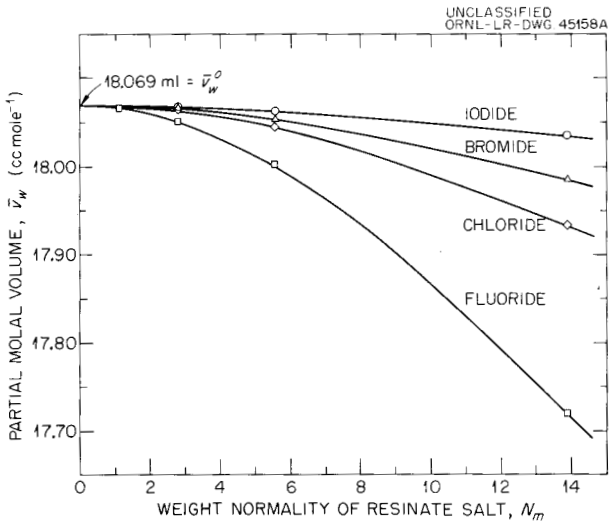

Fig. 15. Variation of Partial Molal Volume of Water with Weight Normality of Resinate Salt.

iodide salt form. Partial molal volume differences $(\bar{v}_1 - \bar{v}_2)$ were evaluated using the equation:[26]

$$(\bar{v}_1 - \bar{v}_2) = (V_1 - V_2) - \int_0^{x_w} \left(\frac{\partial \bar{v}_w}{\partial x_2}\right)_{x_m} dx_w \quad . \qquad (4)$$

A comparison of these values is made in Fig. 16 with the corresponding differences evaluated from density data on concentrated aqueous potassium and cesium halide solutions. The agreement, especially for $N_m = 0$, was gratifying.

---

[26] G. E. Myers and G. E. Boyd, *J. Phys. Chem.* **60**, 521 (1956).

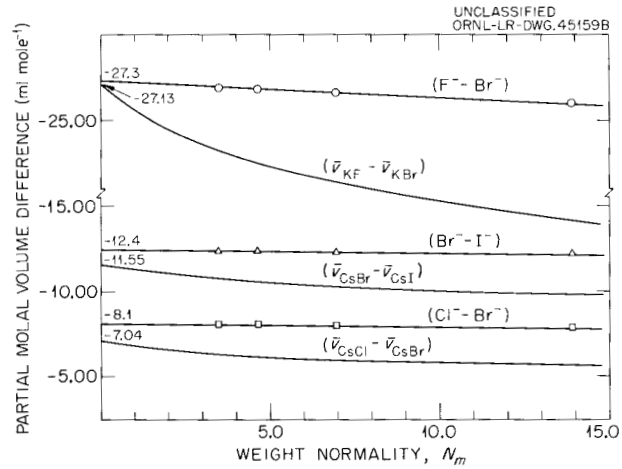

Fig. 16. Variations of Partial Molal Volume Differences of Resin Halides with Weight Normality.

CHEMISTRY OF CORROSION

ANION EFFECTS IN PASSIVE CORROSION SYSTEMS

R. F. Sympson[1] F. A. Posey

Previous reports[2-5] have summarized the history and results of studies on the effect of chloride and thiocyanate ions on the reduction of cupric species on passive stainless steel in oxygenated acidic sulfate solutions. More recent potentiostatic and galvanostatic measurements, together with spectrophotometric studies on important association equilibria in the systems, have provided considerable insight into the mechanism whereby thiocyanate ion catalyzes the over-all reduction rate of cupric species on passive stainless steel.

If it is assumed that the only effect of thiocyanate is the complexing of cupric ion to form the 1:1 complex (which is known to be the only important thiocyanato complex at the concentration levels studied[6]), potentiostatic experiments may be analyzed by use of Eq. (1):

$$\frac{i - i_0}{CD} = kK - K\frac{i}{C} \,. \qquad (1)$$

Here, i is the reduction current density of all cupric species at a fixed electrode potential, i_0 is the reduction current density of cupric ion in the absence of thiocyanate, k is the electrochemical specific rate constant for the reduction of $CuSCN^+$, K is the 1:1 association quotient of Cu^{++} and SCN^-, C is the total concentration of cupric ion in both forms, and D is the concentration of thiocyanate ($D >> C$). Plots of $(i - i_0)/CD$ vs i/C therefore allow determination of both k and K.

Analysis of a large amount of data shows that the form of Eq. (1) is essentially correct for describing the results of potentiostatic experiments, and that the rate constant k varies with electrode potential in a manner quite similar to that reported earlier for the reduction of cupric ion in the absence of thiocyanate.[7,8] However, spectrophotometric studies proved that calculated values of K are not even of the order of magnitude of the 1:1 association quotient of Cu^{++} and SCN^-. Moreover, K is a function of electrode potential, having a maximum in the potential region of a transition from one rate-determining step to another in the mechanism of cupric ion reduction. In addition, both k and K are functions of sulfate ion concentration and acidity.

Recognizing that, in fact, there are several important equilibria operative in the systems examined, and hence a number of cupric species with different specific rate constants for reduction, it is possible to understand the phenomenology outlined above. Together with the bisulfate ion dissociation equilibrium,[9] the reaction scheme of Eq. (2) adequately describes experimental observations:

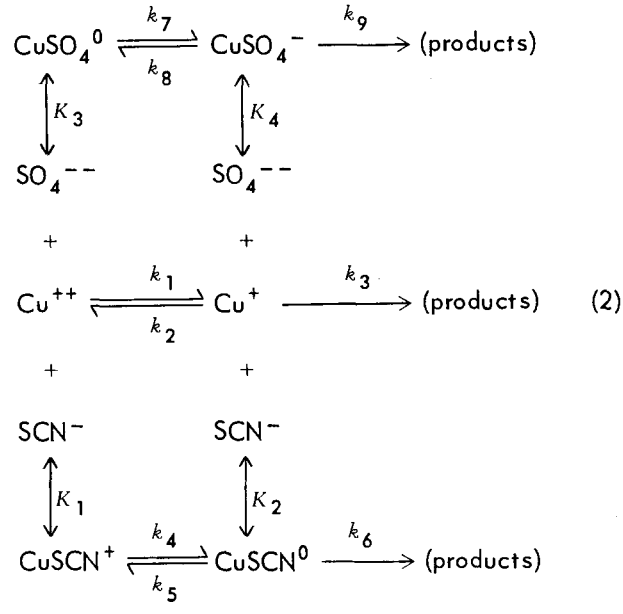

(2)

[1] Summer employee from Ohio University, Athens, Ohio.

[2] R. F. Sympson and G. H. Cartledge, *J. Phys. Chem.* **60**, 1037 (1956).

[3] G. H. Cartledge and R. F. Sympson, *Chem. Semiann. Prog. Rep. Dec. 20, 1955*, ORNL-2046, p 10.

[4] G. H. Cartledge, *Chem. Semiann. Prog. Rep. June 20, 1956*, ORNL-2159, p 66.

[5] R. F. Sympson and F. A. Posey, *Chem. Ann. Prog. Rep. June 20, 1959*, ORNL-2782, p 57.

[6] N. Tanaka and T. Takamura, *J. Inorg. & Nuclear Chem.* **9**, 15 (1959).

[7] F. A. Posey, *Chem. Ann. Prog. Rep. June 20, 1958*, ORNL-2584, p 65.

[8] F. A. Posey, G. H. Cartledge, and R. P. Yaffe, *J. Electrochem. Soc.* **106**, 582 (1959).

[9] F. A. Posey, *Chem. Ann. Prog. Rep. June 20, 1959*, ORNL-2782, p 56.

Here, Cu^{++}, $CuSCN^{+}$, and $CuSO_4^{0}$ are stable species in the bulk of the solution and at the interphase, Cu^{+}, $CuSCN^{0}$, and $CuSO_4^{-}$ are intermediates in the electrochemical reduction reactions at the passive interphase, K_1 through K_4 are association quotients, and k_1 through k_9 are electrochemical specific rate constants. Under certain experimental conditions, diffusion of stable cupric species from the bulk of the solution to the interphase, as well as diffusion of the intermediates away from the interphase, must be considered.

Equations for the over-all reduction current of the general case and of special cases of the reaction network of Eq. (2) have been derived. In addition, these have been put into the form of Eq. (1) so that k and K are expressible in terms of complicated functions of rate constants and equilibrium quotients of Eq. (2). However, the analysis is tedious and some of the detailed predictions cannot be confirmed experimentally because of certain limitations inherent in the passive system itself and because some important quantities cannot be evaluated using steady-state techniques and are not available from the literature. Nevertheless, gross features are accounted for, and considerable experience has been gained in dealing with complex kinetic situations where association reactions exert an important influence on observable electrochemical properties.

SPECTROPHOTOMETRY OF SULFATO AND THIOCYANATO CUPRIC COMPLEXES

F. A. Posey

Analysis of electrochemical kinetic data on systems containing cupric, sulfate, and thiocyanate ions is generally complicated due to complexing effects, and conversely may be greatly facilitated with a knowledge of association quotients of important equilibria. Although accurate values of the 1:1 association quotients of cupric ion with sulfate and with thiocyanate ions have been reported for the conditions 25°C and ionic strengths of zero or unity,[6,10–13] no reliable experimental data exist on the values of these quotients at more elevated temperatures and intermediate ionic strengths. Accordingly, a spectrophotometric study has been devoted to determining values of the 1:1 association quotients of Cu^{++} with SCN^{-} and of Cu^{++} with SO_4^{--} as a function of temperature from 25 to 65° in sodium perchlorate–perchloric acid solutions of selected ionic strength.

The 1:1 association quotient of Cu^{++} with SCN^{-} was determined in the spectral region 320–390 mμ by fitting experimental data at 15 wavelengths to Eq. (3):

$$\frac{CD}{I} = \frac{1}{\epsilon K_c} + \frac{C}{\epsilon} \quad . \tag{3}$$

Here, C is total cupric concentration, D is total thiocyanate concentration, K_c is the 1:1 (concentration) association quotient, I is the measured absorbancy vs H_2O in 1-cm cells, and ϵ is the molar extinction coefficient of the 1:1 complex, $CuSCN^{+}$. The absorbancy of uncomplexed cupric ion is negligible in this spectral region at the concentration levels employed, and the molar extinction coefficient of $CuSCN^{+}$ for the same region is given approximately as a function of temperature and wavelength by Eq. (4):

$$\log \epsilon(CuSCN^{+}) = 2.63_5 + 10^{-3}t - 2.01 \times \times 10^{-4}[\lambda - (340 + 0.167t)]^2 \quad . \tag{4}$$

In Eq. (4), t is temperature in degrees centigrade, and λ is the wavelength in millimicrons. Association quotients were measured at the temperatures 25, 34, 49, and 63°C for the ionic strengths 0.05 and 0.50.

Results are summarized in Eqs. (5) and (6) (T is absolute temperature):

$$\log K_c(\mu = 0.05) = -0.283 + 6.79 \times 10^2 \frac{1}{T} \quad , \tag{5}$$

$$\log K_c(\mu = 0.50) = -0.391 + 6.44 \times 10^2 \frac{1}{T} \quad . \tag{6}$$

Calculated energetic quantities have the following values: $\Delta H^{\circ}(\mu = 0.05) = -3.11$ kcal/mole; $(\Delta S^{\circ} - R \ln K_{\gamma})(\mu = 0.05) = -1.30$ e.u.; $\Delta H^{\circ}(\mu = 0.50) = -2.95$ kcal/mole; and $(\Delta S^{\circ} - R \ln K_{\gamma})(\mu = 0.50) = -1.79$ e.u. These quantities were calculated

[10] R. Näsänen, *Acta Chem. Scand.* **3**, 179, 959 (1949).

[11] S. Fronaeus, *Acta Chem. Scand.* **4**, 72 (1950).

[12] R. Näsänen and B. Klaile, *Suomen Kemistilehti* **27B**, 50 (1954).

[13] W. D. Bale, E. W. Davies, and C. B. Monk, *Trans. Faraday Soc.* **52**, 816 (1956).

from Eqs. (5) and (6) and the thermodynamic relation, Eq. (7):

$$\log K_c = \frac{\Delta S^\circ - R \ln K_\gamma}{2.303R} - \frac{\Delta H^\circ}{2.303R}\frac{1}{T} . \quad (7)$$

Here, ΔH° and ΔS° have their usual significance, R is the gas constant, and K_γ is the ratio of molar activity coefficients corresponding to K_c. Values of K_c calculated from Eqs. (5) and (6) for the temperature 25°C are in excellent agreement with values of other workers.[6]

A similar technique was used to obtain values of the 1:1 association quotient of Cu^{++} with SO_4^{--} in the spectral region 238–275 mμ, except that experimental data were fitted to Eq. (8):

$$\frac{CB}{\Delta I} = \frac{1}{\Delta\epsilon K_c} + \frac{B}{\Delta\epsilon} . \quad (8)$$

Here, C is total cupric concentration, B is total sulfate concentration, K_c is the (concentration) association quotient, ΔI is the difference in absorbancy of solutions with and without added sulfate at constant C, and $\Delta\epsilon$ is the difference in the molar extinction coefficients of $CuSO_4^0$ and Cu^{++}.

Measurements were made at 18 wavelengths in the region 238–275 mμ for the temperatures 25.0, 34.8, 44.0, 54.0, and 65.3°C at an ionic strength of 0.30, and the results are described by Eq. (9):

$$\log K_c(CuSO_4) = 2.01 - 3.26 \times 10^2 \frac{1}{T} . \quad (9)$$

From Eqs. (7) and (9), it may be seen that $\Delta H^\circ = +1.49$ kcal/mole and $\Delta S^\circ - R \ln K_\gamma = +9.20$ e.u. The large positive entropy change on complexing may be due to decreased solvent interaction with the uncharged complex as compared with the charged reactants.

POTENTIOSTATIC AND GALVANOSTATIC STUDIES ON PASSIVE STAINLESS STEEL

F. A. Posey

Systematic studies have begun on transients observed in potentiostatic and galvanostatic step-function experiments on passive stainless steel in aqueous solutions. Compared with the more commonly studied two-phase corrosion systems, passive stainless steel exhibits extremely slow transients, which may be measured precisely and conveniently with conventional recording equipment. Analysis of transients in passive systems is capable of yielding important information about the potential and charge-density profiles across the complex interphase between metal and solution as well as information about the Faradaic impedance of barriers to charge-transfer steps of processes occurring in the interfacial system.

Although no comprehensive, quantitative kinetic theory of the passive state exists, an electrical analog or equivalent circuit has been developed which exhibits transient behavior identical with that of the real passive systems. The chosen analog is a two-terminal network consisting of "leaky" capacitors in series, the exact number being determined by experimental criteria. The form of the particular circuit developed is dictated not only by the accuracy with which experimental data may be described, but also by the severe requirement that circuit elements be readily interpretable in terms of physical and kinetic parameters. Specifically, the potential difference across each capacitor is assumed to be the analog of a potential difference across an interphase or between consecutive electrochemical potential minima in the passive oxide. The magnitude of a capacitor is a function of the charge-density profile at the position of interest and of non-Faradaic processes which affect only transient behavior. In addition, each shunting resistor is the analog of the impedance of energy barriers to Faradaic processes in the system.

General equations have been derived, by use of matrix and Laplace transform techniques, for the response of the two-terminal equivalent circuit to step functions of current (galvanostatic experiment) or of potential (potentiostatic experiment). Direct application of the general equations to the analysis of experimental data in terms of the properties of the analog is possible provided changes of independent variables (potential or current) in an experiment are limited in magnitude, so that the behavior of the linear elements of the analog is a sufficiently good approximation to the nonlinear behavior of the real system. However, this is not a severe restriction in practice, and comparison of quantities calculated from transient and from steady-state measurements provides a sufficient check on the degree of approximation.

Results of preliminary transient experiments have provided remarkable confirmation of the validity of the "dual-barrier" model deduced earlier[7] to explain values of electrochemical transfer coefficients in the reduction of cupric ion on passive stainless steel. A comprehensive survey has begun on the effect of changes in such variables as temperature, acidity, and identity and concentration of cathodic reactants on the properties of the analog. It is anticipated that experiments of this type will provide necessary fundamental data on which the development of any kinetic theory of passivity must depend.

THE ELECTROCHEMISTRY OF ZIRCONIUM

R. E. Meyer

Film Formation[14]

Using an electrochemical method, rates of film growth in oxygenated sodium sulfate solutions have been measured on polycrystalline zirconium at temperatures ranging from 25 to 88°C. The resulting rate-time plots are roughly hyperbolic. A model is proposed which when treated by electrode kinetics is shown to give this type of behavior.

Reduction Processes

During the formation of a film on corroding zirconium, cathodic reduction of oxygen or other oxidizing agents proceeds at a total rate equal to the rate of the anodic process (film formation). A detailed study of some of these reduction processes was therefore undertaken. In all cases the environment was aqueous 0.1 M Na_2SO_4 in the pH range 2–5. The experimental portion of the work involved the determination of the constant α_z and the order p in the equation for the rate of reduction,

$$i = Ka^p \exp \frac{-\alpha_z FE}{RT} ,$$

where K is constant, a is the activity of the oxidizing agent, E is the electrode potential, and RT/F has the usual significance. The constant α_z is determined by measuring i as a function of E at constant a, and p is determined by measuring i as a function of a at constant E. Table 21 shows some results for crystal-bar zirconium. The current densities, i_{-100}, were measured at $a = 5 \times 10^{-4}$ M and $E = -100$ mv vs S.C.E.

Table 21. Reduction Rates on Passive Zirconium

Oxidizing Agent	i_{-100} (amp/cm^2)	Temperature (°C)	p	α_z
O_2	7×10^{-8}	75	0.7–1	0.31
UO_2^{++}	5×10^{-10}	75	1	~0.6
Cu^{++}	4×10^{-6}	66	0.66	0.3
H_2O_2	2×10^{-8}	66	0.4–0.6	0.25

The results for the current densities are not strictly comparable, since those for Cu^{++} and H_2O_2 were obtained at 66° and those for O_2 and H_2O_2 were measured at 75°. However, it is clear (*a*) that in any equimolar mixture of the oxidizing agents, almost all of the current would be carried by the copper, and (*b*) that the rate of reduction of UO_2^{++} would be small compared with that of the other oxidizing agents.

The measurements are not sufficient to determine detailed mechanisms for these reductions. However, all evidence obtained so far suggests that a two-step process is involved, the one corresponding to the ordinary double-layer process and the other to a process within the film. Kinetic equations derived from this model predict that fractional orders and α_z constants in the range 0.2 to 0.35 should be observed under some of the conditions encountered in these experiments. As shown in Table 21, these predictions have received some experimental verification.

Alloy Studies

Two alloys were selected for comparison with crystal-bar zirconium, namely, Zircaloy-2 and zirconium–15 wt % niobium. The work on the latter alloy has just begun, but considerable work was done on Zircaloy-2 in aqueous Na_2SO_4 in the pH range 2–5 and the temperature range 25–85°C. As with crystal-bar zirconium, reproducible results were obtained only if the sample was annealed in vacuum after a chemical polish. The results were interesting in that they showed no significant differences between Zircaloy-2

[14] Abstract of paper published in *J. Electrochem. Soc.* 106, 930 (1959).

and crystal-bar zirconium. Thus the 1.5% tin and the other alloying elements appeared to have no effect at all upon the rate-time behavior or the polarization characteristics of Zircaloy-2.

THE SIGNIFICANCE OF THE "EQUIVALENT REDOX POTENTIAL" IN IRRADIATED SYSTEMS

G. H. Cartledge

The so-called "equivalent redox potential"[15] refers to a single-electrode potential which was presumed to be characteristic of the solvent in irradiated solutions containing a redox couple. On the basis of electrochemical measurements made in this laboratory[16] and elsewhere, a qualitative interpretation of the phenomena was developed from kinetic considerations. It was concluded that the observed single potential is not a unique property of the solvent or its primary radiolytic products. Rather, the chief electrochemical effects may be ascribed to the longer-lived products H_2, O_2, and H_2O_2, so that the measured potential depends upon all factors that affect their activities at the surface of the electrode, as well as upon the polarization characteristics of the different electrode processes. The analysis has been published,[17] and the conclusions have received confirmation from further very recent experimental work at Harwell.[18]

STUDIES ON THE MECHANISM OF PASSIVATION

G. H. Cartledge

In the last progress report[19] brief reference was made to studies designed to determine the comparative roles of oxygen and reducible inhibitors in maintaining the passivity of iron. These studies have been extended, and the first two papers in the series will soon be published.[20] It was shown, by measurements of polarization, that reduction of oxygen alone on passive iron is rapid enough, at potentials in the passive region, to overcompensate the continuing steady-state corrosion current density. In an oxygenated pertechnetate solution under inhibiting conditions, reduction of oxygen was shown to be faster than that of the pertechnetate ion by more than an order of magnitude. It was found also that the reduction product, $Tc(OH)_4$, accelerates the cathodic processes significantly. Reduction of the chromate ion also was shown to be slow, in comparison with reduction of oxygen, and the reduction product does not accelerate cathodic processes. With OsO_4 as passivator, reduction of oxygen plays a subordinate role, and, again, the reduction product, $Os(OH)_4$, acts as an accelerator of cathodic processes. The results strengthen the previous assumption that adsorption of unreduced inhibitor plays a dominant role in the inhibitory process.

Further experiments were made to determine the ability of films on passivated iron to enter into ion exchange equilibria with solute species. Iron that had been passivated in an aerated pertechnetate solution was well washed with water and then with NH_4OH, which Kraus *et al.* have shown to displace chromate ions from bulk-oxide ion exchangers.[21] By counting the beta activity, it was shown that if TcO_4^- interacts at all by ion exchange with the passive film, only a small fraction of a monolayer is involved. Preliminary experiments with the chromate ion as inhibitor show an appreciable interaction.

INHIBITION OF THE DISSOLUTION OF IRON BY IODIDE IONS OR CARBON MONOXIDE

K. E. Heusler[22]

The effects of iodide ions and carbon monoxide as inhibitors for the dissolution of iron in 0.5 *f* sulfate at different pH values were presented in a previous report.[23] By use of tracer I^{131}, a study was made of the quantity of I^- adsorbed on the iron surface as a function of concentration and anodic current density. With no external

[15] F. S. Dainton and E. Collinson, *Discussions Faraday Soc. No. 12*, 251 (1952).

[16] W. E. Clark and G. H. Cartledge, *Chem. Semiann. Prog. Rep. June 20, 1956*, ORNL-2159, p 71.

[17] G. H. Cartledge, *Nature* **186**, 370 (1960).

[18] F. S. Feates, AERE-C/R 2801 (February 1960); F. S. Feates and B. Knight, AERE-R3091 (April 1960).

[19] G. H. Cartledge, *Chem. Ann. Prog. Rep. June 20, 1959*, ORNL-2782, p 51.

[20] G. H. Cartledge, *J. Phys. Chem.* (in press).

[21] K. A. Kraus *et al.*, *Proc. U.N. Intern. Conf. Peaceful Uses Atomic Energy, 2nd, Geneva, 1958*, **28**, 3 (1958).

[22] Present address, Max Planck Institut für Sondermetalle, Stuttgart, West Germany.

[23] K. E. Heusler, *Chem. Ann. Prog. Rep. June 20, 1959*, ORNL-2782, p 52–55.

current passing, the adsorption came to equilibrium within a few minutes; the process was shown to be reversible, and the quantity adsorbed could be related to the activity by either a Langmuir or a Temkin isotherm. From the Langmuir isotherm, a maximum adsorption of 2×10^{15} atoms per square centimeter of projected area was calculated for the open-circuit potentials. The adsorption was found to be decreased by passage of anodic current exceeding *ca.* 1 ma/cm^2. It is possible to account for the observations by a mathematical analysis which assumes an adsorption rate dependent upon the activity of I^- and the bare surface area, as in the Langmuir treatment, together with a rate of desorption which depends on both the covered surface area and the anodic current density.

THE CORROSION OF IRON IN THE PRESENCE OF BENZOATE IONS

E. J. Kelly

The study of the action of the benzoate ion as an inhibitor[24] has been extended by more detailed measurements in the active region. In deoxygenated perchlorate solutions, it was shown that, over a pH range from 0.8 to 4.5, the corrosion potential E_c of iron becomes less noble by $2.303RT/F$ per unit increase in pH; that is,

$$E_c = -0.060 \text{ pH} - 0.194 \ ,$$

where E_c is in volts vs the normal hydrogen electrode, at 30°C. Measurement of E_c at higher pH values is precluded by the lack of buffering action in perchlorate solutions. In this same pH region, the corrosion rate i_c of iron is independent of pH and has a value equivalent to approximately 1×10^{-4} amp/cm^2 (ref 25).

When benzoic acid is added to an acidic perchlorate solution at a fixed pH, the corrosion characteristics of iron remain essentially unaltered until the concentration of the inhibitor, benzoic acid plus benzoate ions, reaches a value of about 1×10^{-3} *f*. As the concentration is increased from 1×10^{-3} to 1×10^{-1} *f*, there is an adsorption of the inhibitor on the iron surface, this process being accompanied by an ennobling of the corrosion potential and a sharp decrease in the corrosion rate. At a fixed inhibitor concentration, the corrosion potential varies with pH just as in the noninhibited solution; that is, the corrosion potential drops about 60 mv per unit increase in pH. Furthermore, at a fixed inhibitor concentration, the corrosion rate is independent of pH, again as in the case of the noninhibited solution. These facts may be derived from the galvanostatic cathodic polarization curves shown in Fig. 17.

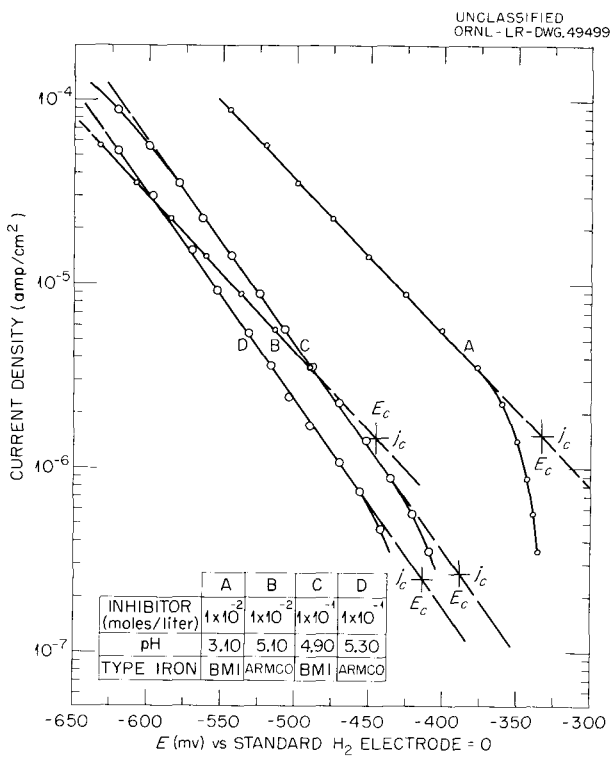

Fig. 17. Cathodic Polarization of Iron in Benzoate Solutions at 30°C. E_c and i_c are the observed open-circuit potential and indicated corrosion current density respectively.

Curves *A* and *B* were obtained for solutions having an inhibitor concentration of 1×10^{-2} *f* at pH values of 3.10 and 5.10 respectively. It is seen that the corrosion potential varies by approximately 60 mv per pH unit, and the corrosion rate i_c is constant at a value of 4.3×10^{-6} amp, or a current density i_c of 1.5×10^{-6} amp/cm^2. Curves *C* and *D* were obtained for solutions having an inhibitor concentration of 1×10^{-1} *f* at

[24] E. J. Kelly and G. H. Cartledge, *Chem. Ann. Prog. Rep. June 20, 1959*, ORNL-2782, p 51.

[25] K. F. Bonhoeffer and K. E. Heusler, *Z. physik. Chem.* (Frankfurt) 8, 390 (1956).

pH values of 4.90 and 5.30 respectively. Again, the corrosion potential varies by 60 mv per pH unit, and the corrosion current density is constant at 2.7×10^{-7} amp/cm^2. The results may be generalized at a pH of 5.10. At this pH, E_c = −0.501, −0.445, and −0.400 mv and $j_c = 1 \times 10^{-4}$, 1.5×10^{-6}, and 2.7×10^{-7} amp/cm^2 for 0, 1×10^{-2}, and 1×10^{-1} *f* inhibitor solutions respectively.

It was found that the corrosion characteristics of Armco iron and very pure zone-refined electrolytic iron (BMI) are essentially identical. For comparative purposes, it was also shown that the addition of $NaClO_4$ up to 0.5 *f* has no specific effect on the corrosion characteristics of iron in benzoic acid solutions.

The results of this investigation suggest that benzoic acid functions as an inhibitor by being adsorbed on the iron surface and thereby reducing the surface concentrations of the adsorbed intermediates of the anodic[26] and cathodic processes, [$FeOH^+$] and [H·] respectively, and, consequently, reducing the rates of these processes.

---

[26]K. E. Heusler, *Z. Elektrochem.* **62**, 582 (1958).

NONAQUEOUS SYSTEMS AT HIGH TEMPERATURE

HAZARDS OF FISSION PRODUCT RELEASE FROM IRRADIATED URANIUM

G. W. Parker

Continuing fuel-element catastrophe investigations have included a study of GE-ANPD fuel, which has been reported;[1] a study of UO_2 fuels suitable for power reactor use, which is in progress; and a recently completed study[2] of the oxidation of uranium in various atmospheres and of the attendant fission product release from irradiated uranium. The results of some experiments in which uranium was incompletely oxidized in air were summarized in a previous report.[3] The present report includes oxidation data obtained in CO_2, steam, and air and fission product release values obtained when irradiated uranium was completely oxidized (except in a steam atmosphere, where complete oxidation would have required an excessively long time).

Oxidation rates of irradiated uranium (0.2 at. % burnup) and unirradiated uranium in air, CO_2, and steam were compared at 800, 1000, and 1200°C. Irradiated uranium oxidized more rapidly than unirradiated uranium under the same conditions, both above and below the melting point of uranium. This shows that oxidation rates measured with unirradiated uranium cannot be applied directly to predictions of the oxidation behavior of highly irradiated uranium present in operating reactors. Figure 18 shows oxidation data obtained in different atmospheres by use of a thermobalance at 1200°C.

Fission products released when uranium irradiated at trace level was partially oxidized in air and steam were measured. Fission products released on oxidizing irradiated uranium (0.2 at. % burnup) in air, CO_2, and steam were also measured, and some experiments were performed to determine the fission products released when uranium irradiated at trace level and at 0.2 at. % burnup was melted in helium. Comparison of fission product release data obtained at 1200°C by another investigator[4] using uranium irradiated at trace level with data obtained in the present investigation, using uranium irradiated to a higher burnup level, showed that several fission products, including strontium, cesium, and rare gases, were released to a greater extent at the higher irradiation level.

The rare gases were essentially completely released on oxidizing irradiated uranium in air at 1000 to 1200°C, even with short burning times and low amounts of oxidation. After 20 min in air at 1000°C, uranium was about 50% oxidized and the iodine release approached 65%, cesium ~2%, and strontium ~0.05%. At 1200°C, uranium was 75% oxidized in 20 min; under these conditions about 70% of the iodine, 70% of the tellurium, 18% of the cesium, 2% of the ruthenium, and 2% of the strontium were released. The high ruthenium release values obtained from completely oxidized samples, as compared with the low values observed in partial oxidation experiments, indicated that ruthenium was released mainly near the end of the oxidation process.

Fractional releases of iodine and tellurium when irradiated uranium was oxidized in CO_2 at 1000 and 1200°C were comparable with those obtained in air. Ruthenium and cesium release values obtained in CO_2 were approximately one-tenth of the values in air at these temperatures. The release values obtained in steam were much lower than those obtained in CO_2 and air, except that at 1200°C tellurium was released to about the same extent in all three types of oxidizing atmospheres. A comparison of fission product release data obtained in different atmospheres is given in Table 22.

Fission product ratios calculated from the release data obtained in air at 1200°C were in very good agreement with reported fission product ratios calculated from measurements of fallout

[1] G. W. Parker, G. E. Creek, and W. J. Martin, *Preliminary Report on the Release of Fission Products on Melting GE-ANP Fuel*, ORNL CF-60-1-50 (January 1960).

[2] G. W. Parker *et al.*, *Fuel Element Catastrophe Studies: Hazards of Fission-Product Release from Irradiated Uranium*, ORNL CF-60-6-24 (June 1960).

[3] G. W. Parker, G. E. Creek, and W. J. Martin, *Chem. Ann. Prog. Rep. June 20, 1959*, ORNL-2782, p 15.

[4] R. K. Hilliard, *Fission Product Release from Uranium Heated in Air*, HW-60689 (August 1959).

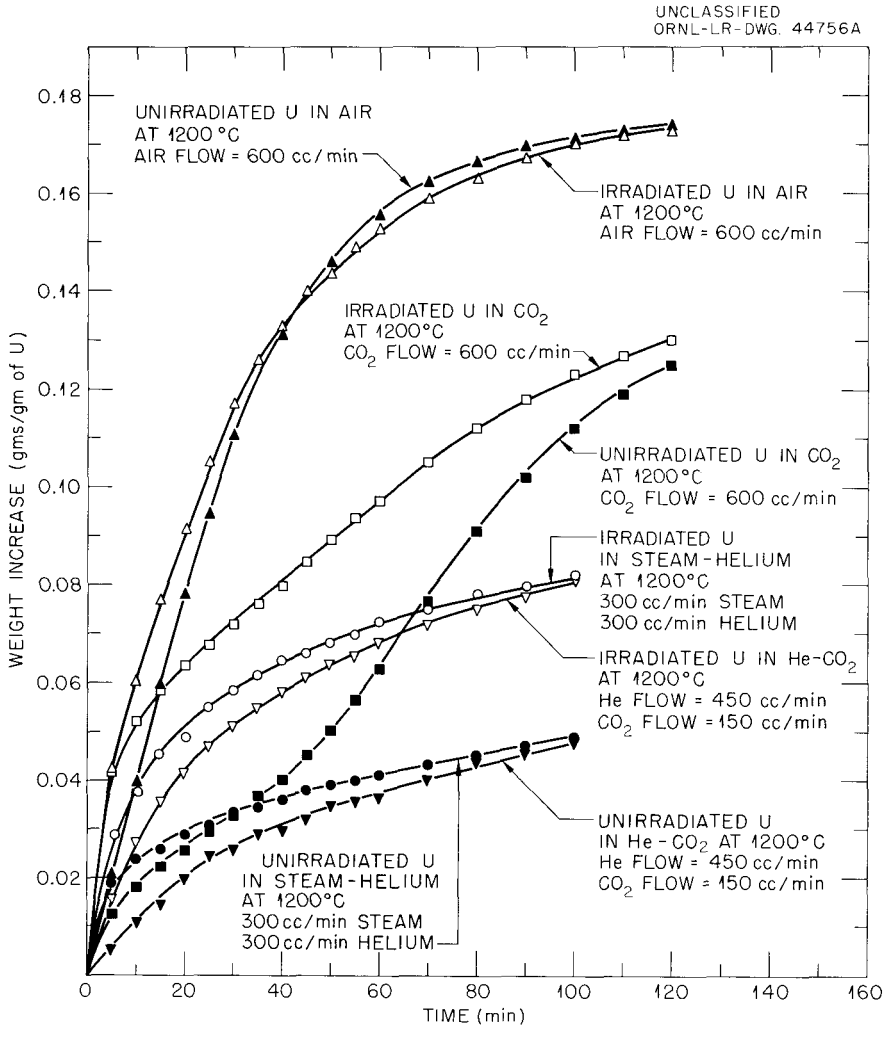

Fig. 18. Comparison of Oxidation Rates of Irradiated and Unirradiated Uranium in Steam, Air, and CO_2 at 1200°C.

following the Windscale incident.[5] The results of this comparison are shown in Table 23.

An interesting profile of the rate of rare-gas release by heating and cooling irradiated uranium in helium (Fig. 19) shows an accelerated release rate at the freezing temperature (1132°C) and at the β-α inversion temperature (660°C). Rapid cooling below 600° showed a final accelerated gas release which indicates that a concurrent increase in density may explain each of the accelerated releases.

[5]D. V. Booker, *Physical Measurements of Activity in Samples from Windscale*, AERE HP/R 2607 (October 1958).

Table 22. Comparison of Fission Product Release from Irradiated Uranium Heated in Various Atmospheres at 1200°C

Atmosphere	Run No.	Per Cent of Uranium Oxidized	Per Cent of Total Activity Released						
			Xe-Kr	I	Te	Cs	Ru	Sr	Zr
0.2 at. % Burnup									
Air	9-9-1	65.4	99.4	57.3	71.3	13.0	1.8	0.85	~0.05
Air	H-83	100	99.2	89.8	95.9	~14.0	85.0		0.01
CO_2	H-31	100	~99	52.7	69.4	1.7*	1.95	0.01*	0.1
CO_2-helium	H-62	90		68.4	95.2	0.93		0.01*	0.6
Steam-helium	H-61	65		15.3	79.4	0.2*	0.01	0.02*	0.2
Helium	8-12-1	4.1	97.7	47.0	0.6	2.0		0.9	
Trace-Level Irradiation									
Air	4-6-2	91.7	80.6	92.4	66.3	~1.0	0.6	~0.01	0.007

*Release values probably low due to chemisorption in mullite porcelain furnace tube.

Table 23. Analysis of Windscale Fission Product Release

Nuclide Observed	Activity Ratio from Fallout Filter Samples[a]	Approximate Ratio in Fuel on October 11[b]	Calculated Per Cent of Total Released[c]	Predicted Per Cent of Total Released[d]
I^{131}	100	1.0	70	~70
Te^{132}	58	0.75[e]	55	~70
Cs^{137}	2.6	0.08	15	~18
Sr^{89}	1.0	1.6	1.1	~2
Ru^{103}	2.0	1.0	1.4	~1.7
Zr^{95}	0.1	2.2	0.3	~0.04

[a]Data from D. V. Booker, *Physical Measurements of Activity in Samples from Windscale*, AERE HP/R 2607 (October 1958).

[b]Fission yield times per cent saturation, assuming 360 days irradiation; relative to I^{131} = 1.0.

[c]Assuming ~75% oxidation; based on 70% for I^{131}.

[d]Assuming average temperature of 1200°C; maximum reported was 1300°C.

[e]Ratio includes decay from October 7.

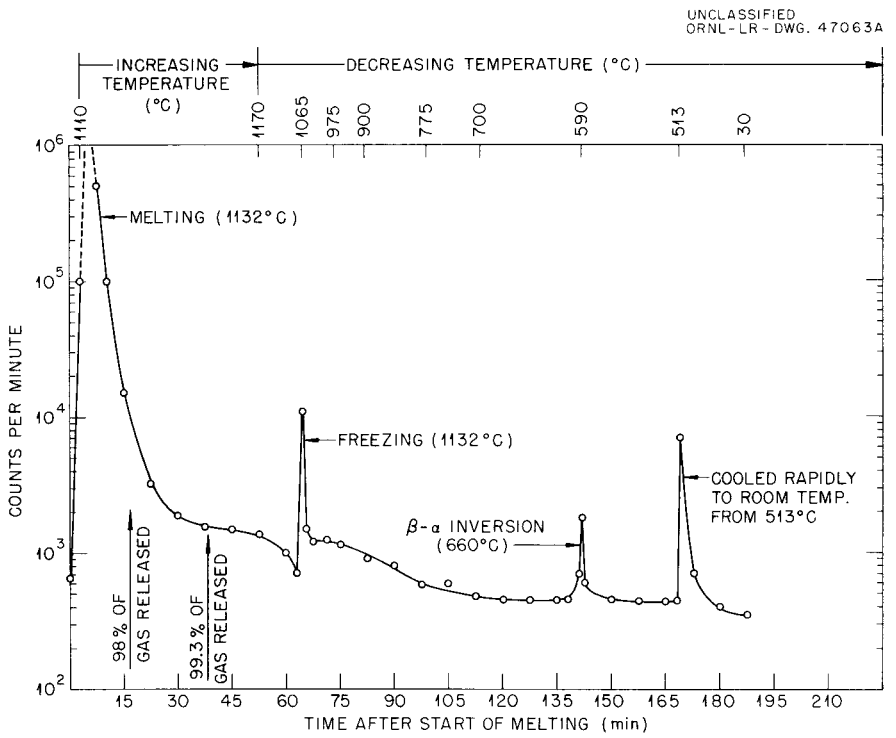

Fig. 19. Release of Fission Gas (Kr^{85}) from Irradiated Uranium (0.2% Burnup) Melted in Flowing Helium.

MOLTEN-SALT–METAL SOLUTIONS

Lithium–Lithium Chloride and Lithium–Lithium Iodide Systems

H. R. Bronstein A. S. Dworkin
M. A. Bredig

Attempts to determine the metal-salt phase equilibria in these systems by thermal analysis were unsuccessful. In the Li-LiF system,[6] thermal halts for liquid-liquid phase separation at 1300°C had been barely discernible at moderate lithium concentrations and none could be observed at lower concentrations because of the small temperature dependence of the solubility. Thus, recourse had to be taken to an equilibration-and-sampling method. An apparatus was built which permitted the direct sampling of the solution at temperature, as in some measurements on the sodium–sodium halide systems.[7]

The apparatus was a smaller modified version of the conductivity apparatus,[8] having only one entry port on the rotatable turret. Operation of the apparatus was similar to that for the conductivity measurements.[8] The lithium was introduced into the molten salt by means of a perforated stainless steel basket which was attached to a stainless steel rod and acted both as a container for the lithium and as a stirrer. The basket was removed after equilibration at temperature with stirring, and a sample of the molten salt-rich phase was taken by means of a sampling device previously described.[8]

The solubility of lithium in lithium chloride was found to increase from a value of 0.5 ± 0.2 mole % at 600°C to 1.0 ± 0.2 mole % at 1000°C. The solubility of lithium in lithium iodide increased from a value of 1.2 ± 0.5 mole % at 550°C to 2.5 ± 0.5 mole % at 950°C. These values are the lowest found as yet among the alkali-metal solubilities in their halides.

[6] M. A. Bredig, J. E. Sutherland, and A. S. Dworkin, *Chem. Ann. Prog. Rep. June 20, 1958*, ORNL-2584, p 74.

[7] M. A. Bredig and H. R. Bronstein, *J. Phys. Chem.* 64, 64 (1960); *Chem. Ann. Prog. Rep. June 20, 1959*, ORNL-2782, p 61–63.

[8] H. R. Bronstein and M. A. Bredig, *J. Am. Chem. Soc.* 80, 2077 (1958).

Cerium in Molten Cerium Trichloride

H. R. Bronstein A. S. Dworkin
M. A. Bredig

Investigations of the Ce-$CeCl_3$ system have lately yielded rather surprising results, such as a strange dependence of the electrical conductance on metal concentration,[9] a proposal of a novel, monovalent rare-earth ion, Ce^+, as the solute species,[10] and the enormous apparent molar volume of 500 cc per mole of mobile electrons, in dilute solution.[9] The recent discovery[11] of solid halides of divalent neodymium and praseodymium supports our own view that cerium enters the solution in molten $CeCl_3$ as Ce^{++}, but clarification of the aforementioned findings appeared desirable.

In agreement with available thermodynamic data, we found that refractory oxides such as sintered alumina (Morganite Triangle RR) or sapphire single crystals are not suited for use with even dilute solutions of cerium in molten $CeCl_3$, as they react readily to form cerium oxychloride according to:

$$M_xO_y + \frac{2y}{3}\,Ce + \frac{y}{3}\,CeCl_3 \longrightarrow y\,CeOCl + x\,M$$

On the basis of these findings it is certain that the data obtained in the emf and conductivity measurements which had been carried out in Morganite crucibles[9,10] did not pertain to the Ce-$CeCl_3$ system! Rather, the added cerium must have been largely, if not completely, converted to CeOCl. Although under the circumstances any attempt at interpretation of those measurements must be inadequate, the observed emf[10] may perhaps be ascribed to a cell such as

$$Mo\,|\,MoO_2(solid),\ CeOCl,\ CeCl_3\,||\,CeCl_3\,|\,Cl_2$$

with variable oxygen concentration in the form of CeOCl. We are now in the process of developing methods of investigating the Ce-$CeCl_3$ and similar systems in such a manner as to avoid reaction with unsuitable container materials. Of particular interest is the question whether the simultaneous presence of two valence states of cerium, Ce^{++} and Ce^{+++}, leads to a high electron mobility.

[9] G. W. Mellors and S. Senderoff, *J. Phys. Chem.* **64**, 294 (1960).

[10] S. Senderoff and G. W. Mellors, *J. Electrochem. Soc.* **105**, 224 (1958).

[11] L. F. Druding and J. D. Corbett, *J. Am. Chem. Soc.* **81**, 5512 (1959).

The Electrical Conductivity of Molten Salts: LiI, CsF, and $CeCl_3$

H. R. Bronstein A. S. Dworkin
M. A. Bredig

In the course of electrical conductivity measurements on solutions of lithium metal in molten lithium halides, which failed due to reaction of the solutions with the cell material (MgO), the conductivity of pure LiI was measured.

The method of measurement has been described previously.[8] The apparatus has been modified as described above ("Lithium–Lithium Chloride and Lithium–Lithium Iodide Systems," this report). The conductivity cell was made from a single crystal of MgO, and the crucible containing the molten salt, the cell holder, and the electrode were molybdenum.

The specific conductivity κ over a temperature range of about 150°C is shown in Table 24. The temperature is defined to ±1°C, and the precision of κ is about ±0.2%. Our results are from 10 to 15% higher than those of Yaffe and Van Artsdalen.[12]

[12] I. S. Yaffe and E. R. Van Artsdalen, *J. Phys. Chem.* **60**, 1125 (1956).

Table 24. Specific Conductivity of Molten Salts

Salt	Temperature (°C)	κ ($ohm^{-1} \cdot cm^{-1}$)
LiI	481	4.01
	507	4.13
	541	4.31
	561	4.40
	603	4.59
	647	4.76
$CeCl_3$	828	1.12
	844	1.17
	868	1.23
	895	1.30
	931	1.38
CsF	737	2.51
	749	2.68
	758	2.65
	784	2.73
	813	2.85
	852	3.03

This is believed to be due to the reported partial decomposition of their LiI, which appears not to have occurred in our measurements.

An unsuccessful attempt to measure the conductivity of the Ce-$CeCl_3$ system was made, as reported in the preceding section ("Cerium in Molten Cerium Trichloride," this report). In the process, the conductivity of pure $CeCl_3$ was measured using a synthetic sapphire cell and a molybdenum container, cell holder, and electrode. The results, good to about ±1%, are shown in Table 24. They are about 22% higher than those reported by Senderoff.[9]

It was noted that among the alkali halides, the equivalent conductance decreases with increasing cation size when the anion is constant. Cesium fluoride was an exception, its reported conductivity[13] being greater than those for the fluorides of the remaining alkali metals. Since the conductivity of KF reported by Yaffe and Van Artsdalen[13] had already been found to be in error,[14,15] it was decided to repeat the CsF measurements. A magnesia cell and a platinum container, cell holder, and electrode were used. The results, shown in Table 24, are about 25% lower than those of Yaffe.[13] This places the equivalent conductance of CsF below those of the other fluorides, in agreement with the trend noted above.

Heat of Fusion Measurements

A. S. Dworkin M. A. Bredig

The determination of the heats of fusion of the alkali halides by means of a copper block calorimeter[16] was completed. The following additional values (in kcal/mole) were obtained: NaCl, 6.69; RbF, 6.15; RbCl, 5.67; RbBr, 5.57; and RbI, 5.27. The calorimetric heats of fusion of the rubidium halides are much larger than the noncalorimetric heats reported in the earlier literature.

A description of the apparatus, a comparison of our heats with those in the literature, and a discussion of the trends in the heat and entropy of fusion of the alkali halides were given in detail in a paper published recently.[17]

Neutron and X-Ray Diffraction Study of Molten Cesium Fluoride

P. A. Agron M. D. Danford
M. A. Bredig H. A. Levy

Diffraction patterns of molten cesium fluoride obtained with neutrons and x rays are shown in Fig. 20. The procedures for collection and treatment of data were substantially as described previously[18] with some modification to ensure containment of this reactive salt at high temperature. In the x-ray study, a platinum tray was designed to minimize creep of the melt, and an enclosing cup of molybdenum, with a delta ring gasket of the same material, incorporating a 0.0005-in. molybdenum foil window gold-brazed to its walls, replaced the beryllium enclosure previously described. For the neutron study, a cell of high-purity vanadium was successful in containing the melt over a period of about a week.

In Fig. 21, curves *A* and *B* show the radial distribution functions derived respectively from the x-ray and neutron data. As in the previous study, the peak at the shortest distance is attributed to the anion-cation nearest-neighbor configuration; from the x-ray and neutron curves are obtained the estimates 2.85 A for the most frequent nearest-neighbor distance and 3.7 ± 0.1 for the number of nearest neighbors. As in studies of other alkali halides,[18] both of these are significantly smaller than found at the melting temperature in the solid, 6 neighbors at 3.12 A (by extrapolation).

The second peak of each function is attributed to the unresolved superposition of like-atom second neighbors, that is, Cs-Cs and F-F. In this case, comparison of the x-ray and neutron curves suggests a partial differentiation between these distributions. Since F is the stronger scatterer for neutrons and Cs for x rays, F-F should be the more prominent peak in the neutron curve. The lesser distance, 4.25 A, found in this curve thus probably indicates a closer approach of

[13] I. S. Yaffe and E. R. Van Artsdalen, *Chem. Semiann. Prog. Rep. June 20, 1956*, ORNL-2159, p 79.

[14] H. R. Bronstein and M. A. Bredig, *Chem. Ann. Prog. Rep. June 20, 1959*, ORNL-2782, p 60.

[15] E. W. Yim and M. Feinleib, *J. Electrochem. Soc.* 104, 626 (1957).

[16] A. S. Dworkin and M. A. Bredig, *Chem. Ann. Prog. Rep. June 20, 1959*, ORNL-2782, p 61.

[17] A. S. Dworkin and M. A. Bredig, *J. Phys. Chem.* 64, 269 (1960).

[18] H. A. Levy *et al.*, *Ann. N. Y. Acad. Sci.* 79, 762–80 (1959).

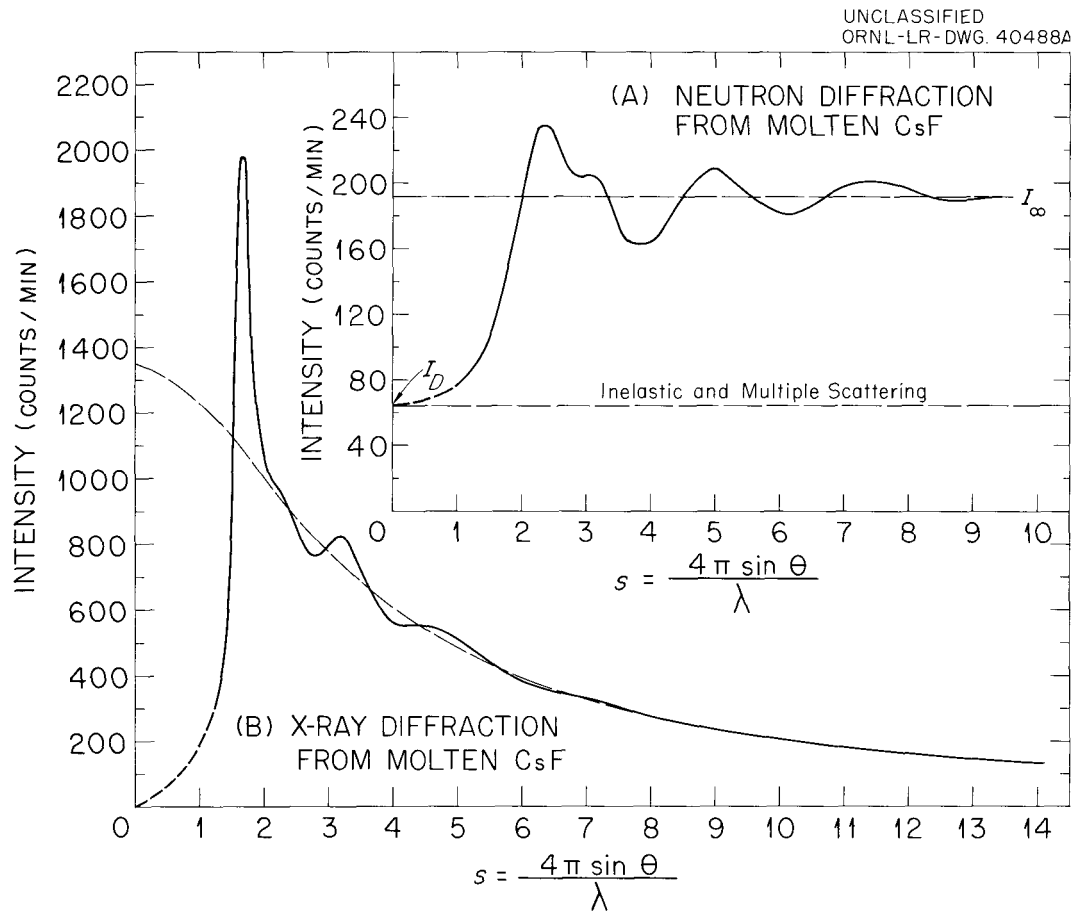

Fig. 20. Neutron (A) and X-Ray (B) Diffraction Patterns for Molten Cesium Fluoride.

F to F than of Cs to Cs, in accordance with the ionic sizes.

Linear combinations of the radial distribution functions derived from x rays and neutrons can be constructed in which one of the three interaction types, Cs-F, Cs-Cs, or F-F, is removed; the result portrays a weighted distribution of the remaining interactions. Curves *C*, *D*, and *E* of Fig. 21 show three such linear combinations in which the Cs-Cs, F-F, and Cs-F interactions, respectively, have been removed, and somewhat improved reduction is consequently available in the remaining function.

If a third independent radial distribution function can be obtained, a complete resolution of the distribution according to interaction type can be accomplished. Plans are under way to collect such data for molten RbCl, using the separated stable isotopes of Rb and Cl.

X-Ray Diffraction Study of Solid and Molten Bismuth(I) Chloroaluminate

P. A. Agron M. D. Danford
M. A. Bredig H. A. Levy

This study was undertaken to provide information on the nature and structure of bismuth(I) species. The compound $BiAlCl_4$ was chosen because it is known to be a well-defined compound with apparently congruent behavior on melting.

The molten state, investigated first, yielded a radial distribution function (Fig. 22, top) having a prominent, relatively sharp peak near 3 A which strongly indicates a polymeric bismuth species. However, because it is unresolved from a broad peak at larger distance, it was not possible to establish its area and, hence, the number of bismuth atoms in the species. Detailed analysis into two peaks was equally successful assuming 2, 3, or 4 bismuth atoms in the configuration,

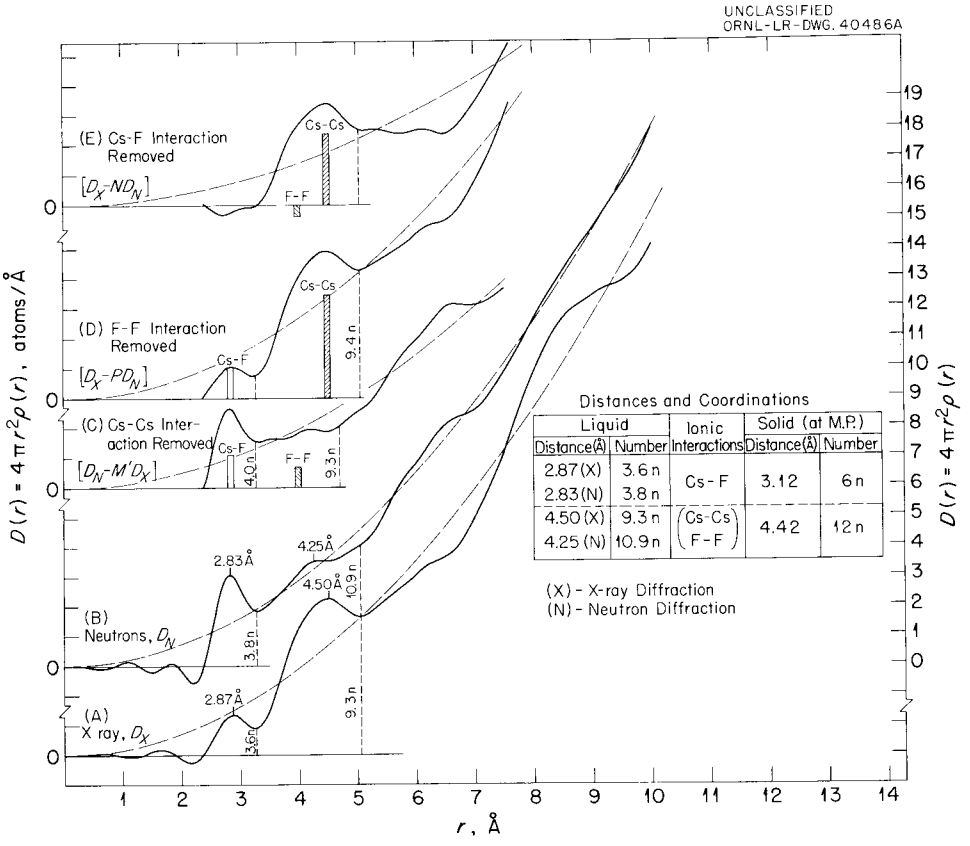

Liquid		Ionic Interactions	Solid (at M.P.)	
Distance(Å)	Number		Distance(Å)	Number
2.87(X)	3.6 n	Cs-F	3.12	6n
2.83(N)	3.8 n			
4.50(X)	9.3 n	(Cs-Cs) (F-F)	4.42	12n
4.25(N)	10.9n			

Fig. 21. Radial Distribution Functions from Molten Cesium Fluoride: (A) from X Rays; (B) from Neutrons; (C), (D), and (E), Linear Combinations Which Remove Respectively the Cs-Cs, F-F, and Cs-F Interactions. The rectangles under curves (C), (D), and (E) indicate the weights associated with one interaction in each curve. Note that F-F has negative weight in curve (E).

except that the number 4 was somewhat disfavored by unreasonable temperature factors.

A study of the solid was then undertaken. Examination of single crystals, reported separately, established the space group and the unit-cell dimensions. However, the difficulty of handling small single crystals, of correcting intensities for strong absorption by bismuth, and the complexity of the problem showed that a complete structure analysis, although highly desirable, would be a major undertaking. As an alternative, it appeared that a study of the crystalline powder, by methods similar to those used on the melt, might provide desirable information concerning the configuration of bismuth atoms with a minimal investment of effort.

The $BiAlCl_4$ was prepared by fusing stoichiometric amounts of Bi, $BiCl_3$, and $AlCl_3$ in vitreous silica under vacuum. The tubes were opened in a dry glove box, and the red solid was ground, screened, and packed into a platinum tray with precautions to minimize preferred orientation. The tray, sealed in a beryllium enclosure cup while in the glove box, was transferred to the diffractometer, and x-ray data were collected by step-scanning methods. Collection of data from the solid covered not only the angular range in which Bragg lines appear, but also the high-angle region in which only thermal-diffuse interferences were observed. This extended angular range is essential if full resolution in the radial distribution function is to be realized.

For study of the melt, the sample was contained in a tray of vitreous silica mounted within a sealed cylinder of the same material, with walls ground to 0.010 in. thickness for transmission of x rays. Data were collected at three temperatures, 265, 235, and 310°C. Only the data taken at 265°C were analyzed in detail.

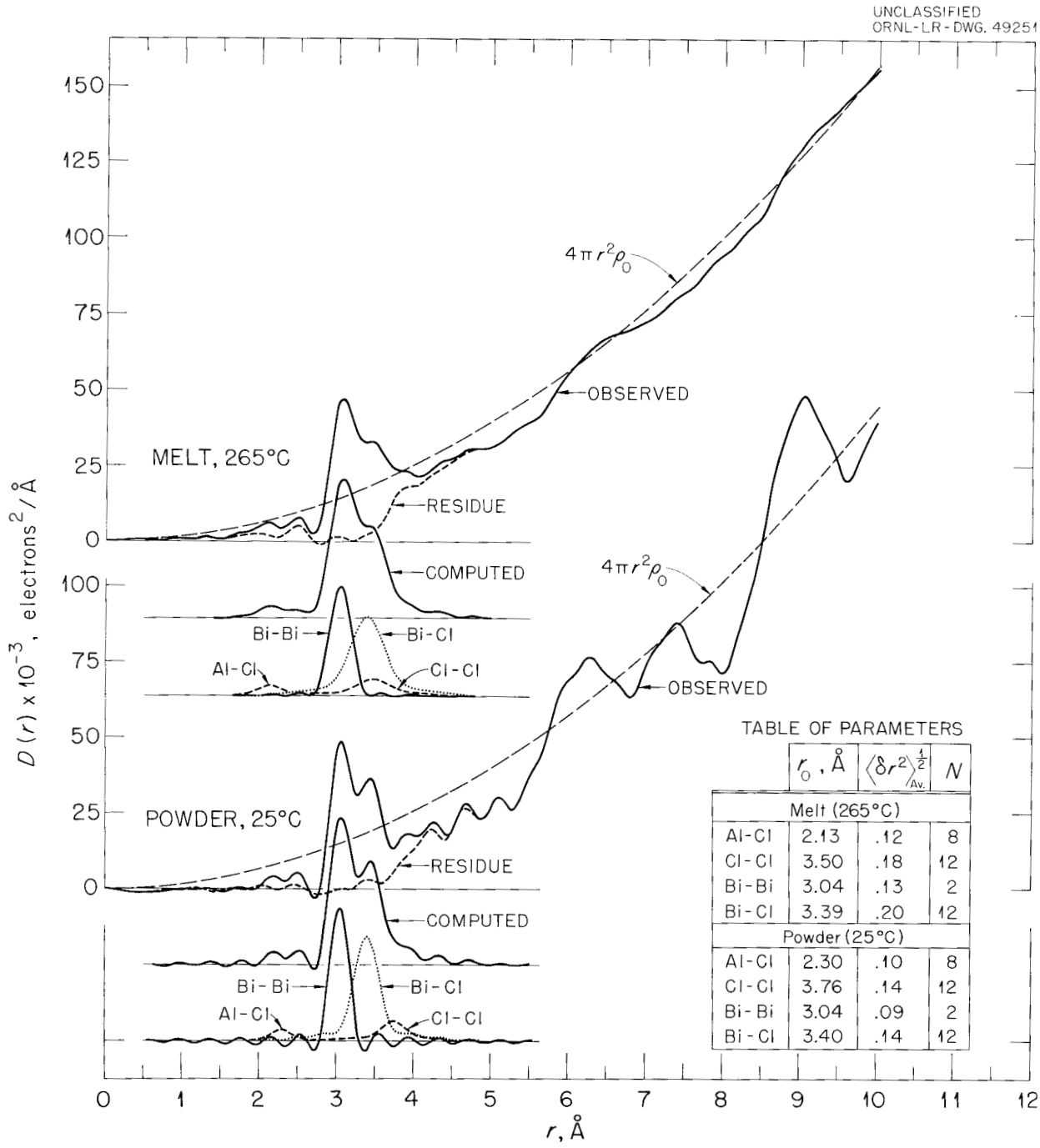

	r_0, Å	$\langle \delta r^2 \rangle_{Av.}^{\frac{1}{2}}$	N
Melt (265°C)			
Al-Cl	2.13	.12	8
Cl-Cl	3.50	.18	12
Bi-Bi	3.04	.13	2
Bi-Cl	3.39	.20	12
Powder (25°C)			
Al-Cl	2.30	.10	8
Cl-Cl	3.76	.14	12
Bi-Bi	3.04	.09	2
Bi-Cl	3.40	.14	12

Fig. 22. Radial Distribution Functions and Summary of Interatomic Distances and Numbers of Interactions for Bismuth (I) Chloroaluminate Melt and Powder.

Examination of the resolved Bragg diffraction lines of the crystalline powder confirmed the identity of the powder and single-crystal samples, and the powder spacings were employed in a least-squares refinement of the unit-cell dimensions.

Figure 22 shows the radial distribution functions from the solid and melt, together with curves indicating the analysis of each into components. Comparison of the solid and liquid functions indicates that configurations in the two states are exceedingly similar. Analysis of the function

from the solid indicates a Bi-Bi separation of 3.04 A and an estimate of two bismuth neighbors per bismuth atom, thus suggesting a trimeric species. This configuration is, in fact, confirmed by the observed space group of the crystal, since the only positions available for equivalent atoms with a separation of 3 A are related by a triad axis. Thus, the trimeric species $(Bi_3)^{+++}$ may be considered to have been established in the solid and to be highly probable in the melt.

Parameters resulting from analysis of the two radial distribution functions are listed in the table inset on Fig. 22. The second prominent peak is attributed to Bi-Cl interactions at about 3.4 A; other features are explained in terms of the Al-Cl and Cl-Cl interactions of an $AlCl_4^-$ tetrahedron.

The diffraction pattern from the melt showed pronounced intensity at scattering angles less than 4°, corresponding to a broad distance spectrum of the order of 50 A. The intensity of this scattering decreased rapidly as the temperature was raised, suggesting that relatively long-range ordering persists above the melting temperature and breaks up as the temperature rises.

The finding of a trimeric species $(Bi_3)^{+++}$ casts considerable doubt on the proposal of the existence in the $BiCl_3$-Bi system of a species $(Bi_2)^{++}$ reminiscent of the neutral gaseous species Bi_2 but involving a double bond.[19] An attempt to reinterpret the cryoscopic and vapor pressure data that appeared to be consistent with $(Bi_2)^{++}$ is under way. The trimeric species is in a sense analogous to the tetrameric neutral molecules P_4 and As_4, which have the configuration of a regular tetrahedron. Removal of one atom along with its six binding electrons leaves a triangular configuration $(M_3)^{+++}$.

[19] M. A. Bredig, *J. Phys. Chem.* **63**, 978 (1959).

CELL SIZE AND SPACE GROUP OF BISMUTH(I) CHLOROALUMINATE

P. A. Agron R. D. Ellison
M. D. Danford H. A. Levy

The crystallographic unit cell size and space group of bismuth(I) chloroaluminate were determined from single-crystal x-ray diffraction patterns taken by means of the Buerger precession camera. The crystal was found to be rhombohedral, with probable space group $C_{3v}^6 - R_3c$, and cell size of $a = 12.115$ A, $\alpha = 58° 23'$. The corresponding hexagonal cell is $a = 11.83$ A, $c = 30.00$ A. Because of the difficulty of handling this very reactive material, the density, 3.0 ± 0.1 g/cc, was found by taking the weight of material fused into a cylindrical container of known dimensions. The theoretical density, based on six molecules in the rhombohedral unit cell (18 in the hexagonal cell), is 3.108 g/cc.

The powder diffraction data referred to in the preceding section of this report ["X-Ray Diffraction Study of Solid and Molten Bismuth(I) Chloroaluminate"] were used to refine the accuracy of the cell-size measurement. The Bragg angles of 12 clearly resolved reflections were corrected for instrumental error by comparison with nearby reflections of yttrium oxide, which was used as an internal standard. These 12 lines were then used to obtain a least-squares fit of the cell: $a = 11.835 \pm 0.003$ A, $c = 29.991 \pm 0.009$ A.

CHEMICAL PHYSICS

CALORIMETRY

Low-Temperature Heat Capacity of Potassium Hexabromorhenate(IV)

R. B. Bevan, Jr. R. H. Busey

The low-temperature heat capacity of K_2ReCl_6 exhibits an unusual series of three cooperative-type transitions with maxima occurring at 76, 103, and 111°K.[1] These observations prompted the determination of the low-temperature heat capacity of the similar compound, K_2ReBr_6. The heat capacity of K_2ReBr_6 was measured with the liquid-helium-cooled calorimeter[2] from 7 to 300°K. The results are presented graphically in Fig. 23. The inset is a detail of the cooperative-type transition with a maximum at 15°K. The curious behavior of the heat capacity above 200°K must correspond to that observed[1] for K_2ReCl_6 from 90 to 120°K. The phenomenon is unexplained for both compounds.

The entropy of the K_2ReBr_6 at 298.15°K is 108.47 cal·deg^{-1}·mole^{-1}. An estimate of the excess entropy associated with the 15°K anomaly is 1.2 cal·deg^{-1}·mole^{-1}. This is approximately half the magnetic entropy of R ln 4 = 2.75 cal·deg^{-1}·mole^{-1} possessed by K_2ReBr_6 at high temperatures due to three unpaired electrons in the 5*d* orbit with their spins free but their orbital momentum quenched by the crystalline field. The magnetic susceptibility[3] of K_2ReBr_6 follows the Curie-Weiss law (80 to 300°K) with a molecular field constant $\Delta \sim 105°$ and a magnetic moment of 3.84 Bohr magnetons (theoretical for three "spin-only" electrons = 3.87). The magnitude of the molecular field constant suggests that a heat capacity anomaly is to be expected around 100°K. The absence of an anomaly around this temperature and the appearance of one at 15°K shows the need for extension of the magnetic susceptibility measurements to liquid-helium temperatures.

To complete the series of measurements on these rhenium compounds the low-temperature heat capacity of K_2ReF_6 will be measured. Because of its quite different chemical properties, K_2ReI_6 is not expected to fall in this class. Heat capacity measurements will be conducted on the corresponding technetium compounds for comparison.

[1] R. H. Busey, H. H. Dearman, and Q. V. Larson, *Chem. Ann. Prog. Rep. June 20, 1956*, ORNL-2159, p 11.

[2] R. B. Bevan, Jr., R. A. Gilbert, and R. H. Busey, *Chem. Ann. Prog. Rep. June 20, 1959*, ORNL-2782, p 73.

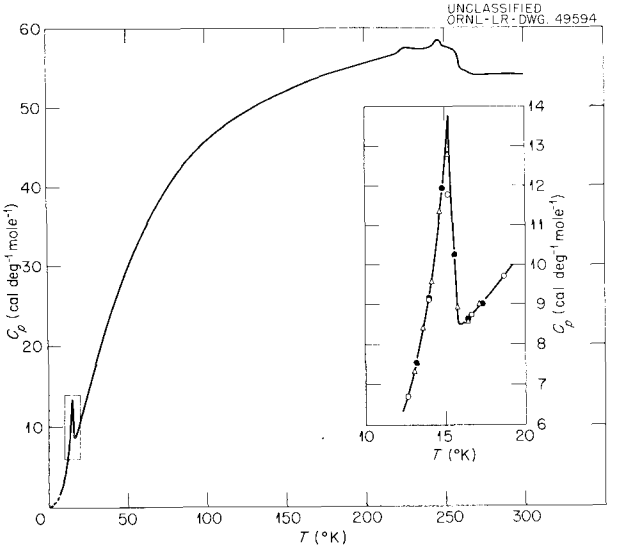

Fig. 23. Low-Temperature Heat Capacity of K_2ReBr_6.

Enthalpy of Standard Al_2O_3 from 0 to 900°C

R. A. Gilbert R. H. Busey

The enthalpy of a Calorimetry Conference standard sample of synthetic sapphire[4] has been measured with the Bunsen ice calorimeter[5] over the range 0 to 900°C. Measurements were made every 100°, several determinations at each temperature being made on the sample capsule and on the sample capsule plus sample. The results are presented in Fig. 24, which gives both the per cent deviation and absolute deviation of the smoothed enthalpies of this research from the smoothed values reported by investigators[4] at the National Bureau of Standards. The results average 0.07 cal/g higher than the NBS values over the temperature range studied. Above 200°C the average deviation is +0.08%; below 200° the per

[3] N. Perakis, *Compt. rend.* **206**, 1369 (1938).

[4] G. T. Furukawa *et al.*, *J. Research Natl. Bur. Standards* **57**, 67 (1956).

[5] R. A. Gilbert, *Chem. Ann. Prog. Rep. June 20, 1958*, ORNL-2584, p 96.

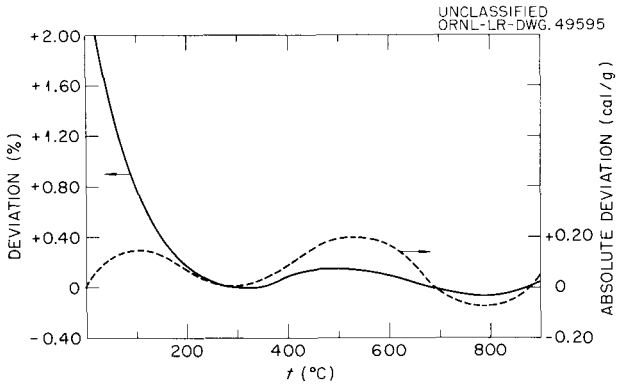

Fig. 24. Comparison Between Smoothed Enthalpies of This Work (ORNL) and the NBS Smoothed Values. Absolute deviation is the ORNL minus the NBS value.

cent deviation rises because of the relatively small magnitude of the enthalpy. The most difficult enthalpy to measure was that at 100°C, where it was most possible to have a temperature difference between the sample and the thermometer since radiation is not yet the preponderant mode of heat transfer at this temperature.

A single determination of the enthalpy of LiF at 898°C has been made as the first step in a study of heats of solution in fused alkali fluoride salt mixtures. The enthalpy obtained, 698.1 cal/g, affords an additional spot check on the accuracy of the calorimeter, since it may be compared with the value 693.8 cal/g reported by NBS investigators.[6] The deviation, +0.6%, approaches the upper limit, ±0.5%, of the absolute error reported by these investigators.

CHEMICAL KINETICS BY MOLECULAR BEAM TECHNIQUES

S. Datz R. E. Minturn
E. H. Taylor

Two papers were published[7] describing the characteristics of thermal emission of positive ions from heated tungsten filaments. Such positive ion emission is a source of noise in the surface ionization gage for the detection of molecular beams. The papers have been abstracted previously.[8]

The detector end of the apparatus used to study chemical kinetics by the crossed-molecular-beams technique[9] was redesigned. The new design allows better angular resolution of scattered signal by providing independent movement, from outside the vacuum system, of the detector slits and the differential detector filaments. Placement of the final collimating slits, the scattering center, and the cross beam source with its collimating system on an optical bench which also holds the detector assembly permits precise adjustment of beam incidence angles and detector filament alignment. Scattering by residual gases and by reflected beams is minimized in the new design by surrounding the reaction center completely with liquid-nitrogen-cooled cold traps.

An investigation of the kinetics of the hydrogen-deuterium exchange reaction by the crossed-molecular-beams technique was initiated. The apparatus, part of which is indicated schematically in Fig. 25, was substantially completed. A beam of hydrogen atoms, from a thermal dissociation source, is to intersect a beam of molecular deuterium emanating from a "wrinkle slit" at liquid-hydrogen temperatures. Reaction products are to be measured as a function of scattering angle by means of a mass spectrometer detector utilizing a 14-stage electron multiplier. The hydrogen atom beam is to be pulsed at a rate of 1.08 kc by a mechanical chopper, and the signal from the multiplier is fed into a phase-sensitive electronic network. For very low product-ion intensities, consideration is being given to detection by pulse counting techniques. The construction of the electronic components of the apparatus is at a well-advanced stage.

ANOMALOUS NEUTRON SCATTERING EXPERIMENTS

H. G. Smith S. W. Peterson

Breit-Wigner dispersion theory implies that the neutron scattering amplitude is complex, thus that there is a component of scattering which is 90°

[6] T. B. Douglas and J. L. Dever, *J. Am. Chem. Soc.* **76**, 4826 (1954).

[7] R. E. Minturn, S. Datz, and E. H. Taylor, *J. Appl. Phys.* **31**, 876 (1960); S. Datz, R. E. Minturn, and E. H. Taylor, *J. Appl. Phys.* **31**, 880 (1960).

[8] R. E. Minturn, S. Datz, and E. H. Taylor, *Chem. Ann. Prog. Rep. June 20, 1959*, ORNL-2782, p 74.

[9] E. H. Taylor and S. Datz, *J. Chem. Phys.* **23**, 1711 (1955).

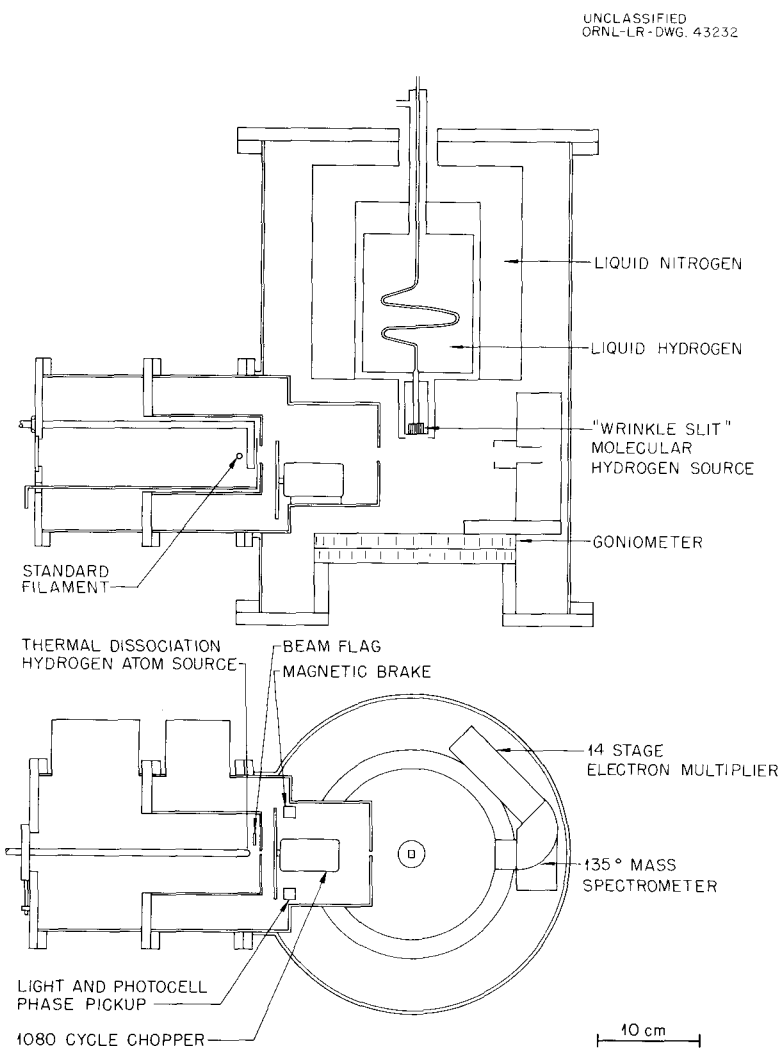

Fig. 25. Schematic Diagram of an Apparatus to Investigate the Kinetics of the Hydrogen-Deuterium Exchange Reaction.

out of phase with normal scattering. This out-of-phase or imaginary component is normally expected to be small at thermal energies except for the case of nuclides with high neutron absorption, and thus strong resonances, in the thermal region. The existence of complex scattering amplitudes implies the existence of corollary crystallographic phenomena such as the failure of Friedel's law for neutron diffraction and an energy dependence of the scattering amplitude. These phenomena are familiar ones in x-ray scattering and have been applied to determination of absolute configuration and to solution of the phase problem in crystal structure analysis. Discovery of the related phenomena in the neutron case has been retarded due to lack of high-intensity neutron beams and suitable crystals. Recent experiments at the ORR have shown decisively that anomalous coherent scattering effects are readily observable in Bragg scattering of neutrons from appropriate materials. Both Friedel's law failure and the energy dependence of the coherent neutron cross section have been demonstrated. In addition, magnitudes of the imaginary contribution to the cross section have been measured as a function of energy, yielding results in good agreement with the Breit-Wigner formulation.

Cadmium Sulfide. – The first clear evidence for the anomalous scattering effect was obtained with cadmium sulfide crystals, chosen because they are noncentrosymmetric and contain a strong neutron absorber, the Cd^{113} isotope. The experiments consisted of measurement of integrated intensities of (hkl) and $(\bar{h}\bar{k}\bar{l})$ mates of a series of

reflections at several wavelengths. Friedel's law states that $I_{hkl} = I_{\bar{h}\bar{k}\bar{l}}$; in other words, the diffracted intensities from the opposite sides of a plane in a crystal should be equal. However, this is known to be strictly true only when the scattering amplitude is real. Therefore, in the absence of other perturbing phenomena, failure of Friedel's law is convincing evidence of a complex amplitude and anomalous scattering.

Figure 26 gives convincing evidence of Friedel's law failure for several pairs of (00*l*) reflections in CdS. The phase relations are such that the (004) and (008) pairs should give equal intensities while the (002), (006), and (0010) pairs can be expected to give unequal intensities if the cadmium scattering amplitude is complex. Approximate values for the scattering amplitudes of cadmium as a function of wavelength, as determined from these measurements, are listed below:

	$\lambda = 0.87$	$\lambda = 0.94$	$\lambda = 1.075$	$\lambda = 1.38$	$\lambda = 1.88$
f'_{Cd}	0.35	0.35	0.35	0.35	0.35
f''_{Cd}	0.21	0.16	0.12	0.08	0.06
$\lvert f_{Cd} \rvert$	0.41	0.38	0.37	0.36	0.35

(λ is in angstroms; f values are cm $\times 10^{12}$).

Cadmium Iodide. – In order to give confirmatory evidence and because the crystal structure was more favorable, crystals of CdI_2 were prepared and checked for anomalous scattering. Observations of Friedel's law failure were made on a considerable number of reflections and at several wavelengths, including the wavelength corresponding to the peak of the cadmium resonance. These results confirm the existence of the anomalous scattering phenomenon for coherent neutron scattering and are expected to yield accurate values for the various scattering parameters.

Crystals of highly enriched $Cd^{113}I_2$ were also prepared, and Friedel's law failure was observed at one wavelength for several reflections. The accuracy of these measurements is in doubt because of the extremely high absorption; however, it is clear that the real component of the Cd^{113} scattering amplitude is negative, as would be expected for neutrons on the low-energy side of the resonance.

Boron Phosphide. – The B^{10} isotope of boron is a strong absorber of thermal neutrons, and it is to be expected that boron should also exhibit anomalous scattering of thermal neutrons. It differs from cadmium in that the boron absorption is attributed to a negative energy level, the magnitude of which is large compared with thermal energies. In this case Friedel's law failure is to be expected, but no energy dependence of the scattering amplitude is to be expected in the thermal region.

Single crystals of boron phosphide which have the noncentrosymmetric cubic zinc sulfide structure were examined for violations of Friedel's law. Although the effects were expected to be small,

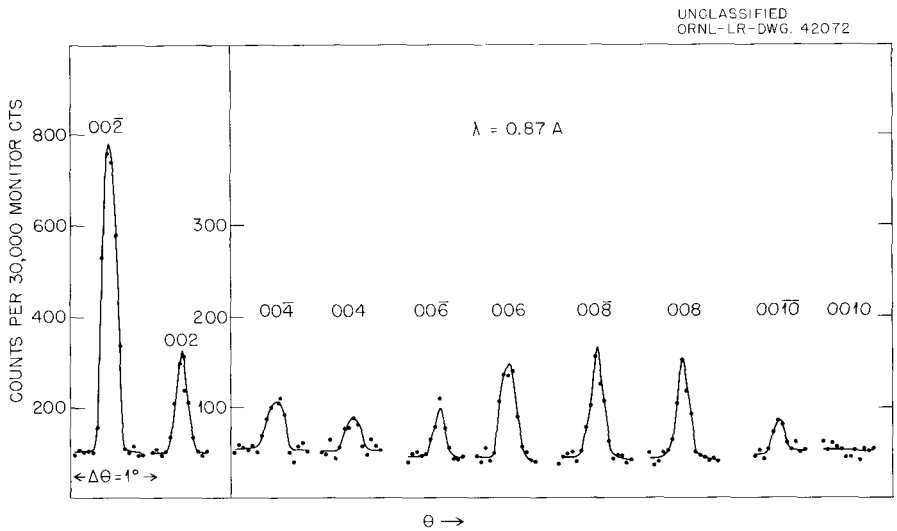

Fig. 26. Anomalous Neutron Scattering from CdS.

they were definitely observed in eight out of nine possible cases. In addition to confirmation of anomalous scattering from boron, a neutron scattering amplitude of approximately 0.5×10^{-12} cm was measured for boron. More precise values of the real and imaginary terms will be available later.

SINGLE-CRYSTAL NEUTRON DIFFRACTION STUDY OF HYDRAZINE

W. R. Busing M. Zocchi[10]
H. A. Levy

An x-ray study of hydrazine, N_2H_4, has been reported by Collin and Lipscomb (refs 11 and 12) who showed the structure to be monoclinic with space group $P2_1/m$ or $P2_1$. Although these authors favored the former symmetry, the hydrogen positions which they proposed would require the latter.

A single-crystal neutron diffraction study of this compound is now in progress, and the intensities of 53 reflections of the $(h0l)$ zone have been measured. A Fourier projection based on this data clearly revealed the four nonequivalent hydrogens and showed that the symmetry must be $P2_1$. A preliminary least-squares refinement gave the following x and z coordinates.

	x	z
N_1	0.036	0.359
N_2	−0.259	0.055
H_1	0.036	0.449
H_2	0.301	0.361
H_3	−0.396	0.009
H_4	−0.129	−0.125

The N_1-H_4 distance in this projection is 1.07_5 A; this is close to the expected bond length, so that this bond must lie nearly in the x,z plane. The other N-H bonds with shorter projections must lie out of this plane, which means that, contrary to the conclusion of Collin and Lipscomb, the molecular configuration is probably either the staggered C_2 or staggered C_{2h} geometry described by these authors.[12]

[10]Guest scientist from the Comitato Nazionale per le Ricerche Nucleari, Rome, Italy.

[11]R. L. Collin and W. N. Lipscomb, *Acta Cryst.* **4**, 10 (1951).

[12]R. L. Collin and W. N. Lipscomb, *J. Chem. Phys.* **18**, 566 (1950).

SINGLE-CRYSTAL NEUTRON DIFFRACTION STUDY OF $Sr(OH)_2 \cdot 8H_2O$

W. R. Busing M. Zocchi[10]
H. A. Levy

Neutron diffraction intensities have been measured for 224 reflections of the (hhl), $(h0l)$, and $(hk0)$ zones of $Sr(OH)_2 \cdot 8H_2O$. The results are consistent with the x-ray structure reported by Smith,[13] and a preliminary least-squares refinement of the parameters, assuming isotropic temperature factors, gave a discrepancy factor of 20% in F^2. The x-ray study did not locate the Sr atom unambiguously, but the present work shows the position postulated by Smith to be correct. Each water molecule is hydrogen-bonded to a hydroxide ion and to another water molecule. The hydroxide ions are hydrogen-bonded to each other in linear chains.

A COMPUTER PROGRAM TO PRODUCE STEREOSCOPIC PICTURES OF CRYSTAL STRUCTURES

W. R. Busing H. A. Levy

A program has been prepared to plot stereoscopic pictures of crystal structures on the cathode-ray-tube output of the IBM-704 computer. Two 35-mm negatives are produced for each view, and these may be mounted directly for use as stereo slides. The input to the program includes the cell parameters, the atomic coordinates, symmetry information, a list of the atoms and bonds to be plotted, and a specification of the directions from which the structure is to be viewed.

Each atom is represented as a number of points distributed on the surface of a sphere of specified radius, and the unit cell edges and interatomic bonds are plotted as loci of points of specified linear density. As the first step in the program, the computer stores the Cartesian coordinates x, y, and z of each of these points, in effect preparing a three-dimensional crystal structure model. Then, for each picture to be plotted, a rotation matrix is generated which transforms the stored points to the coordinate system x', y', z', where z' is parallel to the direction of view. The coordinates of each point on the cathode-ray tube are then obtained from x' and y' by making a correction for perspective which depends on z'.

[13]H. G. Smith, *Acta Cryst.* **6**, 604 (1953).

The intensity of each plotted point is also made a function of z', so that near points appear darker than far ones. Pictures for each eye and for any direction of view are obtained by modifying the rotation matrix appropriately.

A STRUCTURE PROPOSAL FOR $Na_7Zr_6F_{31}$

P. A. Agron R. D. Ellison

A structure for $Na_7Zr_6F_{31}$, one of the binary phase compounds occurring in the NaF-ZrF_4 system, was proposed. The details of this proposal are contained in a published note.[14] Work is continuing to elucidate further details of this structure.

MICROWAVE AND RADIO-FREQUENCY SPECTROSCOPY

Hydrogen Gas and Atomic Hydrogen Yields from Irradiated Acids

R. Livingston A. Weinberger

Earlier reports[15] have described results of assays for atomic and molecular hydrogen from irradiated acids. Solutions of sulfuric, phosphoric, and perchloric acids have been cooled to 77°K, irradiated with gamma rays from Co^{60}, and then assayed for atomic hydrogen by the paramagnetic resonance method. Similarly irradiated samples have been melted and the hydrogen gas collected and assayed. A correspondence between atom and molecule yields was found. The study has been extended to include measurements of the saturation concentration of atomic hydrogen upon prolonged irradiation. Sulfuric acid (0.129 mole fraction) irradiated as a glass at 77°K gives a saturation concentration of 3.4×10^{18} hydrogen atoms per gram, while perchloric acid (0.125 mole fraction) gives 2.9×10^{19}. Other additional experiments have been made to study the scavenging effects of nitric acid and hydrogen peroxide. For example, nitric acid added to 0.129 mole fraction sulfuric acid causes the atomic hydrogen yield upon irradiation to be reduced. A 2% addition of nitric acid completely suppresses the yield of atomic hydrogen. There is an accompanying scavenging effect on the molecular hydrogen yield. This program has now been completed, and all the results have been submitted for publication.[16]

Diluted Single Crystals of α,α-Diphenyl-β-picrylhydrazyl

R. Holmberg R. Livingston

The last annual report[17] described preliminary results on a paramagnetic resonance study of diluted single crystals containing α,α-diphenyl-β-picrylhydrazyl (DPPH). One of the nitrogen atoms of the free radical was to be replaced by N^{15} as an aid in experimentally deducing the two tensors that describe the hyperfine interactions for the two hydrazyl nitrogen atoms. These tensors have been evaluated and interpreted on the basis of an s-p model with the following electron densities: for the α nitrogen, $a_s^2 = 0.011$ and $a_p^2 = 0.263$, with the two parts having the same sign of spin density; for the β nitrogen, $a_s^2 = 0.024$ and $a_p^2 = 0.396$, or $a_s^2 = 0.010$ and $a_p^2 = 0.605$. The two choices for the β nitrogen arise from an ambiguity in interpreting the hyperfine tensor, but with either choice the two parts have the same sign of spin density. The total unpaired electron spin density found on the two nitrogen atoms is 0.694 or 0.889 depending on the choice made for the β nitrogen. This program has been completed and submitted for publication.[18]

Paramagnetic Resonance Study of Irradiated Single Crystals of Calcium Tungstate

H. Zeldes R. Livingston

The initial results of a study of irradiated crystals of calcium tungstate at 77°K have been described.[19] The spectra of two paramagnetic species formed by the irradiation were observed, and experiments indicated these two species to be the related halves of the radiation effect in the

---

[14] P. A. Agron and R. D. Ellison, *J. Phys. Chem.* 63, 2076 (1959).

[15] See, for example, R. Livingston and A. Weinberger, *Chem. Ann. Prog. Rep. June 20, 1959*, ORNL-2782, p 64.

[16] R. Livingston and A. Weinberger, "Atomic and Molecular Hydrogen Yields from Irradiated Acids," to appear in *J. Chem. Phys.*, August 1960.

[17] R. W. Holmberg and R. Livingston, *Chem. Ann. Prog. Rep. June 20, 1959*, ORNL-2782, p 65.

[18] R. W. Holmberg, R. Livingston, and W. T. Smith, Jr., "Paramagnetic Resonance Study of Hyperfine Interactions in Single Crystals Containing α,α-Diphenyl-β-picrylhydrazyl," to appear in *J. Chem. Phys.*, August 1960.

[19] H. Zeldes, R. W. Holmberg, and R. Livingston, *Chem. Ann. Prog. Rep. June 20, 1959*, ORNL-2782, p 64.

initially diamagnetic crystal. Moreover, the measured g values indicate that one of these species contains a surplus electron while the other is electron-deficient (hole). An anomaly in the hyperfine interaction[19] for W^{183} in the electron-deficient center has been explained, and it has clearly been demonstrated that this species contains two tungsten atoms. The hyperfine interaction for this species is isotropic, and the unpaired electron must be highly localized in orbitals of atoms other than tungsten, presumably oxygen. On the other hand, the electron surplus center contains one atom of tungsten, the hyperfine interaction with W^{183} is anisotropic, and the electron could have a large probability distribution in tungsten orbitals. This center could be, for example, WO_4^{---}, but from the symmetry of the measured g values it must be formed near a lattice defect. Experiments with heat-treated crystals indicate lattice defects to be important for this radiation effect.

Paramagnetic Resonance Study of Irradiated Single Crystals of Sodium Nitrite

H. Zeldes

Paramagnetic resonance measurements of single crystals of gamma-irradiated $NaNO_2$ containing a small amount of $AgNO_2$ have been completed and are being analyzed. The spectrum consists of a single group of three well-resolved N^{14} hyperfine lines. From symmetry considerations it is clear that this spectrum arises from a species with point symmetry C_{2v} at the position of the N atom which is responsible for the hyperfine structure. The data fit a Hamiltonian with electron spin of $\frac{1}{2}$ of the form

$$\mathcal{H} = \beta H \cdot g \cdot S + S \cdot A \cdot I \ ,$$

where H is the applied field, S and I are the electron and N^{14} spin operator in units of $\hbar$, β is the Bohr magneton, and g and A are tensors for the spectroscopic splitting factor and the hyperfine coupling respectively.

The g and A tensors are diagonal in the orthorhombic crystal axes. Where the crystal a, b, and c axes are defined by Wyckoff,[20] the principal values of these tensors are

$g_a = 2.0057$ $\qquad A_a/\beta = 98.9$ gauss

$g_b = 2.0015$ $\qquad A_b/\beta = 135.9$ gauss

$g_c = 1.9910$ $\qquad A_c/\beta = 93.5$ gauss

The data are being fitted to a simple model for NO_2, which most likely is the radical giving the spectrum above.

VAPOR-PHASE ASSOCIATION OF ALKALI HALIDES[21]

S. Datz

Molecular association equilibria in alkali halide vapors were studied by measuring the temperature dependence of the molecular weights of gaseous sodium chloride, sodium bromide, sodium iodide, potassium chloride, potassium iodide, rubidium chloride, and cesium chloride. The molecular weights were determined by measurement of the absolute pressure exerted by a known weight of completely vaporized salt contained in an isothermal fused silica bulb of known volume. The pressure-sensing element consisted of a fused silica U-tube manometer containing molten gold, and pressures were determined by measuring the argon pressure necessary to balance the gold manometer. The apparatus was used in the temperature range 1175 to 1430°K, and pressures of from 10 to 40 mm were measured with a precision of ±0.05 mm.

The temperature dependence of the equilibrium constants for the reaction $(MX)_2 \rightleftharpoons 2MX$ yielded dissociation energies (evaluated at 1300°K) ranging from 48.0 kcal/mole for sodium chloride to 34.7 for cesium chloride. The entropies of dissociation were found to fall within a small range, varying from 28.3 e.u. for sodium chloride to 25.0 for potassium iodide, and a statistical calculation of the entropy changes based on an ionic model was found to agree well with the experimental values. It is shown that these systems may be adequately described with an electrostatic model, although closer attention should be paid to the nature of polarization interactions.

[20] R. W. G. Wyckoff, *Crystal Structures*, Interscience, New York, 1951.

[21] Abstract of paper submitted for publication in *J. Chem. Phys.* See also S. Datz and W. T. Smith, Jr., *Chem. Ann. Prog. Rep. June 20, 1959*, ORNL-2782, p 59; S. Datz and W. T. Smith, Jr., *J. Phys. Chem.* 63, 938 (1959).

MASS SPECTROMETRY AND RELATED TECHNIQUES

Studies of Reaction Rates, Free Radicals, and a Stable Intermediate from Catalytic Reactions of $CO_2 + D_2$ and 1-C_4H_8[22]

C. E. Melton

A stable intermediate and free radicals displaced from the surface of a catalyst have been identified by studying heterogeneous reactions occurring within a research mass spectrometer. For this investigation the ion source (Fig. 27) was modified by inserting a Pt catalyst in the ionization chamber. The catalyst was a spiral of 0.5-mm Pt wire, 3 × 13 mm with a surface area of ~1 cm^2. The temperature of the catalyst was directly determined by means of an optical pyrometer and calculated from the known value of the heater current. Evolved products from a heterogeneous reaction on the catalyst passed directly into the electron beam and either positive or negative ions were formed. The resultant ions were accelerated into the analyzer tube, separated by the analyzer magnet, and finally detected by the multiplier. Displaced free radical products were identified by maintaining the energy of the ionizing electrons below that necessary for the appearance of interfering fragment ions from the reactant gases. Products from the heterogeneous reactions were studied as a function of catalyst temperature, pressure, and concentration of each reactant.

The reaction

$$D_2 + CO_2 \xrightarrow{Pt} D_2O + CO \qquad (1)$$

was studied as a function of pressure over the range 0.1–1 mm and as a function of temperature over the range 50–1000°C. A free radical, whose molecular formula is CDO, is shown to be formed by and displaced from the Pt catalyst during the reaction. Experiments using isotopic labeling

[22] Abstracted from a paper submitted for publication in *J. Chem. Phys.*

UNCLASSIFIED
ORNL-LR-Dwg. 42950a

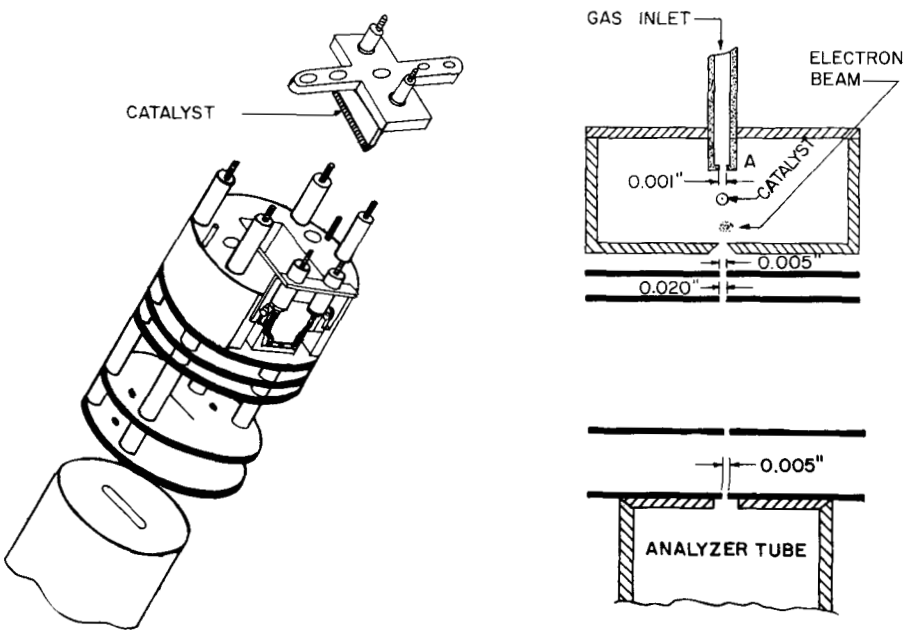

Fig. 27. Mass Spectrometer Ion Source for Catalysis Studies.

suggest that the radical is formed with a C–O–D structure rather than the carbonyl oxygen structure, but probably rearranges in the gas phase to the DCO structure. Both the negative and positive ions from possible intermediates are shown in Table 25. A perusal of this table shows that DCOOD is a possible stable intermediate in the reaction. The D_2CO_3 side product could be formed either on the catalyst or by a reaction in the gas phase. From this study the following rate law was obtained:

$$V = \frac{(CO_2)}{1 + b(CO_2)} \cdot \frac{(D_2)}{1 + c(D_2)} ,$$

where b is less than 0.5 and c is greater than 4. A tentative mechanism is also suggested to be:

$$D_2 + CO_2 \longrightarrow \underset{S}{D} + \underset{S}{COOD}$$

$$CO_2 + \underset{S}{COOD} \longrightarrow CO + COD + \underset{S}{O} + \underset{S}{O}$$

$$\underset{S}{O} + \underset{S}{D} \longrightarrow \underset{S}{OD}$$

$$D_2 + \underset{S}{OD} \longrightarrow D_2O + \underset{S}{D}$$

where S signifies the Pt surface.

The behavior of the D^+ ion intensity from D produced by the reaction

$$D_2 \xrightarrow{Pt} D + D$$

is shown in Fig. 28. Although the observed $D^+/D_2{}^+$ ratio was $\frac{1}{10}$, the concentration of D was probably less than 0.01%. This anomaly is explained on the basis of the higher ionization potential for D_2 (15.4 to 13.6) which results in a much lower detection sensitivity for D_2 than for D with 16-ev electrons. While monitoring the D^+ intensity, CO_2 was admixed to the system. The results, shown in Fig. 29, suggest (*a*) that the D^+ observed is produced by the catalytic decomposition of D_2, and (*b*) the presence of CO_2 inhibits the production of D by poisoning the catalyst. Mechanisms for reaction (1) were not studied at 1000°C, since the reaction has been reported to be both homogeneous and heterogeneous at this temperature; instead the reaction was investigated at 600°.

Free radicals produced by the catalytic decomposition of 1-butene were compared to those known to occur from thermal decomposition at the same temperature. In the catalytic decomposition, the radicals C_4H_7 and C_3H_5 are most abundant as shown in Table 26, the former having the higher intensity, whereas CH_3 and C_3H_5 are most abundant in the thermal decomposition.

Table 25. Free Radicals and Intermediates Detected in the Reaction $D_2 + CO_2 \xrightarrow{Pt} D_2O + CO$

m/e	Ion	Probable Precursor	Probable Source of Precursor
2	D^+, D^-	D	$D_2 \xrightarrow{Pt} D + D$
20	D_3O^+	D_2O, D_3O	D_3O displaced $D_2O^+ + D_2O \longrightarrow D_3O^+ + OD$ $D_2O^+ + D_2 \longrightarrow D_3O^+ + D$
30	CDO^+	CDO	CDO displaced
46	$DCOO^-$	DCOOD, COOD	$CO_2 + D_2 \xrightarrow{Pt}$ DCOOD or COOD
60	CO_3^-	D_2CO_3, CO_3	$D_2O + CO_2 \xrightarrow{Pt} D_2CO_3$ or CO_3
62	DCO_3^-	D_2CO_3, DCO_3	$D_2O + CO_2 \xrightarrow{Pt} D_2CO_3$ or DCO_3

UNCLASSIFIED
ORNL-LR-Dwg. 48198

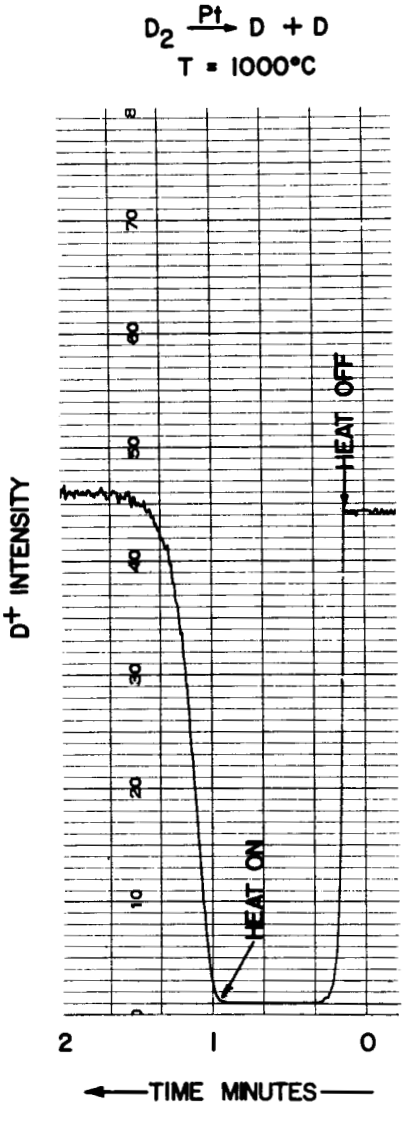

Fig. 28. Dissociation of D_2 on Platinum, Showing the Intensity of D^+ as a Function of the Heating and Cooling Time of the Catalyst.

UNCLASSIFIED
ORNL-LR-Dwg. 48357

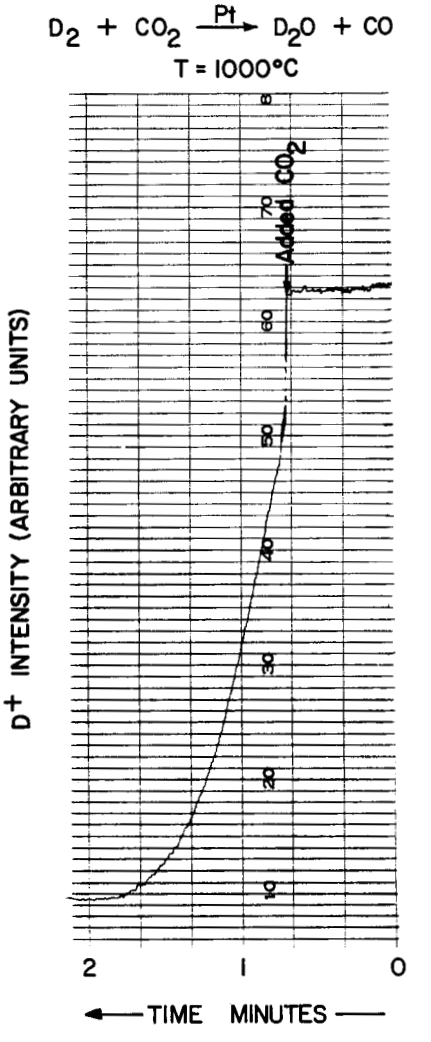

Fig. 29. Inhibition of the Catalytic Production of D by CO_2.

Table 26. Radicals* Detected in the Catalytic Decomposition of 1-Butene over Pt at 1000°C

m/e	Formula	Relative Abundance
15	CH_3	1
39	C_3H_3	29
41	C_3H_5	46
42	C_3H_6	3
43	C_3H_7	3
55	C_4H_7	100

*Radicals with a relative abundance less than 1% are not reported.

Hydrogen Atom Abstraction Reactions by Cyanide Ion-Radicals[23]

T. W. Martin[24] C. E. Melton

Ion-molecule reactions of low energy (0–0.15 ev) CHN^+ and CH_3N^+ were shown conclusively by appearance-potential technique to follow a hydrogen atom abstraction mechanism of the type $XH^+ + YH \rightarrow XH_2^+ + Y$. These reactions are presumably bimolecular, being first order with respect to each reactant over the pressure range 10^{-7}–10^{-3} mm Hg. The rates of these reactions are markedly influenced by the molecular structures of both the cyanide ion and the hydrogen donor (YH). Specific rate constants for these reactions, calculated with the usual approximations, are summarized in Table 27, together with rate constants for the well-known ion-radical reaction, $CH_4^+ + CH_4 \rightarrow CH_5^+ + CH_3$, which were measured to calibrate our method and apparatus. None of these reactions show a discernible temperature dependence over the range 100–215°C; hence, they evidently have no appreciable activation energy. The ratio, k_2/k_1 is approximately equal to (mass D_2/mass H_2)$^{1/2}$, which suggests the difference in these two rate constants, is simply attributable to an isotope effect on their relative collision numbers. The fact that $k_3 > k_1$ shows that the chemical nature of the hydrogen donor can influence the rate of reaction. Similarly, since $k_4 > k_1$, the nature of the cyanide ion-radical plays an important role in the efficiency of the atom abstraction process.

This structural effect of the cyanide ion-radical was further tested in using binary mixtures of

[23] Abstracted from a paper published in *J. Chem. Phys.* 32, 700 (1960).

[24] Summer research participant, Department of Chemistry, Vanderbilt University, Nashville 5, Tennessee.

Table 27. Hydrogen Atom Abstration Reactions by Cyanide Ion-Radicals

Reaction	Electron Energy (indicated ev)	k in Units of 10^{-9} ($cc \cdot molecule^{-1} \cdot sec^{-1}$)*
$C_2H_3N^+ + D_2 \rightarrow C_2H_3DN^+ + D$	14.5	0.3_9
$C_2H_3N^+ + H_2 \rightarrow C_2H_4N^+ + H$	13.8	0.5_7
$C_2H_3N^+ + CH_4 \rightarrow C_2H_4N^+ + CH_3$	12.5	$1._7$
$CHN^+ + D_2 \rightarrow CHDN^+ + D$	14.5	$2._0$
Reference reaction $CH_4^+ + CH_4 \rightarrow CH_5^+ + CH_3$	14.7	$1._3$
	100	$1._3$

*Comparative values for k_x were obtained using the following relationship: $k_x = k_{CH_4} \dfrac{(I_p/I_R)_x}{(I_p/I_R)_{CH_4}}$, where the subscripts x and CH_4 refer to the ion-radical abstraction and the reference reaction respectively, with the ion current ratios taken under identical conditions.

CH_2ClCN, CH_2CHCN, or CH_3CH_2CN with D_2. To our surprise, the parent ions formed from each of these cyanides failed (within our limits of detection) to abstract from D_2. Therefore, HCN and CH_3CN are quite unique in being the only cyanides investigated whose parent ion-radicals show a tendency for hydrogen atom abstraction from D_2. This result is more significant when contrasted with the observation that the parent ion-radicals of all the cyanides mentioned, without exception, will undergo hydrogen self-abstraction reactions in the pressure range 10^{-7}–10^{-3} mm Hg of the type

$$RHCN^+ + RHCN \longrightarrow RH_2CN^+ + (RCN)$$

where (RCN) may represent several uncharged species. Ion-molecule reactions of this type are similar to the hydrogen atom abstraction processes of free radicals, but differ in having no appreciable temperature coefficients (in the range of 100–215°C) and in having much larger rate constants. On the basis of this study, chemical species having unpaired electrons whether charged (ion-radicals) or uncharged (free radicals) were shown to undergo the following similar types of reactions:

I. Ion-radical displacement:

$$\text{e.g., } XM^+ + YN \longrightarrow XMN^+ + Y$$

II. Ion-radical addition:

$$\text{e.g., } XM^+ + YN \longrightarrow XMYN^+$$

III. Ion-radical decomposition:

$$\text{e.g., } XY^+ \longrightarrow X^+ + Y$$

We have shown that ions, particularly the ion-radicals, are both chemically similar to and directly interrelated to free radicals; ion-radicals undergo general reactions analogous to the types known for free radicals, some of which actually generate free radicals as products. Therefore, it seems unreasonable to interpret chemical effects in radiation chemistry without considering both the similarities and interrelationships of ions and radicals. The mass spectrometer is the most definitive tool for the study of ionic reactions, but we believe that further correlations with free-radical data will be increasingly important in achieving an understanding of these reactions.

Evidence for Hydrogen Migration in a Negative Ion-Molecule Reaction[25]

C. E. Melton T. W. Martin[24]
G. A. Ropp

In the course of a previous investigation it was found that the negative ion mass spectra of binary mixtures of the formic acids (HCOOH and DCOOH) showed a small concentration (0.1%) of polymeric negative ions of masses 91, 92, and 93 in the pressure range of 10^{-5} to 10^{-3} mm and at a temperature of 200 ± 25°C in the ionization chamber. A typical scan of these polymeric ions for a 51:49 mole % mixture of HCOOH:DCOOH at a total pressure of 10^{-4} mm is displayed in Fig. 30, together with the reference ions at masses 45 and 46. In the previous investigation it was shown with known gas mixtures that the 45 ($HCOO^-$) and 46 ($DCOO^-$) ion intensities, when isotopically corrected, give an accurate quantitative measure of the partial pressures of HCOOH and DCOOH respectively.

On a statistical basis, the rates of formation of the 91, 92, and 93 product ions would be proportional to a^2, $2ab$, and b^2 respectively. Applying this statistical calculation to the data shown in Fig. 30, we expect the ratios 91:92:93 to be approximately 1:2:1, but we observe 1:1.6:0.6. It follows that this marked departure from statistical behavior is produced by an "isotope effect." The isotope effect can be explained on the basis of the following simple mechanism:

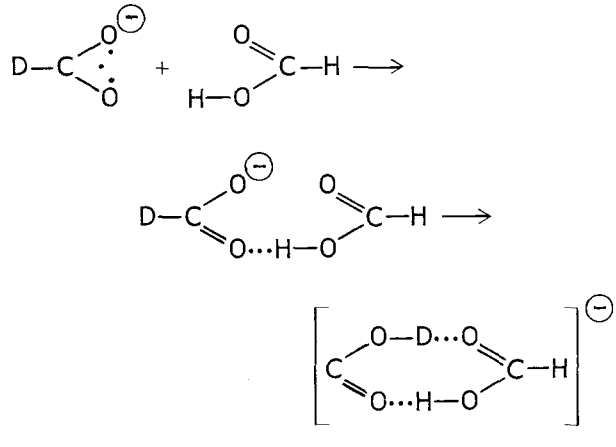

[25] Abstracted from a paper to be published in *J. Phys. Chem.*, September 1960.

UNCLASSIFIED
PHOTO 31086

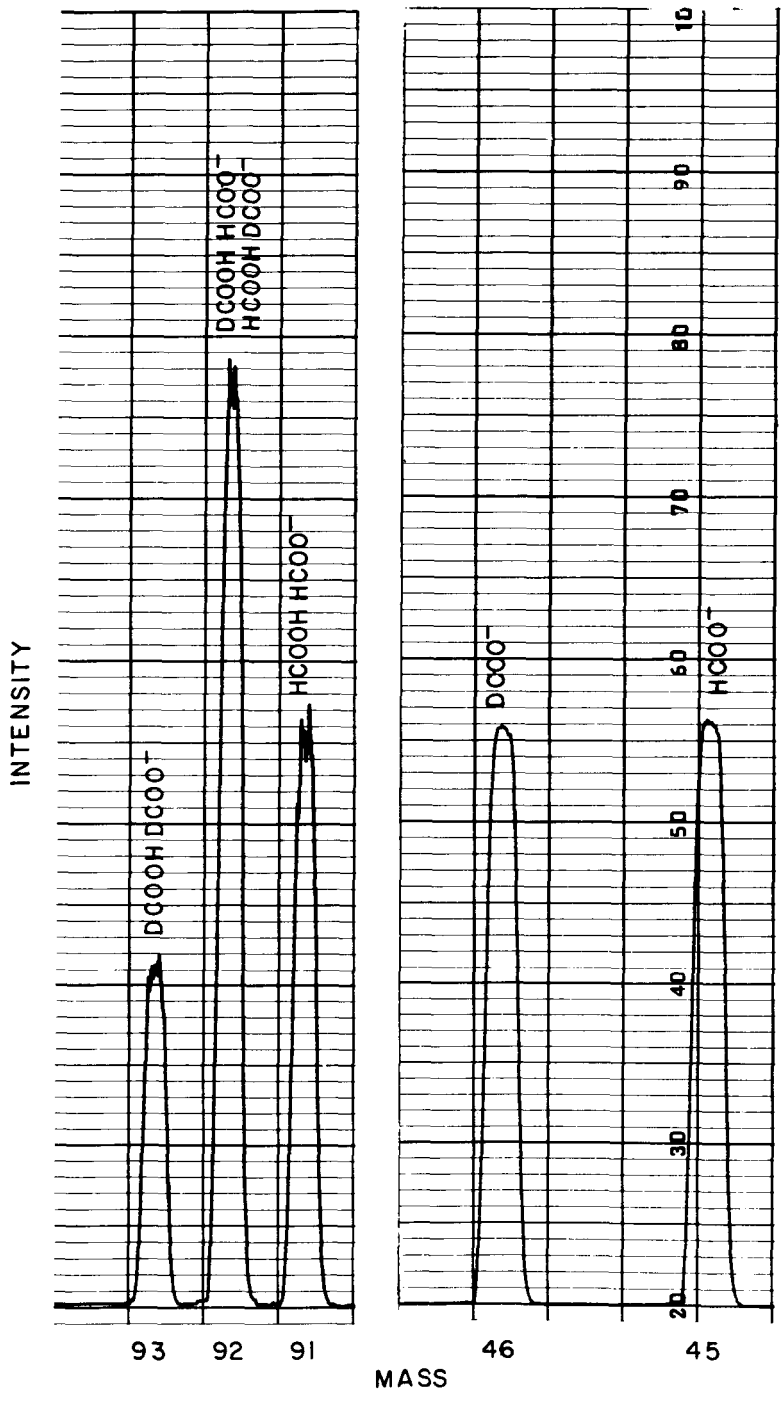

Fig. 30. Polymeric and Parent Ions Formed in a 51:49 Mole % Mixture of HCOOH:DCOOH at a Pressure of 10^{-4} mm.

which assumes that each of the polymeric ions is formed by the rearrangement of the initial collision complex. The rearrangement always involves the migration or tunneling of the hydrogen or deuterium nucleus originally attached to the negative reactant ion, to form the more stable and symmetrical double hydrogen-bonded resonance structure. Since the deuterium would migrate more slowly than hydrogen, the collision complex for 92 and 93 would dissociate more often than that for 91; hence the intensity of 91 would be greater.

Transient Species in the Radiolytic Polymerization of Cyanogen[26]

C. E. Melton P. S. Rudolph

Cyanogen and mixtures of $(CN)_2$ + Xe were irradiated by 135-ev electrons at a pressure of 1 mm in the ionization chamber of the research mass spectrometer. In pure $(CN)_2$ both positive and negative ion-multiplicities of CN up to $(CN)_{10}$ were observed, as shown in Table 28. The ratio

Table 28. Polymer-Ion Mass Spectra of $(CN)_2$ at 1 mm

m/e	Formula	Intensity* (ions/sec)	
		Positive Ions	Negative Ions
26	CN	2.5×10^{11}	2.4×10^{8}
52	$(CN)_2$	9.0×10^{12}	1.9×10^{7}
78	$(CN)_3$	1.6×10^{11}	1.3×10^{6}
104	$(CN)_4$	5.2×10^{13}	2.0×10^{6}
130	$(CN)_5$	6.0×10^{8}	4.5×10^{5}
156	$(CN)_6$	1.2×10^{9}	3.1×10^{5}
182	$(CN)_7$	4.7×10^{6}	5.4×10^{4}
208	$(CN)_8$	1.1×10^{6}	3.7×10^{2}
234	$(CN)_9$	1.0×10^{4}	3
260	$(CN)_{10}$	2.2×10^{4}	5

*Intensities higher than 1×10^5 were calculated from the integrated ion currents.

of CN^+:CN^- was 1000:1. When Xe was admixed with $(CN)_2$ the negative ion intensities were significantly increased; for example, CN^- increased twentyfold. An addition complex, $[Xe(CN)_2]^+$, shown in Fig. 31, was also observed.

[26] Abstracted from a paper to be published in *J. Chem. Phys.*

UNCLASSIFIED
ORNL-LR-Dwg. 48359

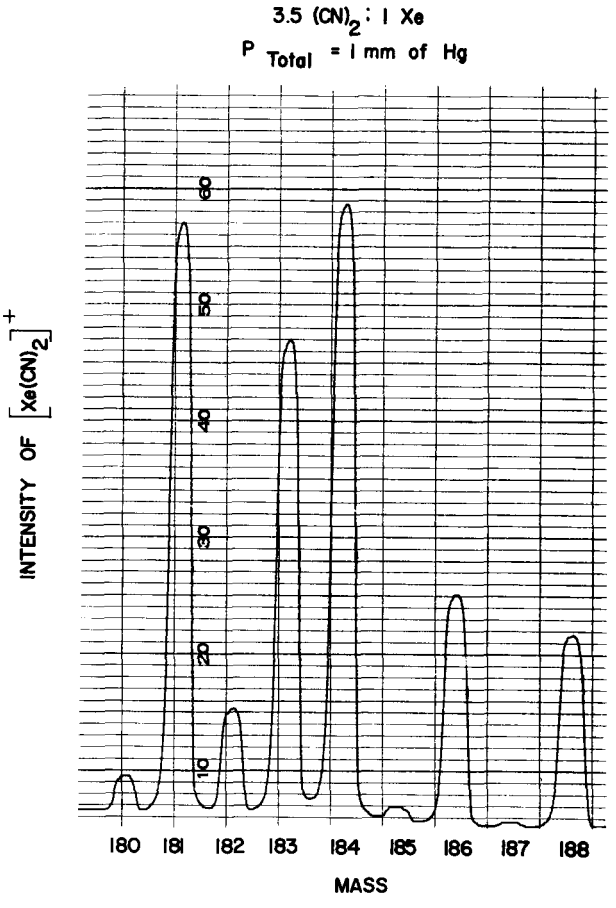

Fig. 31. The Isotopic Pattern of $[Xe(CN)_2]^+$ Observed in a Mixture of 3.5 $(CN)_2$ to 1 Xe at 1 mm Pressure.

The previously observed[27,28] increase in yield of polymerization of $(CN)_2$ in the presence of Xe could not be explained by a charge transfer mechanism, since Xe has the lower ionization potential and thus should diminish the yield. The increased rate of polymerization of $(CN)_2$ upon the admixture of Xe can now be explained on the basis of the reactive complex, $[Xe(CN)_2]^+$, and the increased intensity of negative-ion polymers observed.

[27] S. C. Lind and D. C. Bardwell, *J. Am. Chem. Soc.* 48, 1575 (1926).

[28] D. C. Bardwell and D. K. Naylor, *Radiation Research* 11, 432 (1959).

Charge Transfer Reactions Producing Intrinsic Chemical Change: Methyl, Methylene, and Hydrogen Radicals Produced from Argon and Methane Reactions[29]

C. E. Melton

Charge transfer reactions producing intrinsic chemical changes in the neutral molecule have been proven by mass spectrometric techniques. Reactions were elucidated by catalytic and negative ion studies as well as by the usual pressure and appearance-potential techniques.

The charge transfer reaction

$$Ar^+ + CH_4 \longrightarrow Ar + CH_3^+ + H$$

producing an intrinsic chemical change in CH_4 was found to be more probable by a factor of 5 than the simple charge transfer reaction

$$Ar^+ + CH_4 \longrightarrow Ar + CH_4^+$$

in an Ar + CH_4 system. This mixture was selected because our previous α ionization studies[30] showed that the admixing of 5% of CH_4 to Ar increased the total ionization 2% – decreased the W value (alpha-particle energy divided by the number of ion pairs produced). Values for cross sections and rate constants given in Table 29 show that the 2% decrease in the W value can now be explained on the basis of the CH_2^+ and CH_3^+. These are known to react with CH_4 to form polymeric ions such as $C_2H_5^+$, which when neutralized dissociate and become C_2H_4, etc. In addition, CH_2^+ and CH_3^+ when neutralized become $\cdot CH_2$ and $\cdot CH_3$. Subsequent reactions of these radicals are known to produce C_2H_6 and other hydrocarbons which have a lower ionization potential than that of metastable Ar* and would consequently be ionized by Ar*.

The observation of charge transfer resulting in intrinsic chemical changes in the neutral molecule may in some instances simplify the elucidation of detailed reaction mechanisms in radiolytic studies. However, in most cases the results will be more difficult to interpret, because reactions of this type provide another source of reactants. Charge transfer reactions producing inherent chemical changes in the neutral molecule may be as important in radiation chemistry as simple charge transfer reactions. In systems where charge transfer reactions are energetically possible, but are apparently quite improbable (e.g., C_2H_2 and C_2H_4 systems[31]), charge transfer producing chemical change may explain the seemingly negative results.

[29] Abstracted from a paper to be published in *J. Chem. Phys.*, August 1960.

[30] C. E. Melton, G. S. Hurst, and T. E. Bortner, *Phys. Rev.* **96**, 643 (1954).

Electron-Impact-Induced Charge Transfer Reactions

P. S. Rudolph C. E. Melton

A semiquantitative investigation of electron-impact-induced charge transfer reactions between C_2H_2 or CO and chemically inert gases has been completed in a mass spectrometer. Cross sections (σ) of 10^{-15} cm^2 and rate constants (k) of 10^{-10} $cc \cdot molecule^{-1} \cdot sec^{-1}$ were observed for the reactions summarized below:

$$M^+ + C_2H_2 \longrightarrow M + C_2H_2^+$$

where M is He, Ne, N_2, CO_2, or D_2,

$$He^* + C_2H_2 \longrightarrow He + C_2H_2^+ + e^-$$

$$G^+ + CO \longrightarrow G + CO^+$$

where G is He, Ne, or Xe.

[31] P. S. Rudolph and C. E. Melton, *J. Chem. Phys.* **32**, 586 (1960).

Table 29. Cross Sections and Rate Constants for Charge Transfer Reactions

Probable Reaction	ΔH (ev)	k in Units of 10^{-9} ($cc \cdot molecule^{-1} \cdot sec^{-1}$)	σ in Units of 10^{-16} (cm^2)
$Ar^+ + CH_4 \longrightarrow Ar + CH_4^+$	−2.78	0.3	20
$Ar^+ + CH_4 \longrightarrow Ar + CH_3^+ + H$	−1.36	1.6	104
$Ar^+ + CH_4 \longrightarrow Ar + CH_2^+ + H_2$	−0.16	0.3	20
$Ar^+ + CH_4 \longrightarrow Ar + CH_2^+ + 2H$	4.34	Not energetically probable	

Qualitative electron-impact studies with the dual-leak research mass spectrometer[32] on binary mixtures of CO, CO_2, and O_2 show that the following charge transfer reactions go with a high probability:

$$CO^+ + CO_2 \longrightarrow CO + CO_2^+$$

$$CO_2^+ + O_2 \longrightarrow CO_2 + O_2^+$$

However, the following energetically possible reaction does not go (or goes with a very low probability):

$$CO^+ + O_2 \longrightarrow CO + O_2^+$$

To elucidate these mechanisms, $C^{13}O$ and $C^{13}O_2$ were used in conjunction with normal CO_2 and CO.

Mass Spectrometric Studies of Ionic Intermediates in the Alpha-Particle Radiolysis of Ethylene[33]

C. E. Melton P. S. Rudolph

Two techniques were used for the elucidation of ion-molecule reaction mechanisms in the alpha radiolysis of C_2H_4 in the alpha-particle mass spectrometer.[34] The corresponding variations in the per cent of primary, secondary, and tertiary ions over a pressure range from 0.01 to 0.1 mm were used to postulate the reaction mechanisms. Figure 32 shows the pressure dependence for three ions which are involved in consecutive reactions producing $C_5H_9^+$, the largest polymeric ion observed.

Mixtures of the C_2 hydrocarbons were employed to increase the relative concentration of a specific reactant ion. For example, in order to increase the concentration of $C_2H_4^+$ relative to C_2H_4 and thus test the postulated mechanism for the formation of $C_3H_5^+$, C_2H_6 [the predominant ion of which is $C_2H_4^+$ (49.4%)] was admixed with C_2H_4. The results of the mixture studies confirmed the mechanisms postulated from the pressure studies.

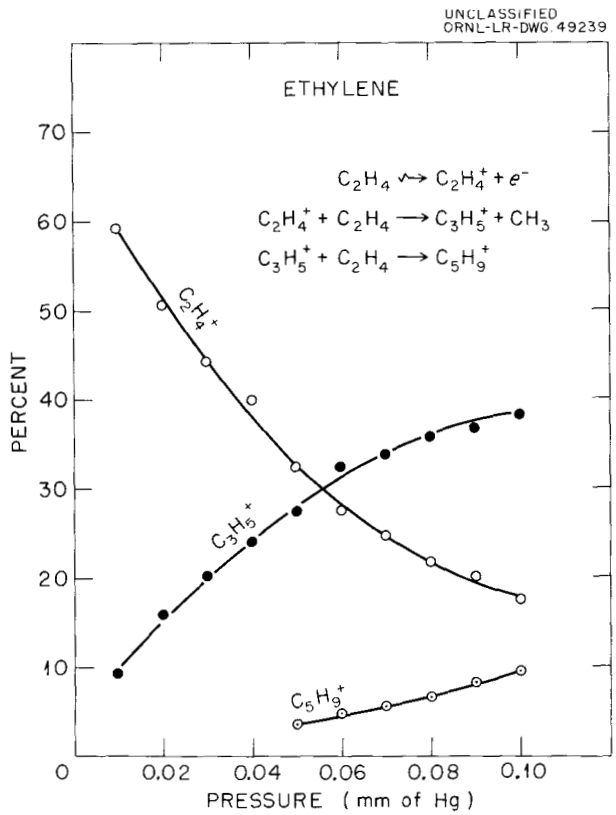

Fig. 32. Typical Curves Showing the Variation in Per Cent Abundance for Ions Involved in a Series of Consecutive Reactions.

Electron Shakeoff Following β^- Decay of He^6

T. A. Carlson[35] C. H. Johnson[36]
F. Pleasonton[36]

Following β^- decay an atom is initially singly charged because of the change in the nuclear charge. The atom may also be sufficiently excited to lose one or more of its electrons and become multicharged. Excitation can result either from the sudden nonadiabatic change in the nuclear charge or from the recoil energy imparted by the beta particle and the neutrino. This phenomenon has been studied experimentally in the past with a number of gases.[37] The investigation of He^6 is of particular interest, however, because the

[32] C. E. Melton and G. A. Ropp, *J. Am. Chem. Soc.* 80, 5573 (1958).

[33] An abstract of a paper published in *J. Chem. Phys.* 32, 1128 (1960).

[34] C. E. Melton and P. S. Rudolph, *J. Chem. Phys.* 30, 847 (1959).

[35] On loan to the Physics Division.

[36] Physics Division.

[37] See, for example, A. H. Snell and F. Pleasonton, *J. Phys. Chem.* 62, 1377 (1958).

availability of appropriate wave functions describing the ground state of He and several states of Li(II) has allowed Winther[38] to calculate the electron shakeoff following β^- decay more rigorously than is generally possible. Using a specially designed mass spectrometer, we have measured the charge and recoil spectra of the resulting lithium ions[39] and have found that one orbital electron is lost in (10.6 ± 1.0)% of the decays while the loss of both electrons occurs in less than 0.02% of the cases. Less than 0.5% of the electron shakeoff can be experimentally attributed to recoil energy, even for ions having the maximum recoil energy of 1500 ev.

These results agree well with Winther's calculations, which would have (10.5 ± 1.5)% of the ions doubly charged and less than 0.1% triply charged. They are also consistent with his estimation that about 0.3% of the ions with the maximum recoil energy would lose an electron due to recoil alone.

---

[38] A. Winther, *Kgl. Danske Videnskab. Selskab. Mat.-fys. Medd.* **27**, 2 (1952).

[39] Preliminary report: C. H. Johnson, F. Pleasonton, and A. H. Snell, *Phys. Ann. Prog. Rep. Mar. 10, 1959*, ORNL-2718, p 5.

PUBLICATIONS

NUCLEAR CHEMISTRY

F. J. Johnston, J. Halperin, and R. W. Stoughton, "The Thermal Neutron Absorption Cross Section of Th^{233} and the Resonance Integrals of Th^{232}, Th^{233}, and Co^{59}," *J. Nuclear Energy* **11**, 95 (1960).

B. H. Ketelle and A. R. Brosi, "Radioactive Decay of Dy^{159}," *Phys. Rev.* **116**, 98 (1959).

J. A. Marinsky and E. Eichler, "A New Fission Product: Ga^{74}," *J. Inorg. & Nuclear Chem.* **12**, 223 (1960).

R. W. Stoughton and J. Halperin, "Heavy Nuclide Cross Sections of Particular Interest to Thermal Reactor Operation: Conventions, Measurements, and Preferred Values," *Nuclear Sci. and Eng.* **6**, 100 (1959).

R. W. Stoughton, J. Halperin, and M. P. Lietzke, "Effective Cadmium Cutoff Energies," *Nuclear Sci. and Eng.* **6**, 441 (1959).

R. W. Stoughton, J. Halperin, and M. P. Lietzke, *Effective Cadmium Cutoff Energies*, ORNL-2833 (March 1960); ORNL-2833 Supplement (May 1960).

ISOLATION AND CHEMICAL PROPERTIES OF SYNTHETIC ELEMENTS

G. E. Boyd, Q. V. Larson, and E. E. Motta, "Isolation of Milligram Quantities of Long-Lived Technetium from Irradiated Molybdenum," *J. Am. Chem. Soc.* **82**, 809 (1960).

CHEMICAL SEPARATION OF ISOTOPES

G. M. Begun, J. S. Drury, and E. F. Joseph, "Automatic Cascade for the Production of Nitrogen-15," *Ind. Eng. Chem.* **51**, 1035 (1959).

G. M. Begun and W. H. Fletcher, "Infrared and Raman Spectra of $N_2^{14}O_4$ and $N_2^{15}O_4$," *J. Mol. Spectroscopy* **4**, 388 (1960).

L. L. Brown and J. S. Drury, "The Fractionation of Oxygen Isotopes Between Water and Sulfur Dioxide," *J. Phys. Chem.* **63**, 1885 (1959).

L. Landau and W. H. Fletcher, "The Infrared Spectrum and Potential Function of Nitrosyl Chloride," *J. Mol. Spectroscopy* **4**, 276 (1960).

D. A. Lee, "The Enrichment of Lithium Isotopes by Ion Exchange Chromatography. II. The Influence of Temperature on the Separation Factor," *J. Phys. Chem.* **64**, 187 (1960).

RADIATION CHEMISTRY

A. R. Jones, "On the Radiation-Induced Gas Phase Polymerizations of Acetylene and Benzene," *J. Chem. Phys.* **32**, 953 (1960).

H. W. Kohn, "Colour Centres Produced by Radiation in Silica Gel," *Nature* **184**, 630 (1959).

H. A. Mahlman, "Activity Concept in Radiation Chemistry," *J. Chem. Phys.* **31**, 993 (1959).

H. A. Mahlman, "Hydrogen Formation in the Radiation Chemistry of Water," *J. Chem. Phys.* **32**, 601 (1960).

C. E. Melton and P. S. Rudolph, "Negative Ion Mass Spectra of Hydrocarbons and Alcohols," *J. Chem. Phys.* **31**, 1485 (1959).

C. E. Melton and P. S. Rudolph, "Mass Spectrometric Studies of Ionic Intermediates in the Alpha-Particle Radiolysis of Ethylene," *J. Chem. Phys.* **32**, 1128 (1960).

P. S. Rudolph and S. C. Lind, "Alpha Radiolysis of CO With and Without Xe," *J. Chem. Phys.* **32**, 1572 (1960).

P. S. Rudolph and C. E. Melton, "Mass Spectrometric Studies of Ionic Intermediates in the Alpha-Particle Radiolysis of the C_2-Hydrocarbons. I. Acetylene," *J. Phys. Chem.* **63**, 916 (1959).

P. S. Rudolph and C. E. Melton, "Ion-Molecule Charge Transfer Reactions in the Alpha Radiolysis of Various Hydrocarbons in a Mass Spectrometer," *J. Chem. Phys.* **32**, 586 (1960).

E. H. Taylor, "Radiation Effects on Solids, Including Catalysts," *J. Chem. Educ.* **36**, 396 (1959).

E. H. Taylor, "Samuel Colville Lind," *J. Phys. Chem.* **63**, 772 (1959).

ORGANIC CHEMISTRY

W. H. Baldwin, *Organic Compounds in Fission Reactors. I. The Dispersion of ThO_2 in Nonpolar Solvents*, ORNL-2758 (July 2, 1959).

W. H. Baldwin, *Differential Thermal Analysis. Qualitative Study of Nitrate–Butyl Phosphate Systems*, ORNL CF-60-1-99 (Jan. 25, 1960).

W. H. Baldwin, *Organic Compounds in Fission Reactors. II. Thorio-Organic Compounds*, ORNL-2864 (Feb. 15, 1960).

J. B. Christie, *The Configurational Relationship of 1,2,2-Triphenylethylamine and 1,2,2-Triphenylethanol*, ORNL-2786 (Sept. 28, 1959).

C. J. Collins and J. B. Christie, "A Radiochemical Criterion for Configurational Relationship," *J. Am. Chem. Soc.* **82**, 1255 (1960).

C. J. Collins and M. H. Lietzke, "The Isotope Effect and Its Relation to the Validity of Isotopic Tracer Experiments," *J. Am. Chem. Soc.* **81**, 5379 (1959).

C. E. Higgins and W. H. Baldwin, "Refractometric Determination of Mutual Solubility as a Function of Temperature. Tributyl Phosphine Oxide and Water," *Anal. Chem.* **32**, 233 (1960).

C. E. Higgins and W. H. Baldwin, "Effect of Centrifugation on Solution Temperature and Solubility of Tributyl Phosphate and Tributyl Phosphine Oxide in Water," *Anal. Chem.* **32**, 236 (1960).

V. F. Raaen and J. F. Eastham, "The Reaction of Cyanogen with Arylmethylmagnesium Halides," *J. Am. Chem. Soc.* **82**, 1349 (1960).

G. A. Ropp, *Curves for Computation of Kinetic Isotope Effects*, ORNL CF-59-12-4 (Dec. 8, 1959).

G. A. Ropp, "Studies Involving Isotopically Labeled Formic Acid and Its Derivatives. V. Studies of the Decarbonylation of Formic, Benzoylformic, and Triphenylacetic Acids in Sulfuric Acid," *J. Am. Chem. Soc.* **82**, 842 (1960).

CHEMISTRY OF AQUEOUS SYSTEMS

R. S. Greeley, W. T. Smith, Jr., R. W. Stoughton, and M. H. Lietzke, "Electromotive Force Measurements in Aqueous Solutions at Elevated Temperatures. I. The Standard Potential of the Silver–Silver Chloride Electrode," *J. Phys. Chem.* **64**, 652 (1960).

J. C. Hayes and M. H. Lietzke, "The Standard Electrode Potential of the Quinhydrone Electrode from 25 to 55°," *J. Phys. Chem.* **64**, 374 (1960).

K. A. Kraus, D. C. Michelson, and F. Nelson, "Adsorption of Negatively Charged Complexes by Cation Exchangers," *J. Am. Chem. Soc.* **81**, 3204 (1959).

K. A. Kraus, H. O. Phillips, T. A. Carlson, and J. S. Johnson, "Ion Exchange Properties of Hydrous Oxides," *Progr. in Nuclear Energy, Ser. IV* **2**, 73 (1960).

K. A. Kraus and R. J. Raridon, "Temperature Dependence of Some Cation Exchange Equilibria in the Range 0 to 200°," *J. Phys. Chem.* **63**, 1901 (1959).

K. A. Kraus, R. J. Raridon, and D. L. Holcomb, "Anion Exchange Studies. XXVI. A Column Method for Measurement of Ion Exchange Equilibria at High Temperature. Temperature Coefficient of the Br^--Cl^- Exchange Reaction," *J. Chromatog.* **3**, 178 (1960).

M. H. Lietzke and R. W. Stoughton, "The Solubility of Silver Sulfate in Electrolyte Solutions. I. Solubility in Potassium Nitrate Solutions," *J. Phys. Chem.* **63**, 1183 (1959).

M. H. Lietzke and R. W. Stoughton, "The Solubility of Silver Sulfate in Electrolyte Solutions. II. Solubility in Potassium Sulfate Solutions," *J. Phys. Chem.* **63**, 1186 (1959).

M. H. Lietzke and R. W. Stoughton, "The Solubility of Silver Sulfate in Electrolyte Solutions. III. Solubility in Sulfuric Acid Solutions," *J. Phys. Chem.* **63**, 1188 (1959).

M. H. Lietzke and R. W. Stoughton, "The Solubility of Silver Sulfate in Electrolyte Solutions. IV. Solubility in Nitric Acid Solutions," *J. Phys. Chem.* **63**, 1190 (1959).

M. H. Lietzke and R. W. Stoughton, "The Solubility of Silver Sulfate in Electrolyte Solutions. V. Solubility in Magnesium Sulfate Solutions," *J. Phys. Chem.* **63**, 1984 (1959).

M. H. Lietzke and R. W. Stoughton, "The Solubility of Silver Sulfate in Electrolyte Solutions. VI. Heats and Entropies of Solution vs Temperature. Species Present in HNO_3 and H_2SO_4 Media," *J. Phys. Chem.* **64**, 133 (1960).

S. Lindenbaum, C. F. Jumper, and G. E. Boyd, "Selectivity Coefficient Measurements with Variable Capacity Cation and Anion Exchangers," *J. Phys. Chem.* **63**, 1924 (1959).

B. McCarroll and M. H. Lietzke, "Indium Sulfate: Raman Spectra and Incomplete Dissociation," *J. Chem. Phys.* **32**, 1277 (1960).

F. Nelson, "Anion Exchange Studies. XXVIII. Comparison of Diffusion in Anion Exchange Resins and Quaternary Amine Solutions," *J. Polymer Sci.* **40**, 563 (1959).

F. Nelson and K. A. Kraus, "Anion Exchange Studies. XXIX. Adsorption of $GeCl_4$ from Gas Streams," *J. Chromatog.* **3**, 279 (1960).

F. Nelson, R. M. Rush, and K. A. Kraus, "Anion Exchange Studies. XXVII. Adsorbability of a Number of Elements in HCl-HF Solutions," *J. Am. Chem. Soc.* **82**, 339 (1960).

W. C. Waggener, "Technique for Liquid Phase Spectrophotometry at Elevated Temperatures and Pressures," *Rev. Sci. Instr.* **30**, 788 (1959).

W. C. Waggener, "Spectrophotometric Studies of Radioactive Aqueous Solutions from 0° to 250°C," CARYGRAPH, vol 1, No. 3, Applied Physics Corporation, Monrovia, California, 1959.

W. C. Waggener, J. A. Mattern, and G. H. Cartledge, "Coordination Properties of the Thiocyanato Radical. I. The Bonding of Silver and Mercury Ions by Thiocyanato Complexes of Cobalt(III) and Chromium(III)," *J. Am. Chem. Soc.* **81**, 2958 (1959).

W. C. Waggener and A. M. Tripp, "Reliable Optical Window for Cells Subjected to Widely Cycling Temperatures and Pressures," *Rev. Sci. Instr.* **30**, 677 (1959).

CHEMISTRY OF CORROSION

G. H. Cartledge, "Action of the XO_4^{n-} Inhibitors," *Corrosion* **15**, 469t (1959).

G. H. Cartledge, "Discussion of a Paper by H. H. Uhlig and P. F. King," *J. Electrochem. Soc.* **106**, 1074 (1959).

G. H. Cartledge, "The Significance of the 'Equivalent Redox Potential' in Aqueous Solutions Under Ionizing Radiation," *Nature* **186**, 370 (1960).

G. H. Cartledge, *Report on Conference on Corrosion in Nuclear Reactors* (Brussels, October 1959), ORNL CF-59-11-39.

R. E. Meyer, "Thin Film Formation on Zirconium," *J. Electrochem. Soc.* **106**, 930 (1959).

NONAQUEOUS SYSTEMS AT HIGH TEMPERATURES

M. A. Bredig and H. R. Bronstein, "Miscibility of Liquid Metals with Salts. IV. The Sodium–Sodium Halide Systems at High Temperatures," *J. Phys. Chem.* **64**, 64 (1960).

A. S. Dworkin and M. A. Bredig, "The Heat of Fusion of the Alkali Metal Halides," *J. Phys. Chem.* **64**, 269 (1960).

H. A. Levy, P. A. Agron, M. A. Bredig, and M. D. Danford, "X-Ray and Neutron Diffraction Studies of Molten Alkali Halides," *Ann. N.Y. Acad. Sci.* **79**, 11 (1960).

G. W. Parker, G. E. Creek, and W. J. Martin, *Preliminary Report on the Release of Fission Products on Melting GE-ANP Fuel*, ORNL CF-60-1-50 (Jan. 29, 1960).

G. W. Parker, G. E. Creek, W. J. Martin, and C. J. Barton, *Fuel Element Catastrophe Studies: The Hazards of Fission Product Release from Irradiated Uranium*, ORNL CF-60-6-24.

CHEMICAL PHYSICS

P. A. Agron and R. D. Ellison, "A Structure Proposal for $Na_7Zr_6F_{31}$," *J. Phys. Chem.* **63**, 2076 (1959).

W. R. Busing and H. A. Levy, *A Crystallographic Function and Error Program for the IBM 704*, ORNL CF-59-12-3 (December 1959).

T. A. Carlson, "Dissociation of C_6H_5T Following Beta Decay," *J. Chem. Phys.* **32**, 1234 (1960).

S. Datz, R. E. Minturn, and E. H. Taylor, "Thermal Positive Ion Emission and the Anomalous Flicker Effect," *J. Appl. Phys.* **31**, 880 (1960).

S. Datz and E. H. Taylor, "Some Applications of Molecular Beam Techniques to Chemistry," p 157 in *Recent Research in Molecular Beams*, Academic Press, New York, 1959.

R. D. Ellison and R. W. Holmberg, "Cell Dimensions and Space Group of 1,1-Diphenyl-2-picryl Hydrazine," *Acta Cryst.* **13**, 446 (1960).

H. A. Levy, P. A. Agron, and M. D. Danford, "X-Ray Diffractometry with Slightly Absorbing Samples," *J. Appl. Phys.* **30**, 12 (1959).

H. A. Levy, M. D. Danford, and P. A. Agron, "X-Ray Diffraction Study of Bismuth Polymer in Aqueous Perchlorate Solution," *J. Chem. Phys.* **31**, 6 (1959).

H. A. Levy and R. D. Ellison, "The Polarization Correction for Upper Level Geometry Using Crystal Monochromatized Radiation," *Acta Cryst.* **13**, 270 (1960).

R. Livingston, "Physical Observation of Radiation-Induced Intermediates," *J. Chem. Educ.* **36**, 349 (1959).

R. Livingston, "Chemical Applications of Pure Quadrupole Spectroscopy," *Record Chem. Progr. (Kresge-Hooker Sci. Lib.)* **20**, 173 (1959).

T. W. Martin and C. E. Melton, "Hydrogen Atom Abstraction Reactions by Cyanide Ion-Radicals," *J. Chem. Phys.* **32**, 700 (1960).

R. E. Minturn, S. Datz, and E. H. Taylor, "Thermal Emission of Alkali Ion Pulses from Clean and Oxygenated Tungsten," *J. Appl. Phys.* **31**, 876 (1960).

H. Zeldes, G. T. Trammell, R. Livingston, and R. W. Holmberg, "Common Error Made in Treating Hyperfine Effects in Electron Paramagnetic Resonance Studies of Free Radicals," *J. Chem. Phys.* **32**, 618 (1960).

PAPERS PRESENTED AT SCIENTIFIC AND TECHNICAL MEETINGS

NUCLEAR CHEMISTRY

E. Eichler,* J. A. Marinsky, G. D. O'Kelley, and N. R. Johnson, "Nuclear Levels of Ge^{74}," American Physical Society, New York, January 27–30, 1960 [*Bull. Am. Phys. Soc.* 5, 10 (1960)].

E. Eichler,* J. W. Chase, N. R. Johnson, and G. D. O'Kelley, "Decay of I^{133}," American Physical Society, Southeastern Section, Gatlinburg, Tennessee, April 7–9, 1960.

N. R. Johnson,* E. Eichler, G. D. O'Kelley, J. W. Chase, and J. T. Wasson, "Decay of I^{134}," American Physical Society, Southeastern Section, Gatlinburg, Tennessee, April 7–9, 1960.

G. D. O'Kelley, "Use of Scintillation Spectrometers in Radiochemical Research," ORINS advanced course in the Use of Radioisotopes in Biochemistry, September 21, 1959.

G. D. O'Kelley, "Special Topics in Scintillation Counting," ORINS Radioisotope Techniques School, August 19, September 17, 1959; January 22, March 11, May 13, 1960; ORINS Third Industrial Training Course, October 23, 1959.

R. L. Robinson,* E. Eichler, and N. R. Johnson, "Decay of I^{132}," American Physical Society, Southeastern Section, Gatlinburg, Tennessee, April 7–9; 1960.

R. W. Stoughton, "Reactor Chemistry," Third Annual Meeting of the South Central Independent College Association of Chemists, Carson-Newman College, Jefferson City, Tennessee, October 2–3, 1959.

R. W. Stoughton,* J. Halperin, and M. P. Lietzke, "Effective Cadmium Cutoffs for Neutrons," American Nuclear Society, Gatlinburg, Tennessee, June 15–17, 1959.

CHEMICAL SEPARATION OF ISOTOPES

J. S. Drury, "Methods of Isotope Separation," Eleventh Annual ONR Nuclear Science Seminar, Oak Ridge, December 4, 1959.

J. S. Drury, "Concepts for Isotope Separation," Sixty-ninth Meeting, Tennessee Academy of Science, Vanderbilt University, Nashville, December 11, 1959.

J. S. Drury, "Chemical Separation of Isotopes," Tennessee Polytechnic Institute, Cookeville, Tennessee, February 11, 1960.

RADIATION CHEMISTRY

C. J. Hochanadel, "Radiation Chemistry," ORINS Industrial Radioisotopes Training Course, Oak Ridge, Tennessee, November 11, 1959, February 8, 1960, March 28, 1960, and May 31, 1960.

C. J. Hochanadel, "Radiation Chemistry of Water," Symposium on the Comparative Effects of Ionizing, Ultraviolet, Visible, and Near Visible Radiations, NRC, San Juan, Puerto Rico, February 16, 1960.

H. A. Mahlman, "The Radiolysis of Aqueous Nitrate Solutions," Gordon Research Conference on Radiation Chemistry, New Hampton, New Hampshire, July 27–31, 1959.

H. A. Mahlman, "Radiation Chemistry of Concentrated Aqueous Nitrate Solutions," Sterling Forest Laboratory, Union Carbide Nuclear Company, Tuxedo, New York, February 12, 1960.

P. S. Rudolph, "Mass Spectra of Organic Ions Produced by 5-Mev Alpha Particles," Gordon Research Conference on Radiation Chemistry, New Hampton, New Hampshire, July 27–31, 1959.

*Denotes speaker.

E. H. Taylor, "The Use of Ionizing Radiation in the Study of Heterogeneous Catalysts," Philadelphia Catalysis Club, Chester, Pennsylvania, May 16, 1960; Saint Joseph's College, Philadelphia, May 17, 1960.

E. H. Taylor, "The Use of Ionizing Radiation in the Study of Catalysts," seminar, Parma Research Center, Cleveland, November 17, 1959.

E. H. Taylor* and H. W. Kohn, "The Use of Ionizing Radiation in Heterogeneous Catalysis," International Atomic Energy Agency Meeting on Applications on Large Radiation Sources in Industry, Warsaw, Poland, September 8–12, 1959.

ORGANIC CHEMISTRY

W. H. Baldwin, "Organic Phosphorus Compounds in the Solvent Extraction of Electrolytes," Oklahoma State University, November 10, 1959; Furman University, November 20, 1959; University of Tennessee, March 10, 1960.

W. H. Baldwin, "The Labeling of Organic Phosphorus Compounds with Radioactive Phosphorus," University of Oklahoma, November 11, 1959; University of Mississippi, November 12, 1959; Furman University, November 20, 1959; University of Louisville, March 2, 1960; St. Mary's College, South Bend, Indiana, March 3, 1960.

C. J. Collins, "Some Recent Experiments on the Mechanism of the Deamination Reaction," American Chemical Society, Southeastern Regional Meeting, Richmond, Virginia, November 5–7, 1959.

C. J. Collins, "The Stereochemistry and Radiochemistry of Deaminations," The Johns Hopkins University Chemistry Colloquium, Baltimore, April 12; the Harvard University Organic Chemistry Colloquium, Cambridge, Massachusetts, April 19, 1960.

C. J. Collins, "Some Aspects of Deuterium Isotope Effects in Mechanism Studies," New York Academy of Sciences Conference on Deuterium Isotope Effects in Chemistry and Biology, New York, May 12–13, 1960.

C. E. Melton and G. A. Ropp,* "Isotopic Studies of Ion-Molecule Reactions in Formic Acid Vapor in the Mass Spectrometer," American Chemical Society, Atlantic City, September 13–18, 1959.

G. A. Ropp, "Studies of the Cyclization of *o*-Benzoylbenzoic-Carboxyl-C^{14} Acid," American Chemical Society, Southeastern Regional Meeting, Richmond, Virginia, November 5–7, 1959.

CHEMISTRY OF AQUEOUS SYSTEMS

J. C. Hayes* and M. H. Lietzke, "The Standard Electrode Potential of the Quinhydrone Electrode from 25° to 55°C," American Chemical Society, Cleveland, April 5–14, 1960.

K. A. Kraus, "Ion Exchange Chromatography," Summer Conference on Recent Advances in Analytical Chemistry, Carleton College, Northfield, Minnesota, June 29–30, 1959.

K. A. Kraus, "Separation of Metals by Anion Exchange," American Chemical Society, Eastern Analytical Symposium, New York, November 6, 1959.

K. A. Kraus, "Ion Exchange," Chemistry Seminar, University of Tennessee, Knoxville, January 14, 1960.

K. A. Kraus, "Ion Exchange," Chemistry Division Seminar, Argonne National Laboratory, Lemont, Illinois, May 4, 1960.

*Denotes speaker.

M. H. Lietzke* and R. W. Stoughton, "Solubility of Silver Sulfate in Electrolyte Solutions. VII. Solubility in Uranyl Sulfate Solutions," American Chemical Society, Cleveland, April 5–14, 1960.

M. H. Lietzke* and R. W. Stoughton, "Analytical Method for Evaluating Activity Coefficients from Osmotic Coefficient Data," American Chemical Society, Atlantic City, September 13–18, 1959.

R. W. Stoughton* and M. H. Lietzke, "Heat of Solution of Silver Sulfate and Species Present in Various Aqueous Media vs Temperature," American Chemical Society, Atlantic City, September 13–18, 1959.

CHEMISTRY OF CORROSION

G. H. Cartledge, "Cathodic Processes in Corrosion," AEC-Euratom Conference, Brussels, Belgium, October 1959.

R. E. Meyer, "Cathodic Processes on Passive Zirconium," Electrochemical Society, Chicago, May 5, 1960.

NONAQUEOUS SYSTEMS AT HIGH TEMPERATURES

P. A. Agron, "Diffraction Studies of Molten Salts," Gordon Research Conference on Molten Salts, Meriden, New Hampshire, August 24–28, 1959.

M. A. Bredig, "Metals in Molten Salts," Gordon Research Conference on Molten Salts, Meriden, New Hampshire, August 24–28, 1959.

M. A. Bredig, "Solutions of Metals in Molten Halides," Lecture to combined Knoxville and Oak Ridge sections of graduate class, Chemistry 573, University of Tennessee, May 19, 1960.

G. W. Parker, "Fuel Element Catastrophe Studies: The Hazards of Fission Product Release from Irradiation Uranium," American Nuclear Society, Chicago, June 15, 1960.

CHEMICAL PHYSICS

C. R. Baldock, "Studies of Ion-Molecule Reactions Produced by the Bombardment of Gases with Alpha Particles and Electrons," Chemical Institute of Canada, Hamilton, Ontario, August 31–September 1, 1959.

C. R. Baldock, "Ions and Ion-Molecule Reactions Produced by the Bombardment of Gases with Alpha Particles and Electrons," American Physical Society, Southeastern Section, Gatlinburg, Tennessee, April 7–9, 1960.

C. R. Baldock, "Charge Transfer Reactions and Ionic Intermediates Induced by Alpha Particles and Electrons," Physics Colloquium, Auburn University, Auburn, Alabama, April 22, 1960.

W. R. Busing, "A Computer Program to Produce Stereoscopic Pictures of Crystal Structures," American Crystallographic Association, Washington, D.C., January 27, 1960.

W. R. Busing, "Chemical Information from Neutron Diffraction," Georgia Institute of Technology, Atlanta, February 25, 1960.

W. R. Busing, "Crystallographic Calculations with High Speed Computers," Massachusetts Institute of Technology, Cambridge, March 3, 1960.

W. R. Busing, "Chemical Information from Neutron Diffraction," Louisiana State University, Baton Rouge, March 22, 1960.

*Denotes speaker.

W. R. Busing and H. A. Levy, "The Effect of Thermal Motion on Diffraction Measurements of Bond Lengths in Crystals," American Crystallographic Association, Washington, D.C., January 25, 1960.

W. R. Busing and M. Zocchi, "Single-Crystal Neutron Diffraction Study of $Sr(OH)_2 \cdot 8H_2O$," Conference on Neutron Diffraction, Gatlinburg, Tennessee, April 22, 1960.

S. Datz, "Collision Mechanics in Crossed Maxwellian Beams," American Chemical Society, Cleveland, April 11–14, 1960.

S. Datz, "Application of Molecular Beam Techniques to Chemically Reactive Collisions," Atomic and Molecular Gas Beams Conference, Denver, June 20–22, 1960.

H. A. Levy, "Some Neutron Diffraction Studies of Hydrogen Locations" and "An Automatic Orienter for Single Crystals," Conference on Neutron Diffraction in Relation to Magnetism and Chemical Bonding, Gatlinburg, Tennessee, April 1960.

R. Livingston, "Paramagnetic Resonance Studies of Irradiated Materials," Union Carbide Corporation Nuclear Subcommittee, Oak Ridge, June 8, 1959.

R. Livingston, "Electronic Resonance in Gamma Irradiated Substances at Low Temperatures," Gordon Research Conference on Magnetic Resonance, New Hampton, New Hampshire, July 10, 1959.

R. Livingston, "Atomic and Molecular Hydrogen Yields from Irradiated Acids," the Fourth International Symposium on Free Radical Stabilization, National Bureau of Standards, Washington, D.C., September 1, 1959; Chairman of Session "Interactions of Free Radicals with Solids," September 2, 1959.

R. Livingston, "Electron Paramagnetic Resonance Studies of Irradiation Effects in Solids," Princeton Section of the American Chemical Society, Princeton, New Jersey, October 22, 1959.

R. Livingston, "Nuclear Quadrupole Resonance," Auburn Section of the American Chemical Society, Auburn, Alabama, May 6, 1960.

C. E. Melton, "Ion-Molecule Reactions Resulting from Bombardment of Gases with Electrons and Alpha Particles," Symposium on Nonanalytical Applications of Mass Spectrometry, American Chemical Society, Atlantic City, September 13–18, 1959.

C. E. Melton, "Hydrogen Abstraction and Migration in Positive and Negative Ion-Molecule Reactions," ASTM Committee E-14 on Mass Spectrometry, Atlantic City, June 26–July 1, 1960.

C. E. Melton, "Charge Transfer Reactions Induced by Electrons and Alpha Particles," American Physical Society, Southeastern Section, Gatlinburg, Tennessee, April 7–9, 1960.

S. W. Peterson, "Neutron Diffraction and Structural Chemistry," symposium in connection with the dedication of the Washington State University reactor, Pullman, Washington, October 1959.

S. W. Peterson and H. A. Levy, "A Single Crystal Neutron Spectrometer for a High Flux Reactor," Cornell Meeting of the American Crystallographic Association, Ithaca, New York, July 1959.

S. W. Peterson and H. G. Smith, "Anomalous Neutron Scattering in α-CdS," Conference on Neutron Diffraction, Gatlinburg, Tennessee, April 20, 1960.

S. W. Peterson and J. Worsham, "Hydrogen Positions in Acetamide Hemihydrochloride," Cornell Meeting of the American Crystallographic Association, Ithaca, New York, July 1959.

E. H. Taylor, "Introduction to the Symposium on Molecular Beams and Chemical Kinetics," American Chemical Society, Cleveland, April 11–14, 1960.

E. H. Taylor, "The Use of Molecular Beams in Chemical Kinetics," University of Illinois, Urbana, November 18, 1959.

H. Zeldes, "Paramagnetic Resonance Studies of Irradiated Materials," University of Louisville, Louisville, Kentucky, April 26, 1960.

ORNL-2983
UC-4 – Chemistry-General

INTERNAL DISTRIBUTION

1. C. E. Center
2. Biology Library
3. Health Physics Library
4-6. Central Research Library
7-26. Laboratory Records Department
27. Laboratory Records, ORNL R.C.
28. Reactor Experimental Engineering Library
29. A. M. Weinberg
30. L. B. Emlet (K-25)
31. J. P. Murray (Y-12)
32. J. A. Swartout
33-37. E. H. Taylor
38. E. D. Shipley
39. S. C. Lind
40. M. L. Nelson
41. W. H. Jordan
42. F. L. Culler
43. A. H. Snell
44. A. Hollaender
45. M. T. Kelley
46. R. A. Charpie
47. K. Z. Morgan
48. T. A. Lincoln
49. A. S. Householder
50. C. S. Harrill
51. C. E. Winters
52. H. E. Seagren
53. D. Phillips
54. J. A. Lane
55. G. E. Boyd
56-63. M. A. Bredig
64. R. W. Stoughton
65. R. B. Briggs
66. G. W. Parker
67. C. J. Borkowski
68. G. H. Jenks
69. K. A. Kraus
70. H. A. Levy
71. R. S. Livingston
72. T. E. Willmarth
73. C. H. Secoy
74. C. J. Hochanadel
75. W. H. Baldwin
76. A. R. Brosi
77. R. N. Lyon
78. S. A. Reynolds
79. P. F. Thomason
80. E. G. Bohlmann
81. C. P. Keim
82. C. D. Susano
83. P. M. Reyling
84. R. S. Cockreham
85. R. Livingston
86. G. H. Cartledge
87. E. R. Van Artsdalen
88. E. Lamb
89. R. W. Johnson
90. J. R. McNally, Jr.
91. G. D. O'Kelley
92. M. J. Skinner
93. D. S. Billington
94. H. G. MacPherson
95. J. L. Gabbard
96. R. H. Busey
97. J. J. Pinajian
98. D. W. Sherwood
99. C. R. Baldock
100. F. F. Blankenship
101. C. J. Collins
102. J. S. Drury
103. W. R. Grimes
104. J. S. Johnson
105. W. L. Marshall
106. H. F. McDuffie
107. G. J. Nessle
108. S. W. Peterson
109. G. A. Ropp
110. G. M. Watson
111. R. F. Newton
112. R. E. Thoma
113. D. R. Cuneo
114. P. S. Rudolph
115. J. D. Roberts (consultant)
116. G. T. Seaborg (consultant)
117. C. E. Larson (consultant)
118. E. P. Wigner (consultant)
119. B. Crawford (consultant)
120. T. H. Davies (consultant)

EXTERNAL DISTRIBUTION

121. H. Miller, Office of Isotope Development, AEC, Washington
122. R. H. Schuler, Radiation Research Laboratories, Mellon Institute, 4400 Fifth Ave., Pittsburgh 13, Pa.
123. Division of Research and Development, AEC, Washington
124. Division of Research and Development, AEC, ORO
125. Boeing Airplane Company
126. Union Carbide and Carbon Chemical Company (South Charleston)
127. North American Aviation, Inc.

128-684. Given distribution as shown in TID-4500 (15th ed.) under Chemistry-General category (75 copies – OTS)

Chemistry Division progress reports previously issued in this series are as follows:

ORNL-65	March, April, May, 1948
ORNL-176	June, July, August, 1948
ORNL-229	September, October, November, 1948
ORNL-336	December, 1948, January and February, 1949
ORNL-286	Period Ending June 30, 1949
ORNL-499	Period Ending September 30, 1949
ORNL-607	Period Ending December 31, 1949
ORNL-685	Period Ending March 31, 1950
ORNL-795	Period Ending June 30, 1950
ORNL-870	Period Ending September 30, 1950
ORNL-1036	Period Ending December 31, 1950
ORNL-1053	Period Ending March 31, 1950
ORNL-1116	Period Ending June 30, 1951
ORNL-1153	Period Ending September 30, 1951
ORNL-1260	Period Ending December 31, 1951
ORNL-1285	Period Ending March 31, 1952
ORNL-1344	Period Ending June 30, 1952
ORNL-1432	Period Ending September 30, 1952
ORNL-1482	Period Ending December 31, 1952
ORNL-1587	Period Ending June 20, 1953
ORNL-1674	Period Ending December 20, 1953
ORNL-1755	Period Ending June 20, 1954
ORNL-1832	Period Ending December 20, 1954
ORNL-1940	Period Ending June 20, 1955
ORNL-2046	Period Ending December 20, 1955
ORNL-2159	Period Ending June 20, 1956
ORNL-2386	Period Ending June 20, 1957
ORNL-2584	Period Ending June 20, 1958
ORNL-2782	Period Ending June 20, 1959